



Fermi National Accelerator Laboratory  
P.O. Box 500 - Batavia, Illinois - 60510

## LCLS-II Prototype Dressed Cavity Technical Design Report ED0001383, Rev. -

Rev.	Date	Description	Prepared By	Reviewed By	Approved By
-	25 MAR 2014	Initial Release	<i>Andrea Palagi</i>	<i>Chuck Grimm</i>	

## Contents

List of Figure .....	4
List of Tables .....	5
Pressure Vessel Design.....	7
Introduction.....	7
Definitions.....	7
Exceptional Vessel Discussion .....	8
Reasons for Exception .....	8
Analysis and use of the ASME Code.....	9
Analytical Tools.....	10
Fabrication .....	10
Hazard Analysis .....	10
Pressure Test .....	11
Description and Identification .....	11
Drawing Tree .....	17
Serial Number of Cells.....	17
Processing History .....	17
Fermi Lever Tuner Description.....	19
Design Verification .....	22
Introduction and Summary .....	22
Non-Code Elements .....	23
Geometry.....	24
Material Properties.....	32
Loadings.....	36
Stress Analysis Approach .....	39
Division 1 Calculations by Rule .....	41
Finite Element Model .....	48
Stress Analysis Results .....	50
System Venting Verification.....	65
Summary.....	65
Detailed Calculations for System Venting.....	66
Welding Information .....	70
Fabrication Information.....	73
Verification of ANSYS Results .....	74

Hoop Stress in Ti Cylinder .....	74
Buckling of Spherical Shell – Approximation to Cell Buckling .....	76
Buckling of Ti Cylinder .....	77
Fatigue Analysis of the Titanium Bellows .....	78
RF Analysis.....	84
Influence of the Tuner Stiffness.....	87
Magnetic Shielding.....	90
Shield Fasteners .....	93
Shield Spacers (2nd Layer).....	93
Shield Material.....	93
Appendix A – Pressure Test Results .....	96
Details for the pressure test steps.....	97
Test Setup.....	97
Appendix B - FESHM 5031.6 DRESSED SRF CAVITY ENGINEERING NOTE FORM.....	99
Statements of Compliance.....	100
References .....	101

**List of Figure**

Figure 1. LCLS II Cavity Assembly (Drawing F10017493) ..... 14

Figure 2. 1.3-GHz Nine Cell RF Cavity Assembly (4904.010-MD-440004) ..... 15

Figure 3. LCLS II Helium Vessel weldment (Drawing F10015802) ..... 16

Figure 4. Map of Half Cells ..... 17

Figure 5. Model of the Slim Blade Tuner (left view) ..... 19

Figure 6. Model of the Slim Blade Tuner (right view) ..... 20

Figure 7. Dressed LCLS II SRF cavity ..... 24

Figure 8. Cavity components included in the analysis ..... 25

Figure 9. Geometric limits of analysis ..... 25

Figure 10. Parts and Material in the Field Probe End ..... 26

Figure 11. Parts and Materials in the Main Coupler End ..... 26

Figure 12. Welds Numbered as in Table 5 ..... 29

Figure 13. Weld Numbering (Field Probe End) ..... 30

Figure 14. Weld numbering Main Coupler End ..... 30

Figure 15. Assumed fusion zones - welds 1-3 ..... 31

Figure 16. Assumed fusion zones - welds 4-5 ..... 31

Figure 17. Assumed fusion zones - welds 6-8 ..... 32

Figure 18. Assumed fusion zones - welds 9-11 ..... 32

Figure 19. Volumes for Pressure/Vacuum ..... 36

Figure 20. Largest penetration in the Ti shell ..... 43

Figure 21. Smaller penetrations in the Ti shell ..... 43

Figure 22. Definitions of the parameters X and Y for the calculation of the reinforcement ..... 44

Figure 23. Parameters to determine the Available Area and the Requested Area for the reinforcement ..... 45

Figure 24. The Finite Element Model ..... 48

Figure 25. Mesh Details ..... 49

Figure 26. Stress Classification Lines ..... 51

Figure 27. Lowest buckling mode of Nb Cavity ( $P_{cr} = 96.7$  MPa) ..... 60

Figure 28. Buckling of the conical heads ..... 61

Figure 29. Weld Locations, as numbered in Table 24 ..... 71

Figure 30. Path for hoop stress plot ..... 74

Figure 31. Hoop Stress in Ti Cylinder along line 1-2 for Pressure of 0.205 MPa ..... 75

Figure 32. Single cell - radius for spherical shell buckling calculation ..... 76

Figure 33. ANSYS linear buckling of the Ti cylindrical shell ..... 77

Figure 34. Result of the Electro Magnetic analysis to find the resonant frequency  $f_0$  ..... 85

Figure 35. Axial displacement of the dressed cavity assembly when a pressure of 1 bar is applied in the zones where is located the Helium bath ..... 86

Figure 36. Result of the Electro Magnetic analysis to find the resonant frequency  $f_1$  ..... 87

Figure 37. Graph putting in evidence the influence of the tuner stiffness in the analysis of the pressure sensitivity ..... 89

Figure 38. Cavity prior to Magnetic Shield Installation ..... 90

Figure 39. Cavity Complete with 1<sup>st</sup> layer Magnetic Shielding ..... 91

Figure 40. 2-Cavity string with complete 1<sup>st</sup> layer shielding ..... 91

Figure 41. Cavity complete with 2<sup>nd</sup> layer Magnetic Shielding ..... 92

Figure 42. 2-Cavity string with complete 2 layers of Shielding ..... 92

Figure 43. Close-up of Shields with bellows restraint ..... 93

Figure 44. Permeability vs. Temperature curves for Cryoperm10 and for Amumetal 4K ..... 94

Figure 45. Typical Set-Up of Dressed SRF Cavity for Pressure Test. .... 98

**List of Tables**

Table 1. Areas of Exception to the Code - Safety .....9

Table 2. Areas of Exception to the Code – Design and Manufacturing Issues ..... 10

Table 3. Drawing Tree for the G3 Helium Vessel RF Cavity Assembly..... 18

Table 4. Summary of the Movement and Forces on the Slim Blade Tuner Assembly.....21

Table 5. Summary of Weld Characteristics .....28

Table 6. Material Properties .....33

Table 7. Allowable Stresses for Each Stress Category (Units in MPa) ..... 34

Table 8. Allowable Stress “S” (Units in MPa [PSI])..... 35

Table 9. Load Cases.....38

Table 10. Applicable Code, Div. 1 Rules for 1.3 GHz Cavity .....40

Table 11. Definition of Stresses, Coefficients in the Bellows Analysis, following the Code, Division 1, Appendix 26. ....46

Table 12. Complying with Appendix 26 Rules for Internal Pressure of 2.0-bar (30-psi).....46

Table 13. Load Case 1 - Stress Results .....52

Table 14. Load Case 2 - Stress Results .....53

Table 15. Load Case 3 - Stress results .....54

Table 16. Load Case 4 - Stress Results .....55

Table 17. Load Case 5 - Stress Results .....56

Table 18. Maximum Allowable Sum of Principal Stresses .....58

Table 19. Local Failure Criterion - Niobium .....58

Table 20. Local Failure Criterion - Ti-45Nb .....59

Table 21. Local Failure Criterion - TiGr2.....59

Table 22. Estimated Load History of Dressed SRF Cavity.....62

Table 23. Reproduction of Table 5.9 of Part 5, “Fatigue Screening Criteria for Method A” ..... 63

Table 24. Weld summary for LCLS II cavity .....70

Table 25. Weld Exceptions to the Code .....72

Table 26. Results of the influence of the tuner stiffness over the pressure sensitivity of the dressed cavity .....88

Table 27. Pressure Test Steps .....97



## Pressure Vessel Design

### Introduction

The LCLS II 1.3-GHz “dressed cavity” is a niobium superconducting radio frequency (SRF) cavity surrounded by a titanium vessel. The vessel contains liquid helium which surrounds the SRF cavity. During operation of the Dressed SRF Cavity, the liquid helium is at a temperature as low as 1.8°K.

The design of the LCLS II Helium Vessel RF Cavity Assembly has been modified from the TESLA TTF design for more efficient fabrication. The design is the result of collaboration between FNAL and SLAC.

The Dressed SRF Cavity will be fully tested in the Horizontal Test Stand (HTS) at the Meson Detector Building as an individual entity. The final location of the dressed cavity after it has been tested in HTS has not been determined. However, if it is selected to be installed in a LCLS II prototype cryomodule, then the cryomodule will be tested at the New Muon Lab.

This Technical Design Report describes the design and fabrication of the LCLS II 1.3-GHz Dressed SRF Cavity. This document also summarizes how the cavity, as a helium vessel, follows the requirements of the FESHM Chapter 5031.6 for Dressed SRF Cavities <sup>(1)</sup>. The note contains venting calculations for the Dressed SRF Cavity when it is installed in HTS. The note also includes the system venting verification for NML. This document and supporting documents for the dressed cavity may be found in FNAL’s Teamcenter engineering Installation

### Definitions

- FESHM      Fermilab Environment, Safety and Health manual
- FNAL        Fermi National Accelerator Laboratory
- LCLS II     Linac Coherent Light Source upgrade
- MAWP      Maximum Allowable Working Pressure, a term that is used to define the safe pressure rating of a component or a system
- SLAC        SLAC National Accelerator Laboratory
- SRF         Superconducting Radio Frequency
- AES         Advanced Energy System
- RI          Research Instruments
- ASME       American Society of Mechanical Engineers
- NML         New Muon Lab
- DESY       DESY National Accelerator Laboratory in Hamburg, Germany
- HTS         Horizontal Test Stand
- WPS         Weld Procedure Specification
- PQR         Procedure Qualification Record
- WPQ         Welder Performance Qualification
- EBW         Electron Beam Weld

- TIG Tungsten Inert Gas
- (GTAW) Gas Tungsten Arc Welding
- SCL Stress Classification Lines
- FEA Finite Element Analysis
- EJMA Expansion Joint Manufacturers Association

## **Exceptional Vessel Discussion**

### *Reasons for Exception*

Dressed SRF Cavities, as defined in FESHM Chapter 5031.6, are designed and fabricated following the ASME Boiler and Pressure Vessel Code (the Code) <sup>(2)</sup>. The 1.3-GHz Dressed SRF Cavity as a helium pressure vessel has materials and complex geometry that are not conducive to complete design and fabrication following the Code. However, we show that the vessel is safe in accordance with FESHM 5031.6. Since the vessel design and fabrication methods cannot exactly follow the guidelines given by the Code, the vessel requires a Director's Exception. Table 1 lists the specific areas of exception to the Code, where in the note this is addressed, and how the vessel is shown to be safe. Table 2 goes into details of why the design or the fabrication method cannot follow Code guidelines.



*Analysis and use of the ASME Code*

The extended engineering note presents the results of the analysis that was performed on the entire vessel.

**Table 1. Areas of Exception to the Code - Safety**

Item or Procedure	Reference	Explanation for Exception	How the Vessel is Safe
Some category B (Circumferential) welds in the titanium sub-assembly are Type 3 butt welds (welded from one side with no backing strip).	Pg. 18, 23, 39	Category B joints in titanium must be either Type 1 butt welds (welded from both sides) or Type 2 butt welds (welded from one side with backing strip) only (see the Code, Div. 1, UNF-19(a)).	The evaluation of these welds is based on a de-rating of the allowable stress by a factor of 0.6, the factor given in Div. 1, Table UW-12 for a Type 3 weld when not radiographed.
No liquid penetrant testing was performed on the titanium sub-assembly.	Pg. 18, 23	All joints in titanium vessels must be examined by the liquid penetrant method (see the Code, Div. 1, UNF-58(b)).	The evaluation of all welds is based on a de-rating of the allowable stress by a factor given in Div. 1, Table UW-12 for welds not radiographed. For the corner joints, the joint efficiency has to be less than 1.00.
No electron beam welds were ultrasonically examined in their entire length	Pg. 18, 23	All electron beam welds in any material are required to be ultrasonically examined along their entire length (see the Code, UW-11(e)).	The evaluation of all welds is based on a de-rating of the allowable stress by a factor given in Div. 1, Table UW-12 for welds not radiographed.
Fabrication procedure for the niobium cavity assembly does not include WPS, PQR, or WPQ	Pg. 63, 65	The fabrication procedure for the niobium cavity is proprietary. Detailed information on the procedure is not available.	The RF performance of the niobium cavity is acceptable, showing indirectly that all welds in the cavity are full penetration
No liquid penetrant testing was performed on the welds of the bellows sub-assembly.	Pg. 39, 65	All welds in the bellows expansion joint shall be examined by liquid penetrant testing (see the Code, para. 26-11)	The evaluation of the longitudinal weld is based on a de-rating of the allowable stress by a factor given in Div. 1, Table UW-12 for welds not radiographed. The circumferential attachment welds between the bellows and the weld ends are radiographed.

**Table 2. Areas of Exception to the Code – Design and Manufacturing Issues**

Item or Procedure	Reason
Some category B (circumferential) welds in the titanium sub-assembly are Type 3 butt welds (welded from one side with no backing strip).	Use of the Type 3 butt weld was driven by the design requirement for maximal space between the niobium cavity equator and the helium vessel inside diameter, as well as being historically rooted in the helium vessel design in use at DESY for the last 15 years.
No liquid penetrant testing was performed on the titanium sub-assembly.	Any acceptable pores within the weld will hold the liquid penetrant. Temperature changes in the weld, and thus the liquid penetrant, may result in degradation in the weld integrity.
No electron beam welds were ultrasonically examined in their entire length	The geometry of the parts being welded makes it significantly difficult to set up for the ultrasound procedure.
Fabrication procedure for the niobium cavity assembly does not include WPS, PQR, or WPQ	The fabrication procedure is proprietary information.
No liquid penetrant testing was performed on the bellows sub-assembly.	Any acceptable pores within the weld will hold the liquid penetrant. Temperature changes in the weld, and thus the liquid penetrant, may result in degradation in the weld integrity.

*Analytical Tools*

Analysis was done using ANSYS Workbench 14.5 and Mathcad version 14.

*Fabrication*

The x-ray results of the welds for any given dressed cavity helium vessel are located online:

<http://ilc-dms.fnal.gov/Workgroups/CryomoduleDocumentation/folder.2011-04-14.5879929941/PVnotes/WeldFabrication/Xray/>

Fabrication documents, like the weld documents such as the available Weld Procedure Specifications (WPS), Procedure Qualification Record (PQR), and Welder Performance Qualification (WPQ) and the material certifications, are stored online at:

<http://ilc-dms.fnal.gov/Workgroups/CryomoduleDocumentation/folder.2011-04-14.5879929941/PVnotes/WeldFabrication/Xray/>

*Hazard Analysis*

Whether tested in the HTS or a part of a cryomodule at NML, the 1.3-GHz helium vessel is completely contained within a multilayered structure that protects personnel. The 5°K copper thermal shield completely surrounds the helium vessel. The 80°K copper thermal shield, in turn, completely surrounds the 5°K shield, and the outer vacuum vessel encases the 80°K thermal shield. From a personnel safety standpoint, the helium vessel is well contained within

both the test cryostat and the cryomodule. Vacuum safety reliefs vent any helium spill.

### *Pressure Test*

The helium vessel MAWP is 2.05-bar. This means that during testing at HTS and when installed in the cryomodule, the helium vessel maximum allowable pressure differential is 0.205 MPa across the vessel outer wall to insulating vacuum and across the cavity wall to beam vacuum. The helium vessel pressure test takes place at a surrounding environment of atmospheric pressure. So the required test pressure is at least 110% of 29.7 psig. The pressure test goes up to 34.5-psig, which is 116% of the required test pressure.

## **Description and Identification**

The Dressed SRF Cavity is called a an LCLS II Helium Vessel RF Cavity Assembly. The dressed cavity consists of the niobium nine-cell 1.3-GHz cavity, with a unique serial number, and the titanium helium vessel, also with unique serial number. The top assembly drawing of the assembly, drawing F10017493, is shown in Figure 1. The LCLS II Cavity Assembly consists essentially of two sub-assemblies: the niobium SRF (bare) cavity and the titanium helium vessel weldment.

The niobium SRF cavity is an elliptical nine-cell assembly. A drawing of the nine-cell cavity is shown in Figure 2 (drawing 4904.010-MD-440004). A single cell, or a dumbbell, consists of two half-cells that are welded together at the equator of the cell. Rings between the cells stiffen the assembly to a point. Some flexibility in the length of the nine-cell cavity is required to tune the cavity and optimize its resonance frequency. The end units each consist of a half cell, an end disk flange, and a transition flange. The transition flange is made of a titanium-niobium alloy. The iris' minimum inner diameter is 35-mm (1.4-in), and the maximum diameter of a dumbbell is 211.1-mm (8.3-in) (see drawing 4904.010-MD-439173). The length of the cavity, flange-to-flange, is 1247.4-mm (49.1-in.) (see drawing 4904.010-MD-440004). Refer to the section titled "Drawing Tree" for the location of the drawings not shown in this note.

The titanium helium vessel encases the niobium SRF bare cavity. Figure 3 shows the drawing of the titanium vessel assembly (drawing F10015802). The vessel has two helium fill ports at the bottom and in the center of the vessel there is the two-phase helium return line. At the sides of the vessel are tabs which support the vessel within the HTS cryostat or cryomodule. The vessel is flexible in length due to a bellows at the field probe end. This flexibility in the vessel allows for accommodating the change in the nine-cell cavity length due to thermal contraction at cryogenic temperature and for tuning the niobium cavity during operation. A lever tuner supports the vessel at the bellows. Two control systems act on the lever tuner to change the length of the vessel, and thus change the length of the cavity. A slow-control tuner system that consists of a stepper motor that changes the vessel length. The stepper motor extends the length of the cavity by less than 2.0-mm (0.079-in.) to bring it to the desired resonance frequency to counteract the combined effects of thermal contraction and pressurization during cool down. Once the cavity is at cryogenic temperature, the slow tuner system is shut-off. A fast-control tuner system consisting of two piezoelectric actuators prevents detuning of the cavity during operation due to Lorentz Forces and noise sources (microphonics)<sup>(4)</sup>. The piezos provide an increase in bellows length (bellows expansion) of 13- $\mu$ m during operation. The vessel is expected to have a lifetime

of 10-years. The minimum inner diameter of the cylindrical part of the vessel (both the tubes and bellows) is 230-mm (9.1-in.). Refer to the tube drawings F10008818 and bellows drawing F10010529.

The design of the niobium nine-cell cavity is the same as the cavities used in the TESLA facility at DESY (Hamburg, Germany), which has been in operation for the past 10 years. The design of the helium vessel is a modification of the TESLA design. The location of the titanium bellows, along with the lever tuner and control systems, is a modification of the TESLA design that is the result of collaboration between Fermilab and DESY.

The Dressed SRF Cavity will be performance tested in HTS. The results will determine whether or not it will be used in a future cryomodule. The results of the testing will also be feedback in optimizing the design and fabrication process for future LCLS II dressed cavities which will be used in a cryomodule.

The Dressed SRF Cavity has two internal maximum allowable working pressures (MAWP). At a design temperature range of 80°K - 300°K, the (warm) internal MAWP is 2.0-bar. The vessel will be pressure tested in room temperature. The internal MAWP for cold temperatures (1.8°K - 80°K) is 4.0-bar. The external MAWP is 1.0-bar.

The beam vacuum has an internal MAWP of 3-bar (45-psia). At NML, where the string of dressed cavities within the cryomodule is tested, the niobium cavity would operate under vacuum as part of the beam vacuum. The beam pipe venting line has a rupture disk with a set pressure as high as 25-psig (0.18 MPa). In the failure mode where liquid helium leaks into the cavity, and then the cavity is warmed up, the helium would expand and pressurize the cavity.

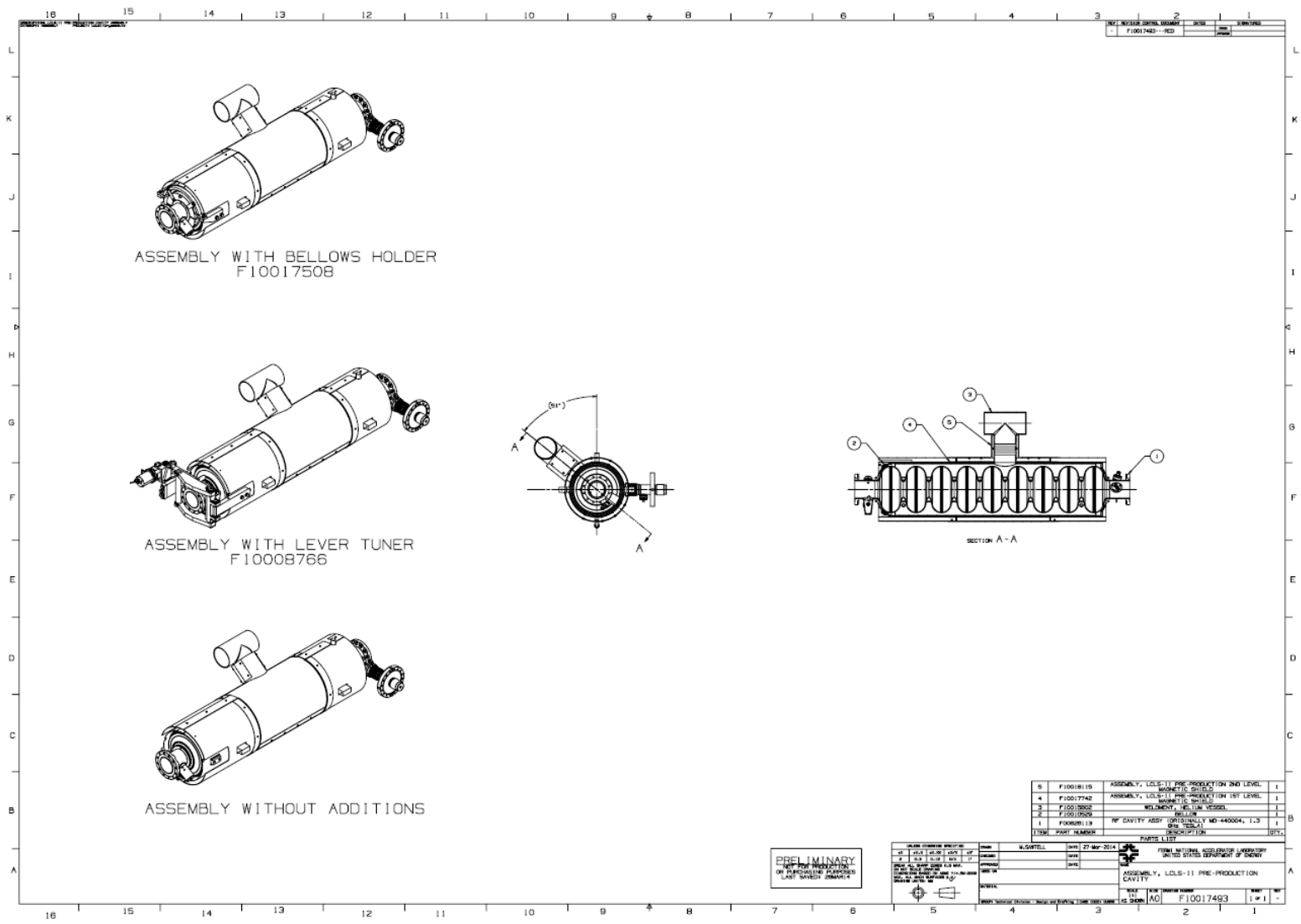


Figure 1. LCLS II Cavity Assembly (Drawing F10017493)

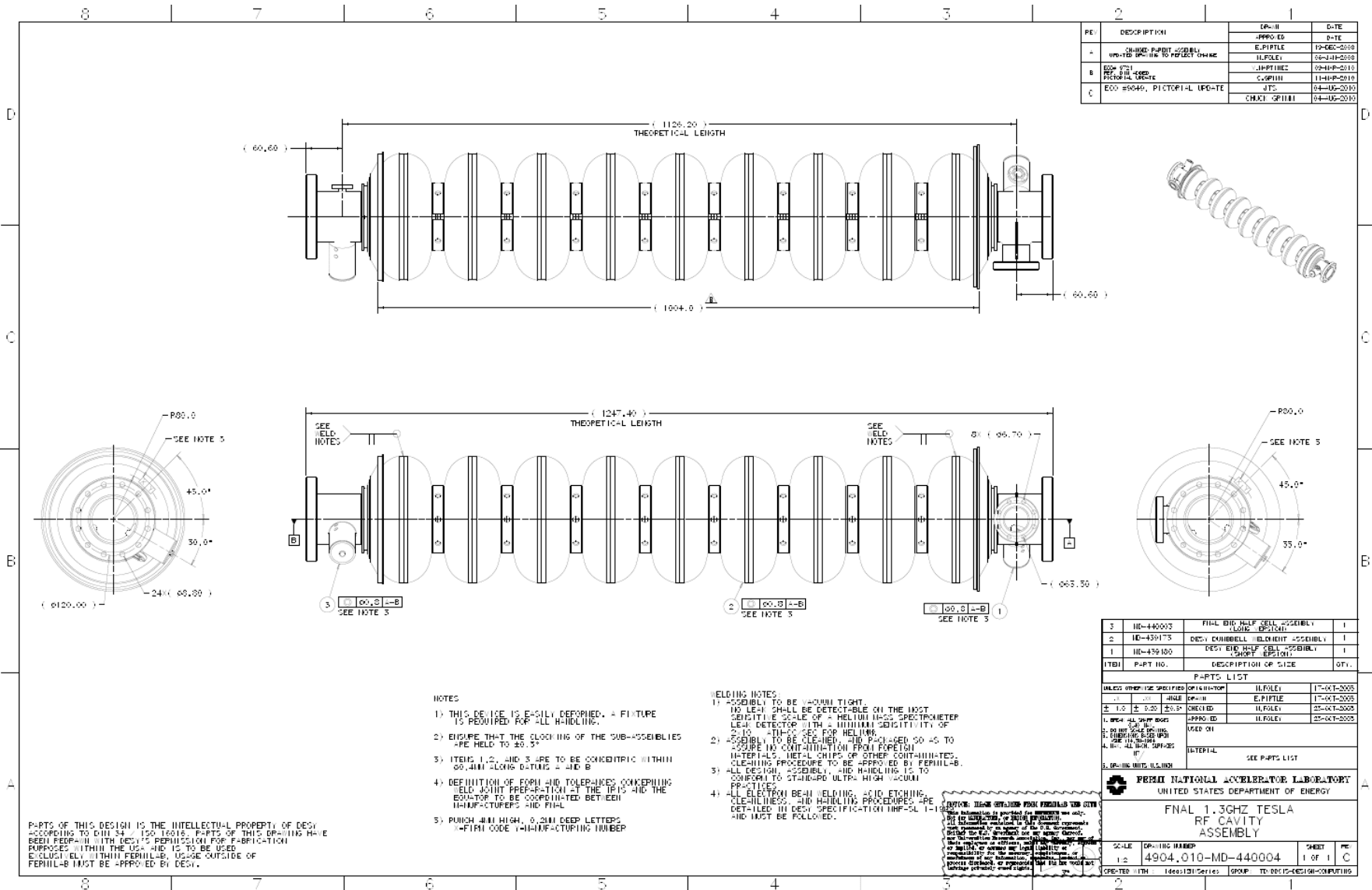


Figure 2. 1.3-GHz Nine Cell RF Cavity Assembly (4904.010-MD-440004)

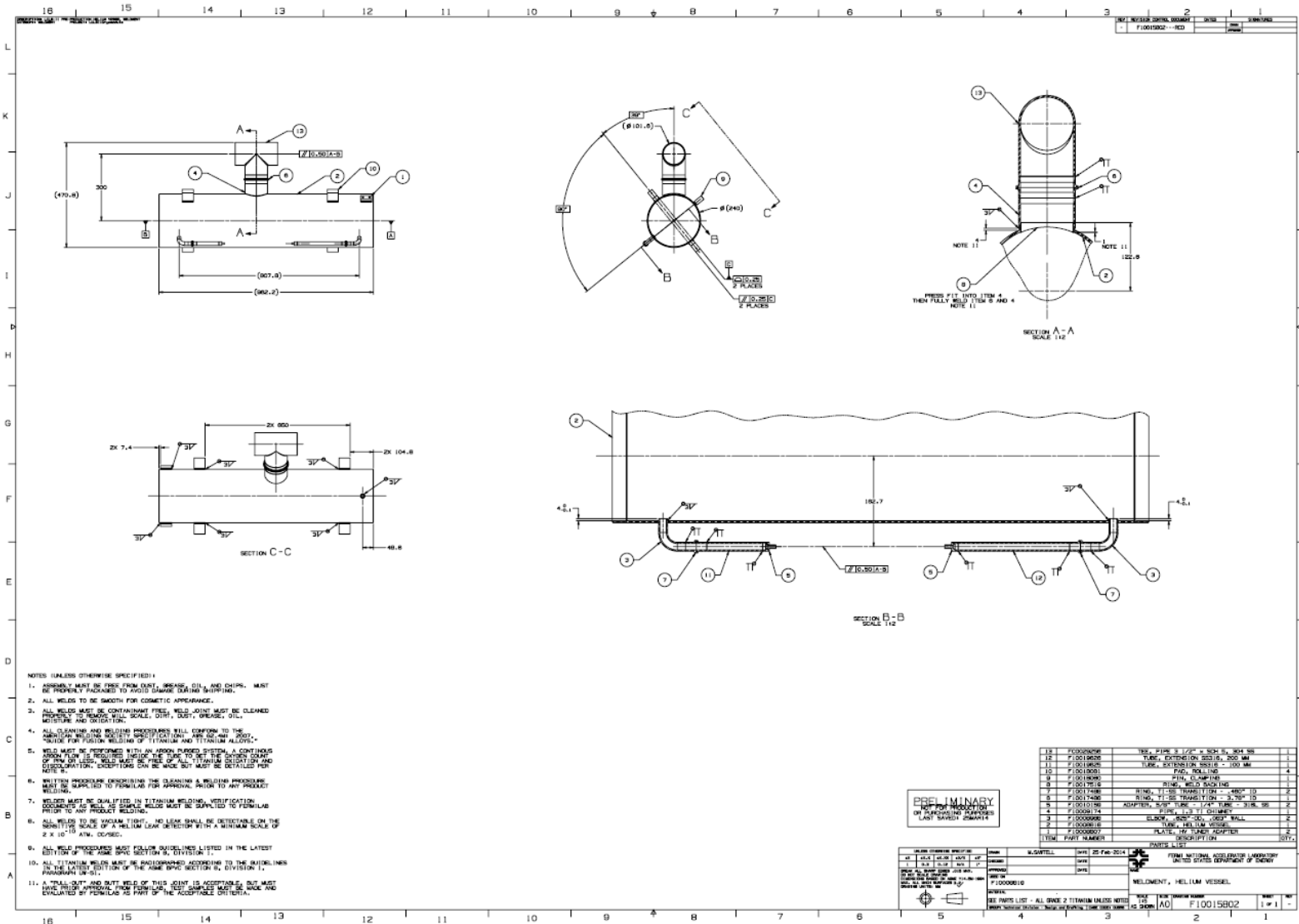


Figure 3. LCLS II Helium Vessel weldment (Drawing F10015802)



*Drawing Tree*

A drawing tree for the LCLS II Helium Vessel RF Cavity Assembly is shown in Table 3. All drawings are located online. The drawings can be found in FNAL’s Teamcenter engineering installation

The RF Cavity Assembly, drawing 440004 is also located in Teamcenter.

*Serial Number of Cells*

As previously discussed, the niobium SRF bare cavity is comprised of nine cells, or 18 half cells. The serial numbers of these half cells are shown in Figure 4 in this sample from the incoming inspection traveler

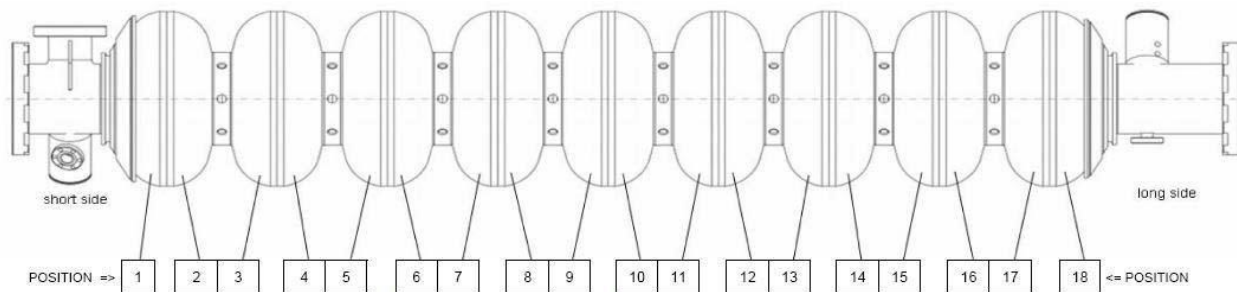


**Figure 4. Map of Half Cells**

Half Cell	Serial #	Half Cell	Serial #
Position 1	FE323	Position 10	FE396
Position 2	FE268	Position 11	FE358
Position 3	FE237	Position 12	FE214
Position 4	FE462	Position 13	FE242
Position 5	FE439	Position 14	FE259
Position 6	FE341	Position 15	FE451
Position 7	FE271	Position 16	FE361
Position 8	FE284	Position 17	FE452
Position 9	FE224	Position 18	FE334

*Processing History*

The processing history of RF cavities includes any or all the following: bulk- and light-electropolishing, centrifugal barrel polishing, an 800°C high temperature bake for 3 hours, and a 120°C bake for 48 hours. The cavity is tested, and then welded to the helium vessel. The complete history for this Dressed SRF cavity can be found in the following device service document:

<https://vector-onsite.fnal.gov/>

**Table 3. Drawing Tree for the G3 Helium Vessel RF Cavity Assembly**

Drawing No.	Rev.	Title
F10017493	--	LCLS II He Vessel RF Cavity Assembly
F10015802	--	LCLS II Helium Vessel Weldment
F10008807	--	Plate, HV tuner adapter
F10008818	--	Tube Helium Vessel
F10008988	--	Elbow, .625" -OD, .083" Wall
F10009174	--	Pipe, 1.3 Ti Chimney
F10010159	--	Adapter, 5/8" tube - 1/3" tube - 316L SS
F10017486	--	Ring, Ti-SS transition - 3.76" ID
F10017488	--	Ring, Ti-SS transition - .460" ID
F10017519	--	Ring, Weld backing
F10018080	--	Pin, Clamping
F10018081	--	Pad, Rolling
F10019625	--	Tube, Extension SS316 - 200 mm
F10019626	--	Tube Extension SS316, 200 mm
F10029256	--	Tee, Pipe 3 1/2" xSCH 5, 304 SS
813175	A	Support Plate Adapter
440004	A	RF Cavity Assembly
449180	D	Short End Half Cell Assembly
439178	B	End Disk Weldment - Short Version
439164	A	End Tube Spool Piece
439152	B	End Cap Flange
439168	--	End Cap Disk (Short Version)
439163	--	RF Half Cell (Short Version)
439177	A	End Tube Weldment - Short Version
439175	--	Short Version HOM Assembly
439166	--	Short Version HOM Formteil Housing
439150	--	HOM Spool Piece
439162	--	Short Version Formteil
439161	B	Short Version End Tube
439171	--	Coupler Spool Piece
439169	--	Coupler Rib
439159	--	NW78 Beam Flange
439158	--	NW40 Coupler Flange
439157	--	NW12 HOM Flange
813185	A	Cavity Transition Ring MC End
439173	-	DESY Dumbbell Weldment
439172	--	Dumbbell
439156	--	Mid Half Cell
439151	A	Half Support Ring
440003	-	FNAL End Half Cell Assembly
439178	B	End Disk Weldment (Long Version)
439164	A	End Tube Spool Piece
439152	B	End Cap Flange
439167	--	End Cap Disk (Long Version)
439155	--	RF Half Cell (Long Version)
440002	B	FNAL End Tube Weldment (Long Version)
439174	--	DESY Long Version HOM Assembly
439165	--	HOM Long Version Formteil Housing
439150	--	HOM Spool Piece
439154	--	Long Version Formteil
440001	--	FNAL Long Version End Tube
439170	A	DESY Antenna Spool Piece
439159	--	DESY NW78 Beam Flange
439160	--	DESY NW8 Antenna Flange
439157	--	DESY NW12 HOM Flange
813195	A	Cavity Transition Ring Field Probe End
F10010529	--	He Vessel Bellows

### *Fermi Lever Tuner Description*

While not an integral part of the pressure vessel design, the blade tuner's function is affected by the performance of the pressure vessel. Figure 1 (drawing 872825) shows the “slim” blade tuner around the titanium bellows on the helium vessel. The blade tuner maintains the tuning of the RF cavity after cooldown of the vessel and during operation of the RF cavity. The design that is used on RI-026 is version 3.9.4.<sup>(18)</sup>

**Error! Reference source not found.** shows the different parts of the blade tuner assembly. The tuner rings (part numbers 844675 and 844685) are welded to the titanium helium vessel.

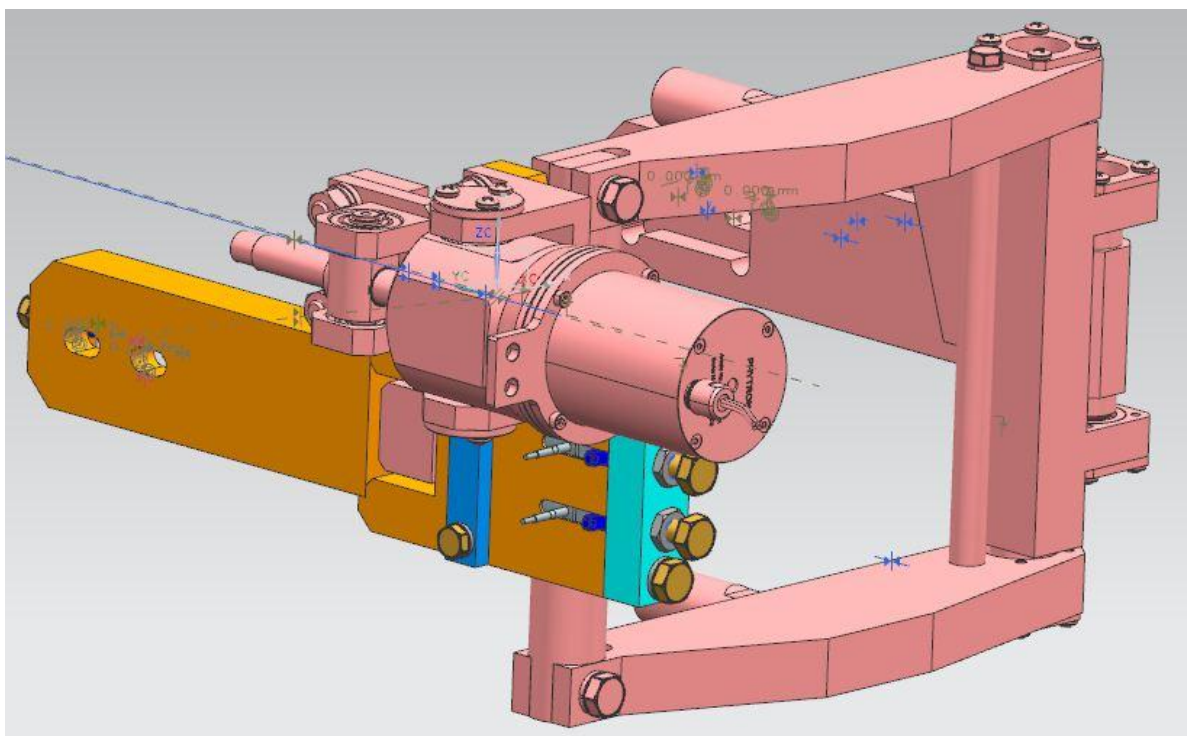


Figure 5. Model of the Slim Blade Tuner (left view)

The tuner assembly is composed of two parts that are defined by their tuning functions: slow tuner assembly and the fast tuner assembly. The slow tuner assembly consists of the stepper motor and the bending system. The bending system consists of three rings. One ring is rigidly attached to the helium vessel by way of the tuner ring (at the coupler end). The central “ring” is divided into two halves. The three rings are connected by thin plates, or blades<sup>(19)</sup>. The stepper motor “is rigidly connected to the helium vessel and produces a rotation of the [central ring halves]. The movement of the [central ring halves] induces the rotation of the bending system that changes the cavity length.” The design of the bending system of the slow tune assembly “provides the amplification of the torque of the stepper motor, dramatically reducing the total movement and increasing the tuning sensitivity.”<sup>(18)</sup>

The fast tuner assembly consists of two piezoelectric actuators that are parallel to each other and

clocked 180° from each other. One side of the fast tuner assembly is fixed to the helium vessel, and the other side is fixed to the bending system of the slow tuner assembly. **Error! Reference source not found.** shows how the piezoelectric actuators are installed.

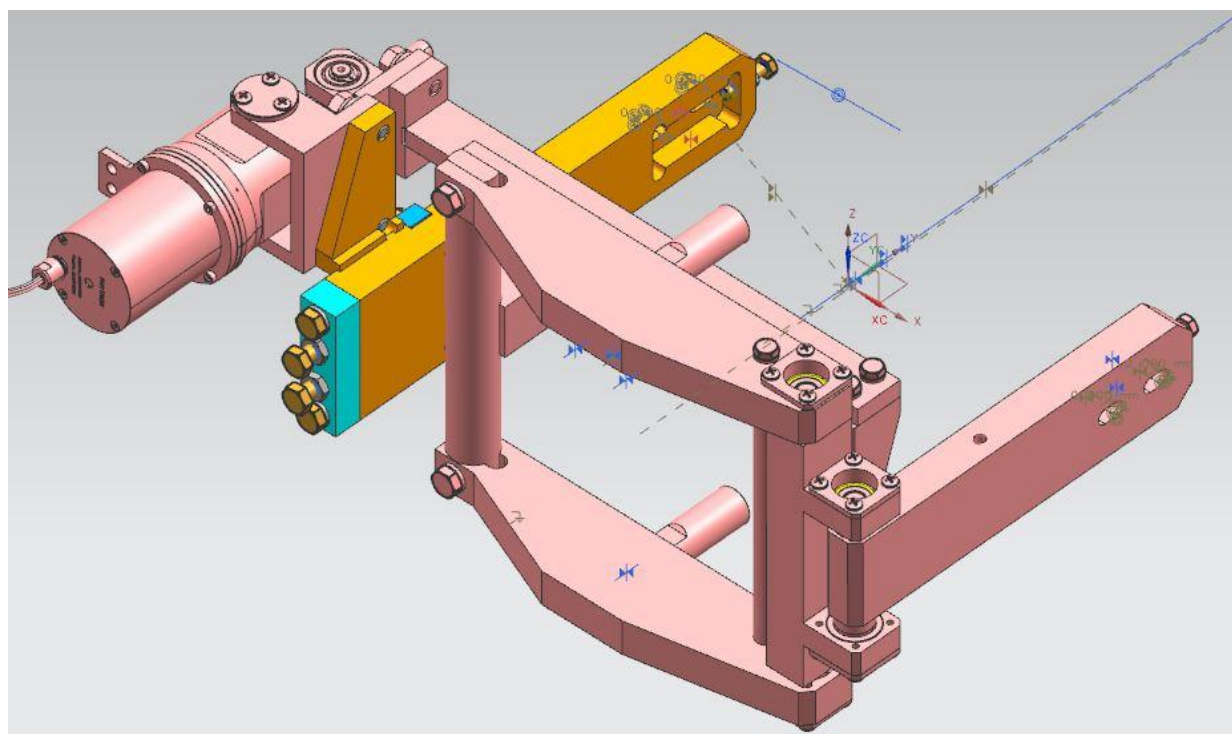


Figure 6. Model of the Slim Blade Tuner (right view)

The slow tuner system lengthens the vessel to maintain the RF cavity tuning after cooldown. The extension compensates for the combined effects of thermal contraction and pressurization, thus bringing the SRF cavity back to its desired resonance frequency. The stepper motor is actuated to increase the vessel length about 1.5-mm after cooldown. During operation of the RF cavity, the beam pulses create a tendency for the RF cavity to decrease in length. This phenomenon is called Lorentz Force Detuning. The piezoelectric actuators increase the vessel length about 13- $\mu\text{m}$  during operation.<sup>(19)</sup>

#### Displacement and Force Limits of the Slim Blade Tuner

The limits of displacement that cause the slim blade tuner to change the length of the vessel are defined by deformation of the tuner assembly. The maximum tuning range of the blade tuner assembly corresponds to 14 steps of the stepper motor (see Section 6.3.3.2 of the Panzeri paper).<sup>(18)</sup> For more than 12 steps of the stepper motor, the tuner assembly goes from yield deformation into plastic deformation. The 12 steps correspond to a displacement of less than 1.8-mm (Figure 37 of the Panzeri paper).

The tuner ring and four threaded rods provide an additional limit on the movement of the tuner assembly. During assembly at room temperature, the outer bolts are installed so that there is a 0.2-mm gap between each bolt and the tuner ring. In the final assembly, the tuner ring is compressing the piezoelectric actuators. The threaded rods act as a safety device in the case of a piezoelectric actuator failure or overpressure of the helium vessel. The threaded rods limit free

movement of the tuner assembly to less than 0.2-mm.

The maximum expected force of compression on the tuner assembly is 3116-N during operation. This would occur when the beam tube is evacuated, the helium vessel is internally pressurized at 1-bar, and the helium vessel is externally pressurized at 1-bar. The expected compressive force is less than the maximum allowed compressive force of 10900-N. Note that the maximum allowed force takes into account a design factor of 1.5.<sup>(18)</sup>

The maximum calculated tensile force on the tuner assembly is 9630-N. This would occur during an emergency scenario when the helium vessel is internally pressurized to its MAWP of 4-bar. The maximum allowed tensile force is 19000-N. So when the vessel is at its internal MAWP, the expected tensile force exerted on the tuner assembly is well within the tuner's allowed tensile force. Note that these calculations took into account material properties at room temperature. The assumption was made that the material properties would be better at cryogenic Temperatures.<sup>(18)</sup>

Table 3 summarizes the limits of movement and forces and the required movement and forces of the slim blade tuner assembly.

**Table 4. Summary of the Movement and Forces on the Slim Blade Tuner Assembly**

	<b>Maximum Allowed</b>	<b>Required Value</b>
<b>Slow tuner movement range</b>	<b>0 – 1.8 mm</b>	<b>0 – 1.5 mm</b>
<b>Free movement range</b>	<b>0 – 0.2 mm</b>	<b>---</b>
<b>Compressive force</b>	<b>10,900 N</b>	<b>3116 N</b>
<b>Tensile force</b>	<b>19,00 N</b>	<b>9630 N</b>

## Design Verification

### *Introduction and Summary*

This analysis is intended to demonstrate that the LCLS II 1.3 GHz SRF cavity conforms to the ASME Boiler and Pressure Vessel Code (the “Code”), Section VIII, Div. 1, to the greatest extent possible.

Where Div. 1 formulas or procedures are prescribed, they are applied to this analysis. For those cases where no rules are available, the provisions of Div. 1, U-2(g) are invoked. This paragraph of the Code allows alternative analyses to be used in the absence of Code guidance.

This cavity contains several features which are not supported by the Code. These are related primarily to materials, weld types, and non-destructive examination, and are addressed in detail in the next section of this report, titled “Non-Code Elements.” These are accepted as unavoidable in the context of SRF cavities, and every effort is made to demonstrate thorough consideration of their implications in the analysis.

Advantage is taken of the increase in yield and ultimate strength which occurs in the Nb and Ti components at the operating temperature of 1.88 K.

The design pressures specified for this analysis are 30 psi (2.0-bar) at 293 K and 60 psi (4.0-bar) at 1.88 K. This analysis confirms that the MAWPs of the vessel can be safely set at these pressures. Negligible margin for increase is available at 293 K, but the cold MAWP could be increased substantially above 60 psi (4.0-bar).

In addition to these fundamental operating limits, the cavity was also shown to be stable at external pressures on the Ti shell of 15 psid (1.0-bar), and internal pressures on the Nb cavity of 15 psid (1.0-bar); these loadings could occur under fault conditions, when the beam and insulating vacuums have been compromised, and the helium volume has been evacuated.

*Non-Code Elements*

With regards to the Design Verification, the LCLS II 1.3 GHz cavity does not comply with Div. 1 of the Code in the following ways:

1. Category B joints in titanium must be either Type 1 butt welds (welded from both sides) or Type 2 butt welds (welded from one side with backing strip) only (see Div. 1, UNF-19(a)). Some category B (circumferential) joints are Type 3 butt welds (welded from one side with no backing strip).
2. All joints in titanium vessels must be examined by the liquid penetrant method. (see Div. 1, UNF-58(b)). No liquid penetrant testing was performed on the vessel.
3. All electron beam welds in any material are required to be ultrasonically examined along their entire length. (see UW-11(e)). No ultrasonic examination was performed on the vessel

The evaluation of the Type 3 butt welds in the titanium is based on a de-rating of the allowable stress by a factor of 0.6, the factor given in Div. 1, Table UW-12 for such welds when not radiographed.

The exceptions listed above do not address Code requirements for material control, weld procedure certification, welder certification, etc. These requirements, and the extent to which the cavity production is in compliance with them, are addressed in the section titled "Weld Information."

## Geometry

### General

This analysis is based on geometry obtained from Dwg # F10017493 and associated details. Figure 7 shows the Dressed SRF Cavity, complete with magnetic shielding, piping and lever tuner.

For the analysis, only the Nb cavity, conical Ti-45Nb heads, and titanium shells and bellows are modeled, as well as the flanges to which the Helium Vessel is constrained. These components are shown in Figure 8.

The geometric limits of the analysis are further clarified in Figure 9.

The individual cavity component names used in this report are shown in Figure 10 and Figure 11.

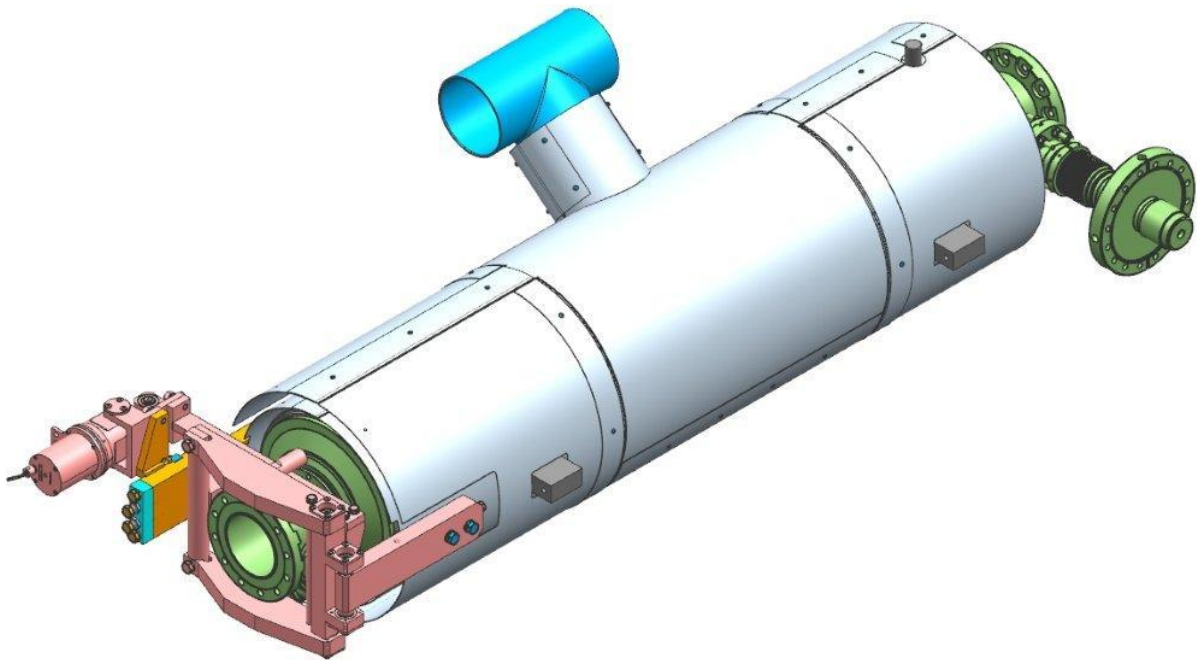


Figure 7. Dressed LCLS II SRF cavity



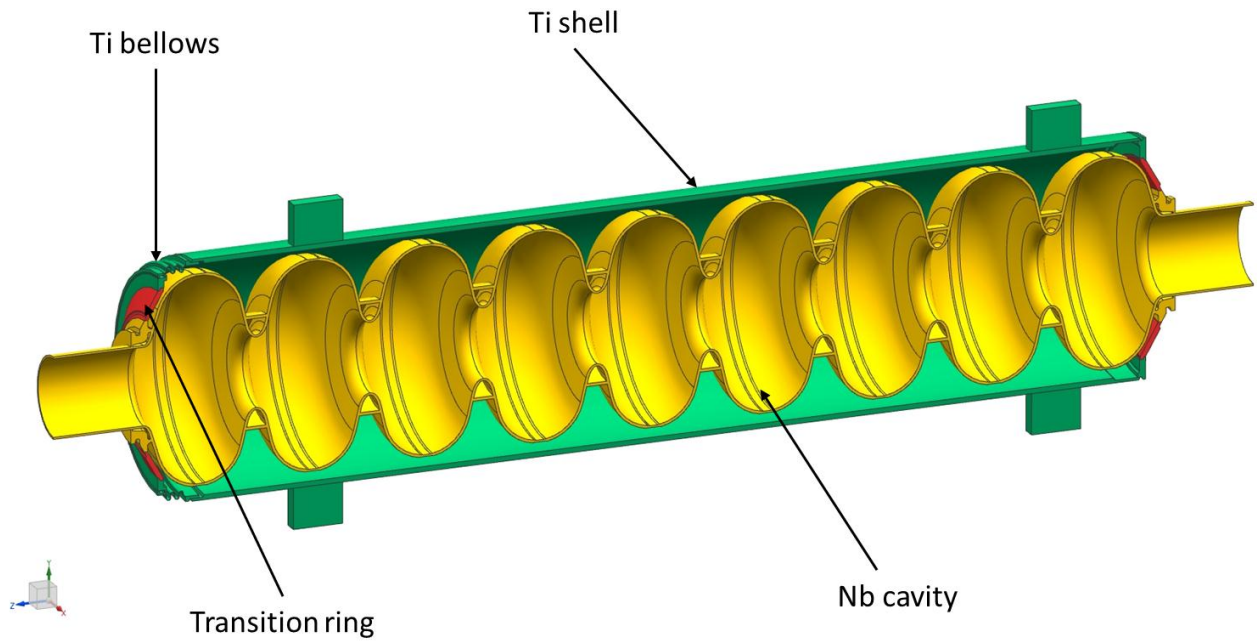


Figure 8. Cavity components included in the analysis

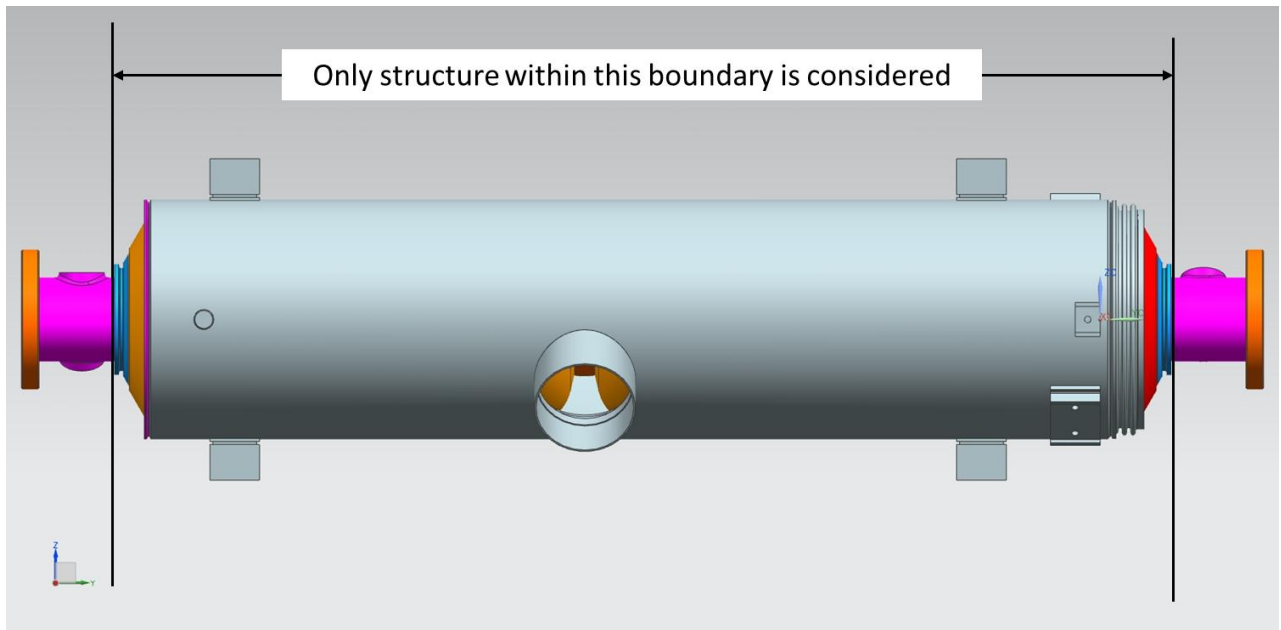


Figure 9. Geometric limits of analysis

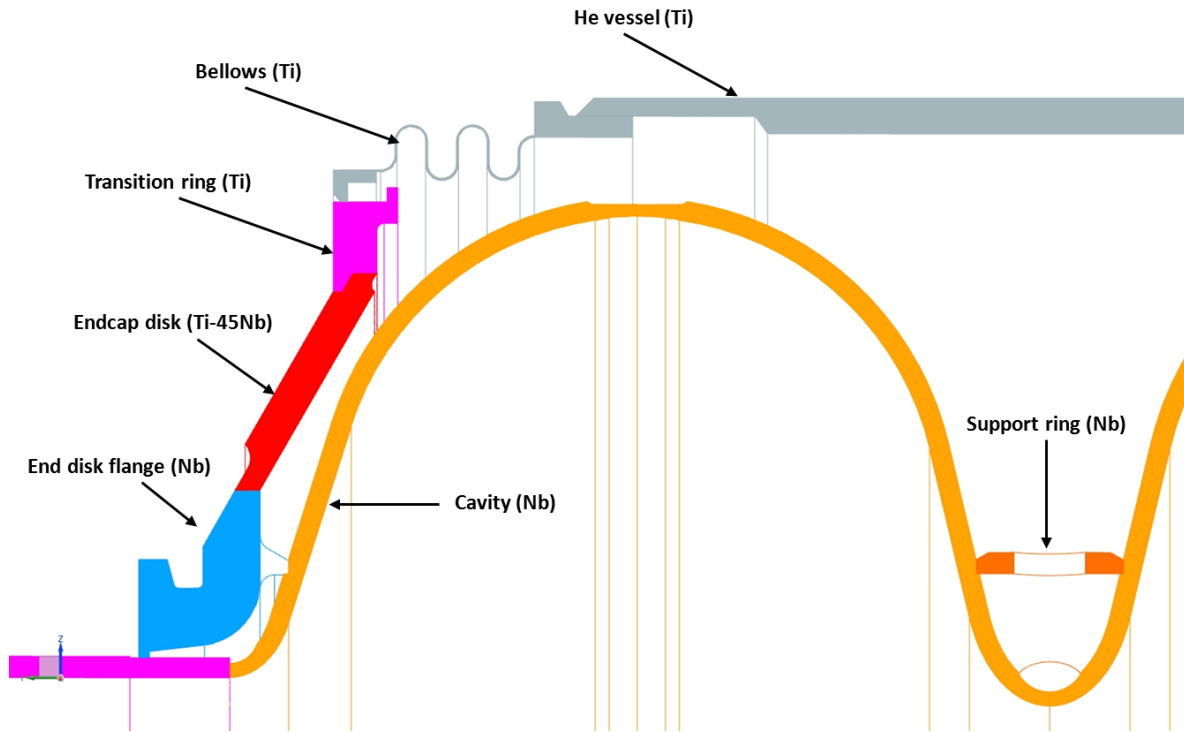


Figure 10. Parts and Material in the Field Probe End

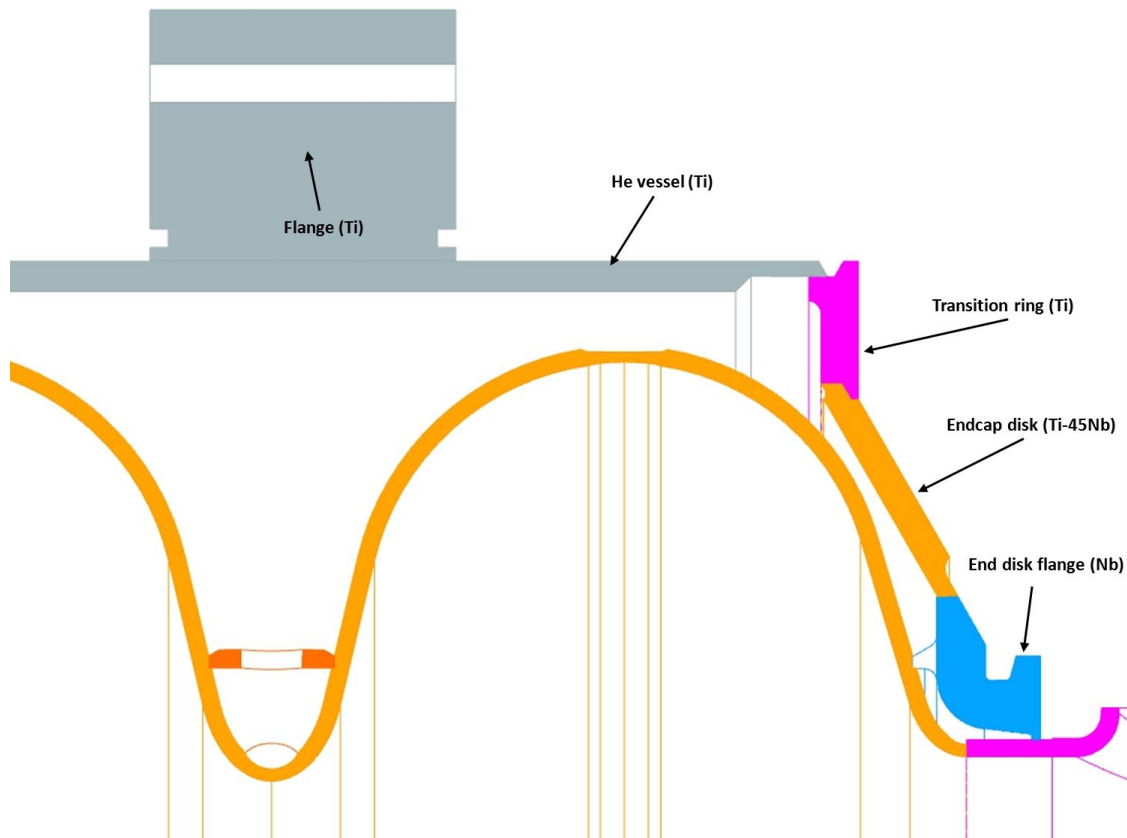


Figure 11. Parts and Materials in the Main Coupler End

## Welds

This section describes the welds as a precursor to the weld stress evaluation. Details regarding the weld fabrication process are shown in a later section of this note titled “Welding Information.”

Welds are produced by the EBW process (in the Nb, and Nb-to-Ti transitions), and the TIG (GTAW) process (Ti-Ti welds).

All welds on the Dressed SRF Cavity are designed as full penetration butt welds. All welds are performed from one side, with the exception of the Ti-45Nb to Ti transition welds. Those welds are performed from two sides. No backing strips are used for any welds.

Table 4 summarizes the weld characteristics, including the Code classification of both joint category and weld type, and the corresponding efficiency.

The locations of the welds as numbered in Table 5 are shown in **Error! Reference source not found.** Detailed weld configurations are illustrated in Figure 13 and Figure 14. Details of the assumed zones of fusion of the welds are shown in Figure 15, Figure 16, Figure 17, Figure 18.

Table 5. Summary of Weld Characteristics

Weld	Weld Description	Drawing	Materials Joined	Weld Process	Joint Category	Code Weld Type	Joint Efficiency
1	End Tube Spool Piece to End Cap Flange	MD-439178	Nb-Nb	EBW	B	3	0.6
2	End Tube Spool Piece to RF Half Cell	MD-439178	Nb-Nb	EBW	B	1	0.7
3	End Cap Flange to RF Half Cell	MD-439178	Nb-Nb	EBW	-	3	0.6
4	End Cap Flange to End Cap Disk	MD-439178	Nb-Ti45Nb	EBW	B	3	0.6
5	End Cap Disk to Transition Ring	MD-439180 MD-440003	Ti45Nb-Ti	EBW	B	1	0.7
6	1.3GHz 9 Cell RF Cavity (Transition Ring) to Bellow Assembly	F10017493	Ti-Ti	TIG	C	7	0.6
7 (FP End)	Bellow Assembly to LCLS II Helium Vessel Assembly	F10010493	Ti-Ti	TIG	B	3	0.7
8	Bellow Convolutions to Weld Cuffs	F10010529	Ti-Ti	EBW	B	3	0.6
9	Support Ring to Half Cell	MC-439172	Nb-Nb	EBW	-	3	0.6
10	Dumbbell to Dumbbell	MD-439173	Nb-Nb	EBW	B	3	0.6
11	Half Cell to Half Cell	MC-439172	Nb-Nb	EBW	B	3	0.6
12 (MC End)	Transition Ring to LCLS II Helium Vessel Assembly	F10017493	Ti-Ti	TIG	C	7	0.6

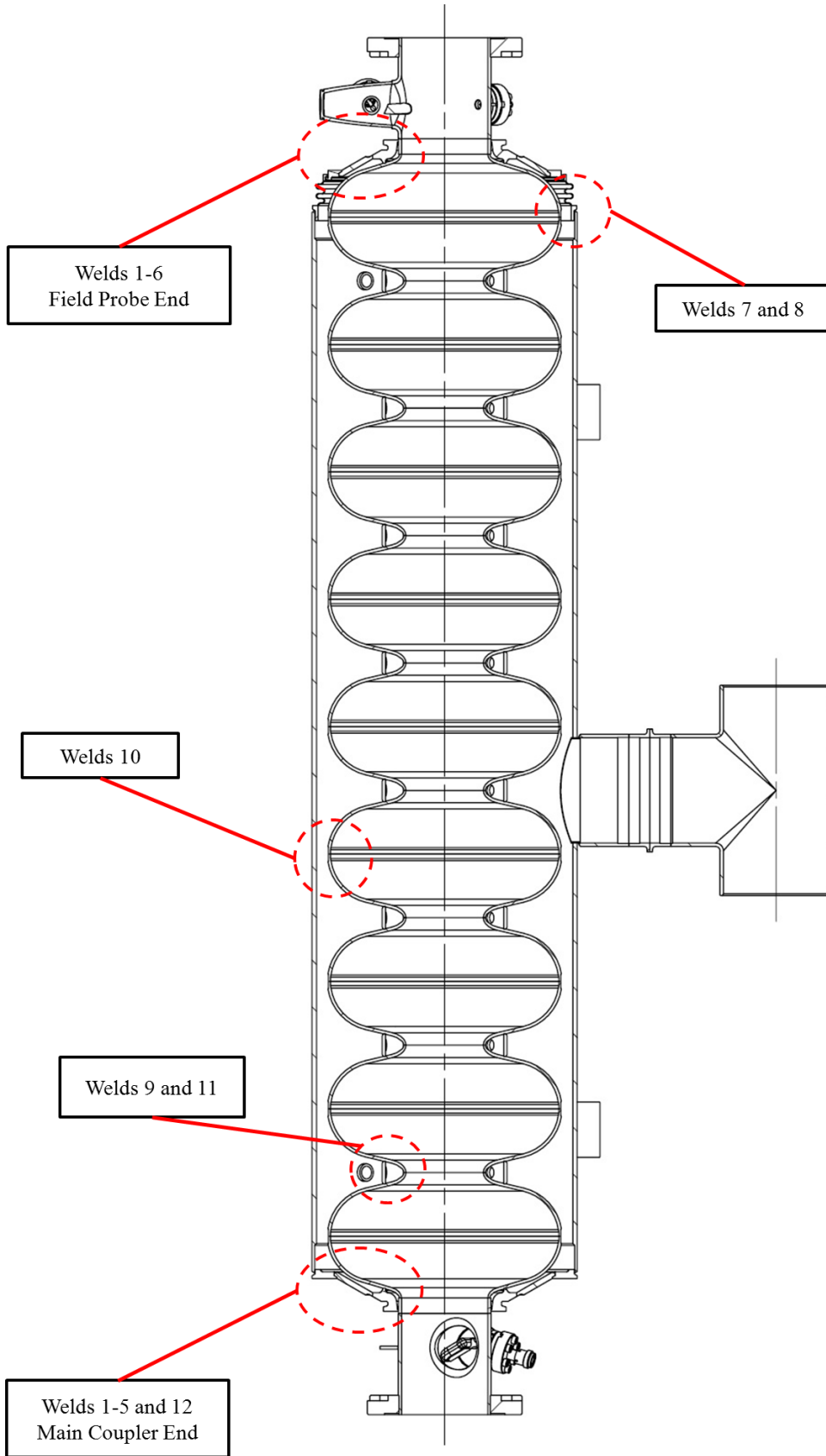


Figure 12. Welds Numbered as in Table 5

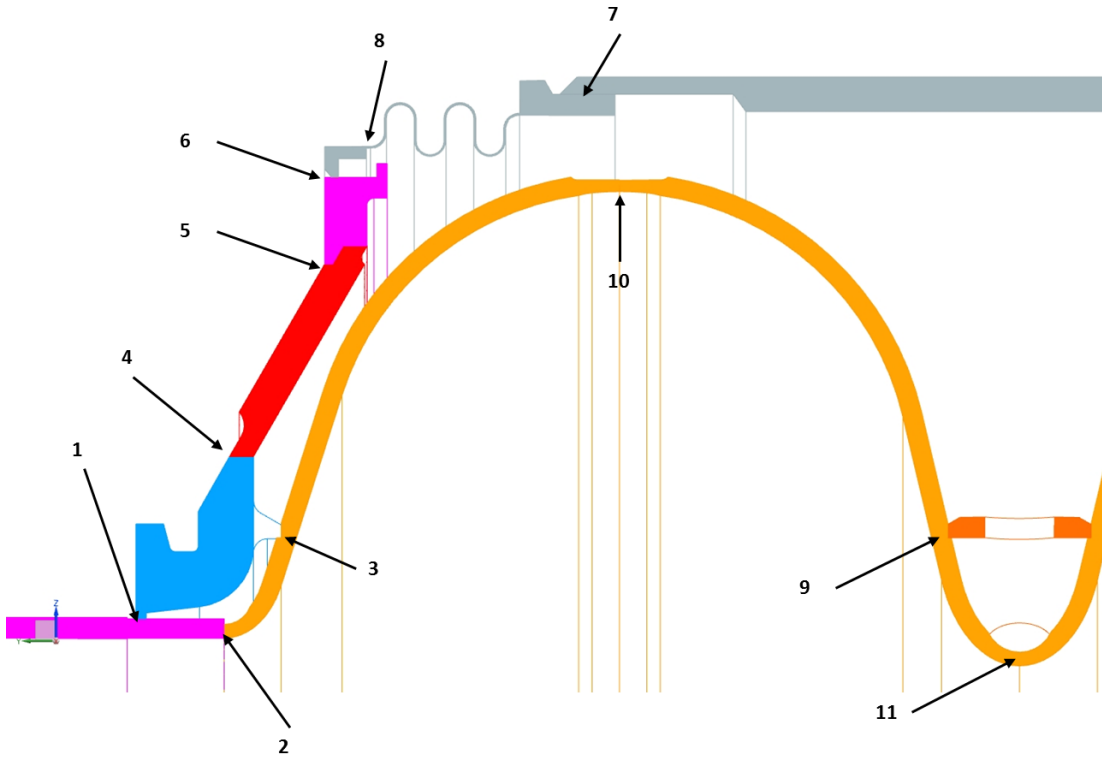


Figure 13. Weld Numbering (Field Probe End)

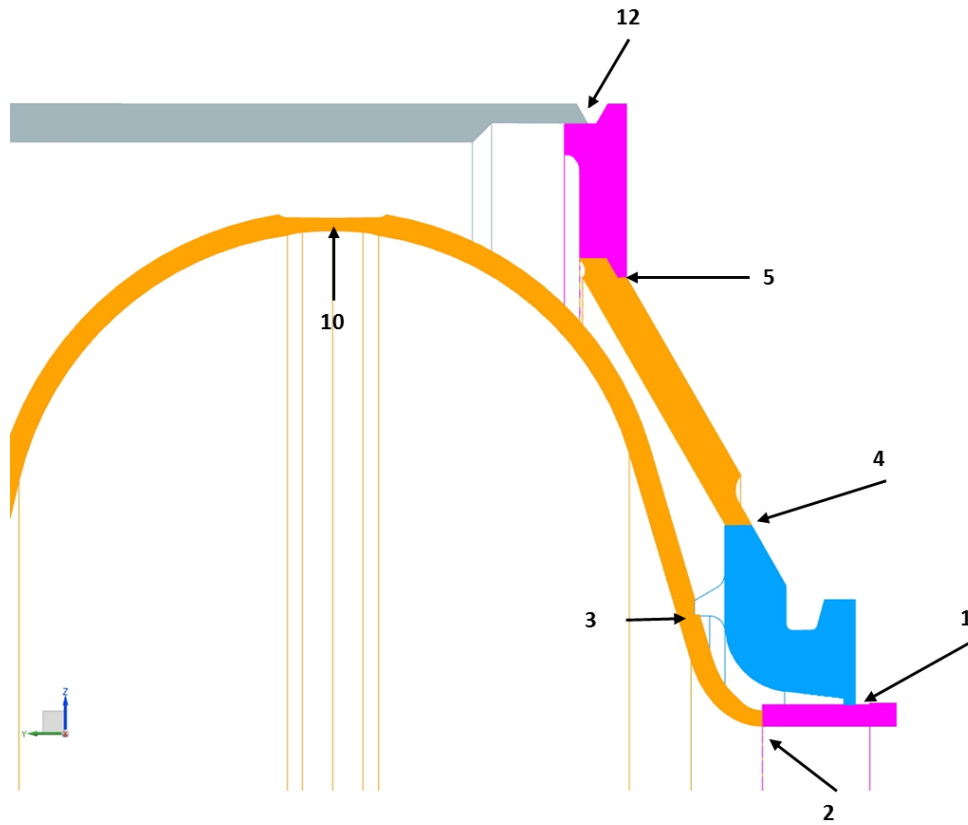


Figure 14. Weld numbering Main Coupler End

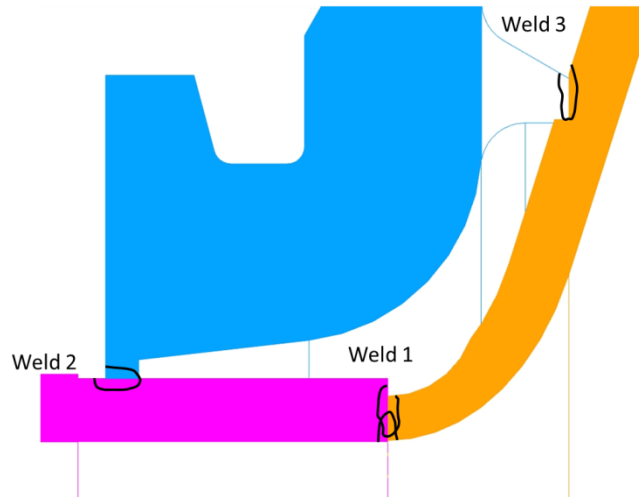


Figure 15. Assumed fusion zones - welds 1-3

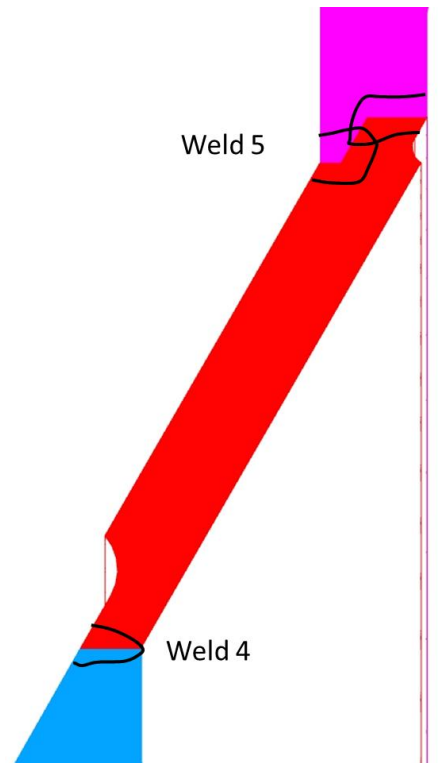


Figure 16. Assumed fusion zones - welds 4-5

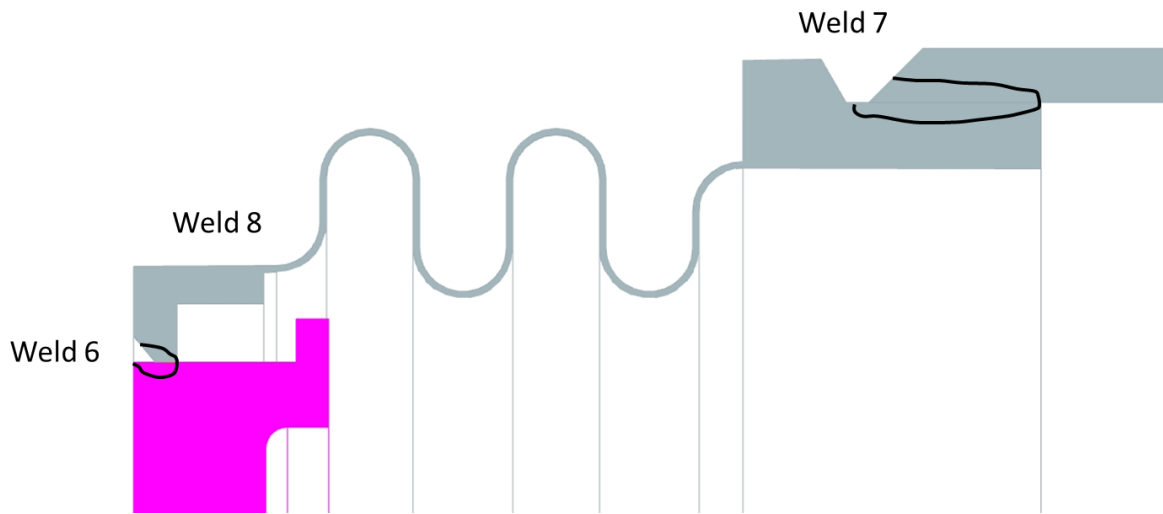


Figure 17. Assumed fusion zones - welds 6-8

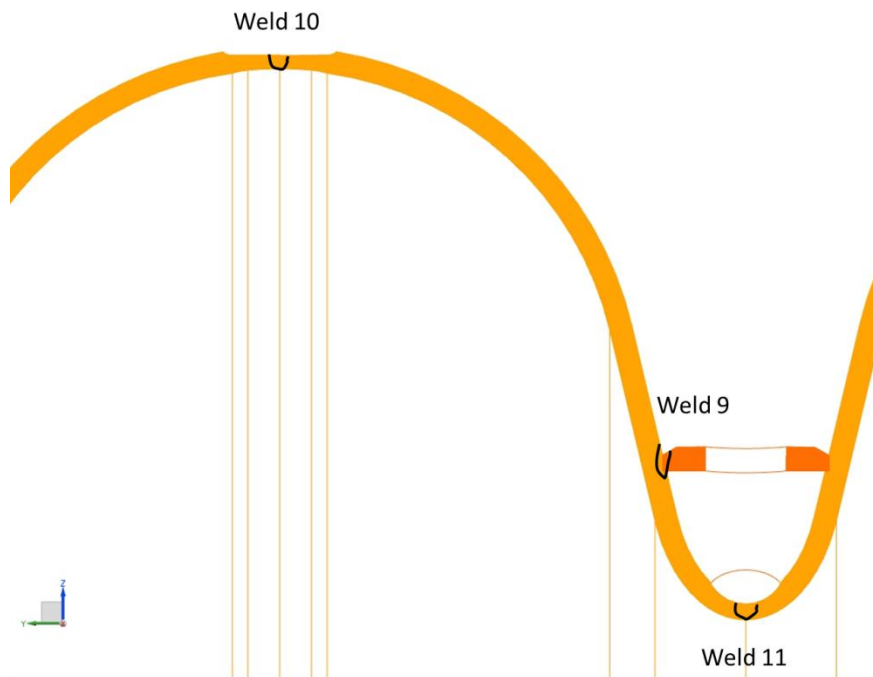


Figure 18. Assumed fusion zones - welds 9-11

## Material Properties

### General

The Dressed SRF Cavity is constructed of three materials: Pure niobium, Ti-45Nb alloy, and Grade 2 titanium. Of these materials, only Grade 2 Ti is approved by Div. 1 of the Code, and



hence has properties and allowable stresses available from Section II, Part D.

The room temperature material properties and allowable stresses for this analysis (are the ones from the Technical Division Technical Note TD-09-005) are identical to those established in the analysis of the 3.9 GHz elliptical cavity<sup>(5)</sup>. The determination of the allowable stresses was based on Code procedures, and employed a multiplier of 0.8 for additional conservatism.

For the cryogenic temperature load cases, advantage was taken of the increase in yield and ultimate stress for the Nb and Ti. As with the room temperature properties, the properties for these materials at cryogenic temperature were also established by previous work related to the 3.9 GHz cavity<sup>(6)</sup>.

Room temperature properties were used for the Ti-45Nb alloy for all temperatures, as no low temperature data on that alloy were available. However, it is highly likely that, like the elemental Nb and Ti, substantial increases in strength occur.

### Material Properties

The elastic modulus, yield strength, ultimate strength, and integrated thermal contraction from 293 K to 1.88 K are given in Table 5 for each material used in the construction of the cavity.

**Table 6. Material Properties**

Material	Property					
	Elastic Modulus (GPa)	Yield Strength (MPa)		Ultimate Strength (MPa)		Integrated Thermal Contraction 293K to 1.88K ( $\Delta l/l$ )
		293K	1.88 K	293K	1.88 K	
Niobium	105	38	317	115	600	0.0014
55Ti-45Nb	62	476	476	545	545	0.0019
Titanium, Gr. 2	107	276	834	345	1117	0.0015

Allowable Stresses

The Code-allowable stresses for unwelded materials for the various categories of stress (see “Stress Analysis Approach” of this report) are given in Table 7.

The Code-allowable stresses for welded materials are calculated by multiplying the values of Table 7 by the joint efficiency given in Table 5.

**Table 7. Allowable Stresses for Each Stress Category (Units in MPa)**

Material	Stress Category							
	$P_m$		$P_l$		$P_l + P_b$		$P_l + P_b + Q$	
	1.88K	293K	1.88K	293K	1.88K	293K	1.88K	293K
Nb	137	20	206	30	206	30	411	61
Ti-45Nb	125	125	187	187	187	187	374	374
Gr. 2Ti	255	79	383	118	383	118	766	237
<p><b>Note:</b></p> <p><math>P_m</math> = primary membrane stress  <math>P_l</math> = primary local membrane stress  <math>P_b</math> = primary bending stress  <math>Q</math> = secondary stress</p>								

The allowed stresses for each Stress Category in Table 6 are defined in the Code, Division 2, Paragraphs 5.2.2.4(e) and 5.5.6.1(d) and are reproduced here, where S is defined in Table 7:

$$P_m \leq S$$

$$P_l \leq 1.5 \cdot S$$

$$(P_l + P_b) \leq 1.5 \cdot S$$

$$(P_l + P_b + Q) \leq 3 \cdot S$$

The allowable stresses for each stress category in Table 7 are based on the value S, which is the allowable stress of the material at the design temperature. Table 8 shows the values of S for each material at 1.88K and 293K. Note that S includes the de-rating factor of 0.8 of the established allowable stress for a material for an experimental vessel. The de-rating follows the guidelines in FESHM Chapter 5031.

**Table 8. Allowable Stress “S” (Units in MPa [PSI])**

Material	Allowable Stress (S)		Established Values	
	1.88°K	293°K	1.88°K	293°K
Nb	137 [19870]	20 [2900]	171 [24801]	25 [3626]
Ti-45Nb	125 [18130]	125 [18130]	156 [22626]	156 [22626]
Gr. 2Ti	255 [36984]	79 [11458]	319 [46267]	99 [14359]

The established material properties used in SRF dressed cavities are stated at temperatures 293 K and 1.88 K. Recent measurements taken by Fermilab of the yield properties of niobium show that, at 77 K, the yield strength is at least 80% of the yield strength at 4 K. This matches what Walsh reported in another cold test in 1999. Walsh also reported that titanium’s yield strength at 77 K is within 74% of the yield strength at 4 K.

Looking at FEA results of Load Cases 2 and 4, where the vessel is modeled at 4-bar, the calculated stresses of the niobium are far less than 40% of allowable at 4K. The calculated titanium stresses are less than 73% of allowable at 4K. So the vessel will remain safe at the higher design temperature for the design pressure of 4.0-bar.

## Loadings

### General

The dressed cavity is shown in cross section in Figure 19.

There are three volumes which may be pressurized or evacuated:

1. The LHe volume of the helium vessel
2. The volume outside the cavity typically evacuated for insulation
3. The volume through which the beam passes on the inside of the Nb cavity itself.

The pressures in these volumes are denoted as  $P_1$ ,  $P_2$ , and  $P_3$ , respectively.

With regards to pressure, typical operation involves insulating vacuum, beam vacuum, and a pressurized LHe volume. Atypical operation may occur if the insulating or beam vacuums are spoiled, and the LHe space simultaneously evacuated. This reverses the normal operational stress state of the device, producing an external pressure on the Ti shell, and an internal pressure on the Nb cavity; however, this pressure is limited to a maximum differential of 1 bar.

In addition to the pressure loads, the cavity also sees dead weight forces due to gravity which are reacted at the Ti blade tuner flanges, as well thermal contractions when cooled to the operating temperature of 1.88 K, and a strain-controlled extension by the blade tuner after cool down.

All of these loadings are considered in this analysis. Specific load cases are defined in the next section.

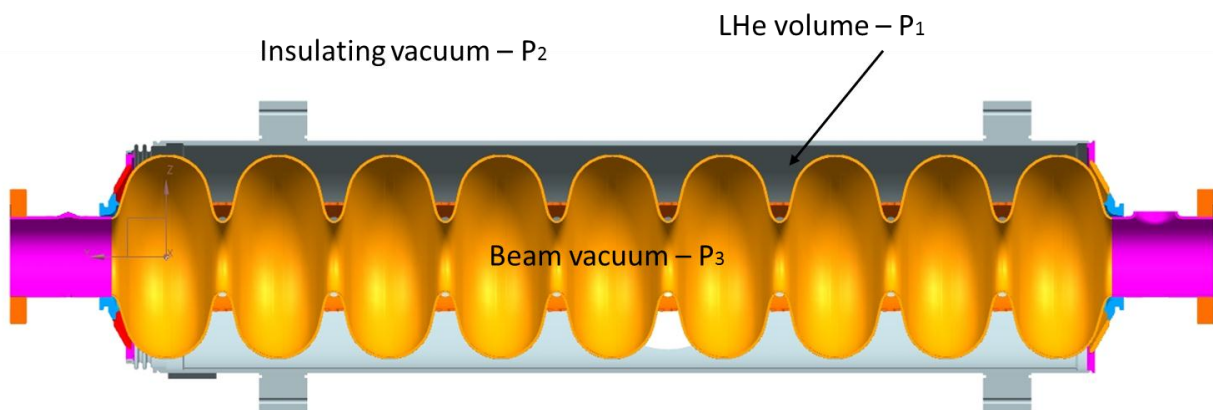


Figure 19. Volumes for Pressure/Vacuum

## Load Cases

The cavity is subjected to five basic loads:

1. Gravity
2. LHe liquid head
3. Thermal contraction
4. Tuner extension
5. Pressure (internal and external)

Three of these loads – gravity, liquid head, and pressure – produce both primary and secondary stresses. The remaining loads – thermal contraction and tuner extension – are displacement-controlled loads which produce secondary stresses only. This results in five load cases. These load cases are shown in Table 9, along with the temperatures at which the resulting stresses were assessed, and the stress categories that were applied.

Table 9. Load Cases

Load Case	Loads	Condition Simulated	Temperature for Stress Assessme	Applicable Stress Categories
1	1. Gravity 2. $P_1 = 0.205$ MPa	Warm Pressurization	293 K	$P_m, P_1, P_1 + Q$
2	1. Gravity 2. LHe liquid head 3. $P_1 = 0.41$ MPa 4. $P_2 = P_3 = 0$	Cold operation, full, maximum pressure – no thermal contraction	1.88 K	$P_m, P_1, P_1 + Q$
3	1. Cool down to 1.88 K 2. Tuner extension of 1.5	Cool down and tuner extension, no primary loads	1.88 K	Q
4	1. Gravity 2. LHe liquid head 3. Cool down to 1.88 K 4. Tuner extension of 1.5mm 5. $P_1 = 0.41$ MPa 6. $P_2 = P_3 = 0$	Cold operation, full LHe inventory, maximum pressure – primary and secondary loads	1.88 K	Q
5	1. Gravity 2. $P_1 = 0$ 3. $P_2 = P_3 = 0.205$ MPa	Insulating and beam vacuum upset, helium volume evacuated	293 K	$P_m, P_1, P_1 + Q$

### *Stress Analysis Approach*

The goal of the analysis is to qualify the vessel to the greatest extent possible in accordance with the rules of the Code, Section VIII, Div. 1. This Division of the Code provides rules covering many cases; however, there are features of this cavity and its loadings for which the Division has no rules. This does not mean that the vessel cannot be qualified by Div. 1, since Div. 1 explicitly acknowledges the fact that it does not prevent formulaic procedures (“rules”) covering all design possibilities. From U-2(g)

“This Division of Section VIII does not contain rules to cover all details of design and construction. Where complete details are not given, it is intended that the Manufacturer, subject to the acceptance of the Inspector, shall provide details of design and construction which will be as safe as those provided by the rules of this Division.”

### Applying Division I Rules to the Cavity

Division 1 rules relate to both geometries and loads. For either, there are few rules applicable to the features of the cavity.

The only components of the cavity which can be designed for internal and external pressure by the rules of Div. 1 are the Ti shells and the Ti bellows. In the Ti shell, there are two penetrations for connection of externals for which the required reinforcement can also be determined by Code rules.

The conical heads have half-apex angles exceeding 30 degrees, and no knuckles; Div. 1, Appendix 1, 1-5(g) states that their geometry falls under U-2(g).

The Nb cavity itself resembles an expansion joint, but does not conform to the geometries covered in Div. 1, Appendix 26. Therefore, U-2(g) is again applied.

UG-22(h) states that “temperature gradients and differential thermal contractions” are to be considered in vessel design, but provides no rules to cover the cavity. In this analysis, all thermal contraction effects are addressed under U-2(g).

The cavity is also subjected to a controlled displacement loading from blade tuner. There are no rules in Div. 1 covering such a loading, so U-2(g) is applied.

The applicable Code rules for each component are summarized in Table

10

Table 10. Applicable Code, Div. 1 Rules for 1.3 GHz Cavity

Component	Loading		
	Internal/External Pressure	Thermal Contraction	Tuner Extension
Nb cavity	U-2(g)	U-2(g)	U-2(g)
Conical heads	U-2(g)	U-2(g)	U-2(g)
Ti shells	UG-27/UG-28	U-2(g)	U-2(g)
Ti bellows	Appendix 26	U-2(g)	U-2(g)

Applying U-2(g)

U-2(g) is satisfied in this analysis by the application of the design-by-analysis rules of the Code, Section VIII, Div. 2, Part 5.

These rules provide protection against plastic collapse, local failure, buckling, fatigue, and ratcheting. The specific sections of Part 5 applied here are:

1. Plastic collapse – satisfied by an elastic stress analysis performed according to 5.2.2.
2. Ratcheting - satisfied by an elastic stress analysis performed according to 5.5.6.1
3. Local failure – satisfied by an elastic stress analysis performed according to 5.3.2
4. Buckling – satisfied by a linear buckling analysis performed according to 5.4.1.2(a).
5. Fatigue assessment – the need for a fatigue analysis is assessed according to 5.5.2.3

In general, an elastic stress analysis begins by establishing stress classification lines (SCLs) through critical sections in the structures according to the procedures of Part 5, Annex 5A, so they are chosen near the discontinuities and are through the thickness of the part. The stresses along these lines are then calculated (in this case, by an FEA), and “linearized” to produce statically equivalent membrane stress and bending stress components. The allowable stress for each component depends on the category of the stress. This category (or classification) depends on the location of the SCL in the structure, and the origin of the load. Stresses near discontinuities have higher allowables to reflect their ability to redistribute small amounts of plasticity into surrounding elastic material. Stresses produced solely by strain-controlled loads (e.g., thermal contractions and blade tuner extension) are given higher allowables regardless of their location in the structure.

Allowable stresses are expressed in terms of multiples of S, which is the allowable general primary membrane stress. The values of S used in this analysis are given in Table 8.



*Division 1 Calculations by Rule*

Ti Cylindrical Shells

*Thickness for Internal Pressure*

The minimum thickness required for the Ti cylindrical shells under internal pressure can be calculated from UG-27(c)(1):

$$t = \frac{P \cdot R}{S \cdot E - 0.6 \cdot P}$$

Where:

- t = required thickness
- P = pressure = 0.205 MPa (warm), 0.41 MPa (cold)
- R = inside radius of the shell = 115 mm
- E = efficiency of seam weld (Type 3 TIG weld: one sided butt weld, no radiography) = 0.6
- S = maximum allowable membrane stress = 79 MPa (warm), 255 MPa (cold)

Substituting, the minimum required thickness when warm and pressurized to 0.205 MPa is 0.49 mm. The minimum required thickness when cold and pressurized to 0.41 MPa is 0.31 mm. The actual minimum thickness of the shells is 2.5 mm (0.098 in). Therefore, the Ti cylindrical shells meet the minimum thickness requirements of UG-27 for internal pressure.

*Thickness for External Pressure (Buckling)*

The minimum thickness required for the Ti cylindrical shells under external pressure can be calculated from UG-28(c). This procedure uses charts found in the Code, Section II, Part D. These charts are based on the geometric and material characteristics of the vessel.

Using: L = 965 mm  
 D<sub>o</sub> = 230 mm  
 t = 1.4 mm

Then: L/D = 2.2  
 D<sub>o</sub>/t = 165

From the Code, Section II, Part D, Subpart 3, Figure G, the factor A is 0.0003..

The allowable pressure is then

$$P = \frac{2}{3} \cdot A \cdot E_m \cdot \frac{t}{D} = 0.11 \text{ MPa}$$

Where E<sub>m</sub> is the Young modulus of Titanium (107 GPa) and the other parameter have already been introduced.

Substituting give  $P = 0.11$  MPa. This is approximately equal to the 0.105 MPa maximum external vessel for which the vessel must be qualified.

The actual minimum thickness of the Ti shell is 2.5 mm. This occurs near the ends, and it is unlikely that the collapse is well predicted by this thickness, due to its short length, and proximity to the conical head, which will tend to stiffen the region. If we assume, however, that the entire shell is this thickness, and repeat the calculations above, the allowable external pressure is 0.23 MPa.

If we assume the collapse is better predicted by the predominant thickness of 5 mm, then the factor  $A = 0.0009$ , and the allowable external pressure is 0.7MPa.

In any case, the required minimum thickness of 1.4 mm is less than the actual minimum thickness anywhere on the Ti cylindrical shell. Therefore, the Ti shell satisfies the Code requirement for external pressure.

### Penetrations

The Ti cylindrical shell contains three penetrations two of which have the same diameter. These are shown in [Figure 17](#). The largest of these penetrations is 2.16 inches (54.8 mm) in diameter.

From UG-36(c)(3):

“Openings in vessels not subject to rapid fluctuations in pressure do not require reinforcement other than inherent in the construction under the following conditions: welded, brazed, and flued connections meeting applicable rules and with a finished opening not larger than 3.5 in diameter – in vessel shells or heads with a required minimum thickness of 3/8 inch or less.”

The minimum required thickness of the shell is largest for the case of 0.205 MPa pressurization (warm). This thickness (calculated in 7.1.1) is 0.49 mm. This is less than 9 mm (3/8 in). The two smaller penetrations have a diameter of 16 mm (0.63 in.) which is smaller than 3.5 in. therefore no additional reinforcement is required for these penetrations. However the largest penetration has a diameter of 95.5 mm (3.76 in.) so for this penetration we need further calculations to see if the reinforcement is needed or not.

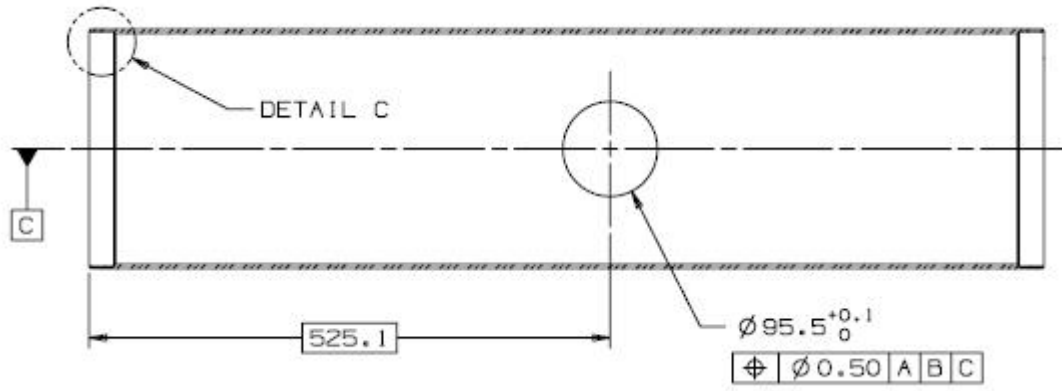


Figure 20. Largest penetration in the Ti shell

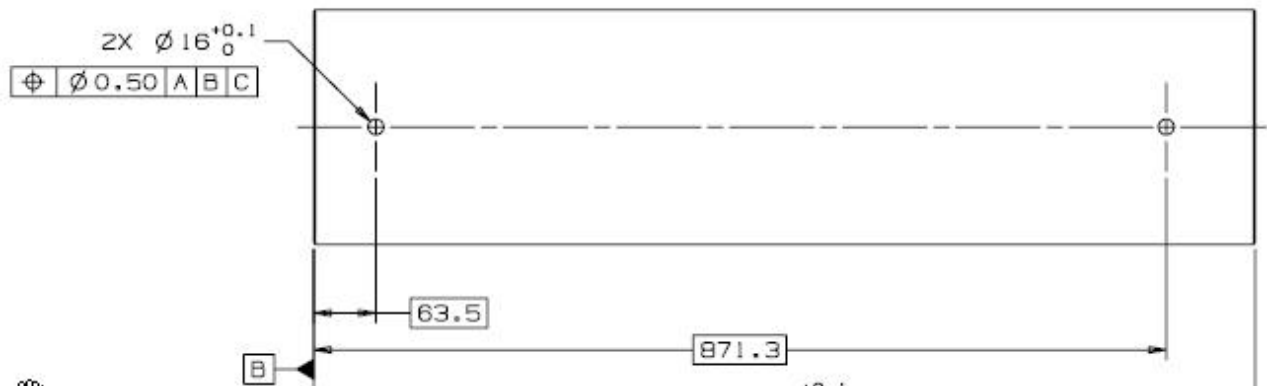


Figure 21. Smaller penetrations in the Ti shell

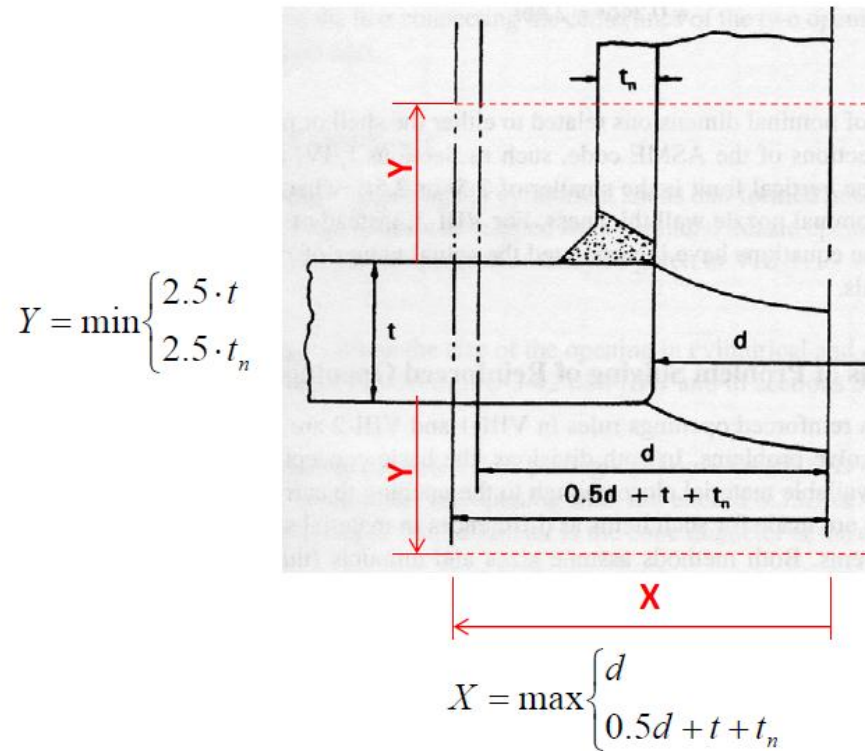


Figure 22. Definitions of the parameters X and Y for the calculation of the reinforcement

From the definitions given by Figure 22 we can write:

- $X = d = 95.5 \text{ mm}$
- $Y = 2.5 t = 12.5 \text{ mm}$

We can now calculate the other parameters introduced in Figure 23:

- $d = \text{diameter of the nozzle} = 95.5 \text{ mm}$
- $t = \text{thickness of the vessel} = 5 \text{ mm}$
- $t_n = \text{thickness of the nozzle} = 1.65 \text{ mm}$
- $t_r = \text{minimum required thickness of the vessel} = 0.49 \text{ mm}$
- $t_m = \text{minimum required thickness of the nozzle} = 0.25 \text{ mm}$

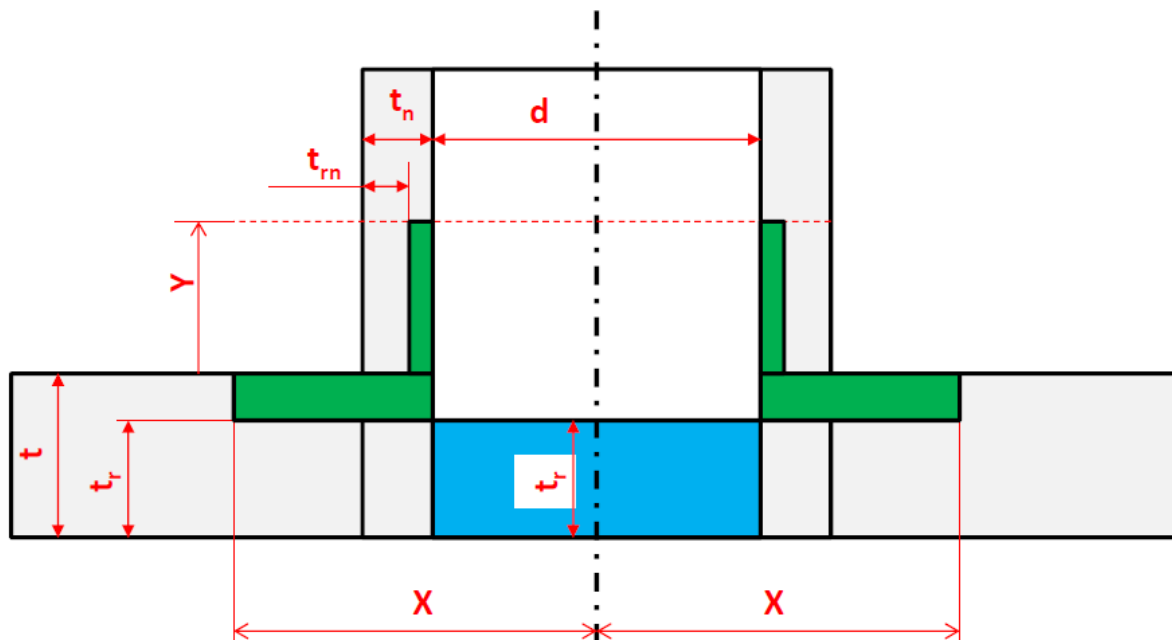


Figure 23. Parameters to determine the Available Area and the Requested Area for the reinforcement

Requested Area:

$$A_r = d \cdot t_r = 48.2 \text{ mm}^2$$

Vessel Available Area:

$$A_1 = (2 \cdot X - d) \cdot (t - t_r) = d \cdot (t - t_r) = 433 \text{ mm}^2$$

Nozzle Available Area:

$$A_2 = 2 \cdot Y \cdot (t_n - t_{rn}) = 5 \cdot t \cdot (t_n - t_{rn}) = 35 \text{ mm}^2$$

Since the Requested Area is smaller than the total Available Area the reinforcement is not needed neither for the dual phase opening.

Ti Bellows

The design of metallic expansion joints (e.g., bellows) is addressed by Appendix 26 of the Code. The formulas permit calculation of internal and external pressure limits. In a bellows, the pressure may be limited not only by stress, but by squirm (internal pressure), and collapse (external pressure.) The analysis shows that the bellows with an internal MAWP of 2.0-bar (30-psi) at room temperature or an external MAWP of 1.0-bar (14.5-psia) follows the rules of Appendix 26. The allowed value S is for titanium at room temperature (see Table 7).

Table 11 defines the stresses that are examined in the bellows analysis. Table 12 summarizes how the calculated or actual stresses comply with the allowed stresses.

The details of the Appendix 26 calculations are presented in Appendix C.

**Table 11. Definition of Stresses, Coefficients in the Bellows Analysis, following the Code, Division 1, Appendix 26.**

		Units
S1	Circumferential membrane stress in bellows tangent, due to pressure P	psi
S2e	Circumferential membrane stress due to pressure P for end convolutions	psi
S2i	Circumferential membrane stress due to pressure P for end convolutions	psi
S11	Circumferential membrane stress due to pressure P for the collar	psi
S3	Meridional membrane stress due to pressure P	psi
S4	Meridional bending stress due to pressure P	psi
P	Design pressure	psi
S	Allowable stress of bellows material	psi
Cwc	Weld joint efficiency of collar to bellows (no radiography, single butt weld)	--
Sc	Allowable stress of collar material	psi
Kf	Coefficient for formed bellows	--
Psc	Allowable internal pressure to avoid column instability	psi
Psi	Allowable internal pressure based on in-plane instability	psi
Pa	Allowable external pressure based on instability	psi

**Table 12. Complying with Appendix 26 Rules for Internal Pressure of 2.0-bar (30-psi)**

Calculated or Actual	Allowed Value	Requirement	Applicable Paragraph
S1 = 428 psi	S = 11500 psi	$S1 < S$	26-6.3.1
S11 = 441 psi	$Cwc * Sc = 6900$ psi	$S11 < Cwc * Sc$	26-6.3.2
S2e = 995 psi	S = 11500 psi	$S2e < S$	26-6.3.3(a)(1)
S2i = 5545 psi	S = 11500 psi	$S2i < S$	26-6.3.3(a)(2)
$S3 + S4 = 4275$ psi	$Kf * S = 34500$ psi	$(S3 + S4) < (Kf * S)$	26-6.3.3(d)
P = 30 psi	$Psc = 64760000$ psi	$P \leq Psc$	26-6.4.1
P = 30 psi	Psi = 198 psi	$P \leq Psi$	26-6.4.2
External pressure = 14.5 psia	Pa = 1077 psi	Ext. pressure < Pa	26-6.5

#### Longitudinal Weld in Bellows Convolution

The allowable stress  $S = 79 \text{ MPa}$  for the bellows convolution assumes a weld joint efficiency of 1.0. The bellows is hydro formed from a rolled tube with a longitudinal (seam) weld that is not radiographed. Let's evaluate the weld by de-rating the allowable stress  $S$  by a factor of 0.6, which is the factor for a Type 3 weld that is not radiographed. The de-rated allowable stress is  $79 \text{ MPa} \cdot 0.6 = 47.4 \text{ MPa}$ . This is still greater than the calculated circumferential stresses of  $S_1$ ,  $S_{2e}$ , and  $S_{2i}$  in the convolutions.

#### Fatigue Analysis for Titanium Bellows

The equations in the Code for fatigue analysis of a bellows are not valid for titanium. The manufacturer of the titanium bellows for the helium vessel provided design calculations following the Standards of the Expansion Joint Manufacturers Association <sup>(7)</sup>. The allowable fatigue life is calculated with the equation

$$N_c = \left( \frac{c}{S_T - b} \right)^a$$

where  $a$ ,  $b$ , and  $c$  are material and manufacturing constants. The manufacturer uses the same material and manufacturing constants as what EJMA uses for austenitic stainless steel. In addition, the manufacturer includes a safety factor of two in their calculation of the allowable number of cycles since the titanium bellows is a custom-made project. The manufacturer calculated an allowable number of cycles to be  $N_C = 375600$ .

The slow tuner system has the capability of increasing the vessel length less than 2.0-mm after each cool down. The bellows extension will occur 200 times over the lifetime of the vessel. This is far less than the allowable number of cycles, so the bellows is designed well within the limits of fatigue failure.

Detailed Code calculations are shown in the section Fatigue Analysis of the Titanium Bellows at Pag 78.

### Finite Element Model

A 3-d finite element half model was created in ANSYS. Elements were 10-node tetrahedra, and 20-node hexahedra. Material behavior was linear elastic.

The lever tuner is very rigid. Axial constraint of the helium vessel was therefore simulated by constraining the outer surface of each flange in the Z (axial) direction. This constraint places the line of action at a maximum distance from the shell, producing the maximum possible moment on the welds between the Ti blade tuner flanges and the shell.

For the cool down loading, the distance between the Ti flanges was assumed to close by an amount equivalent to the shrinkage of a rigid stainless steel mass spanning the flanges.

The constraint against gravity is simulated by fixing the flange outer surface nodes at 180 degrees in the Y (vertical) direction.

The finite element model is shown in Figure 24. Figure 25 shows the mesh detail at various locations within the model.

The complete model was used to demonstrate satisfaction of the plastic collapse, ratcheting, and local failure criteria. Subsets of the model were also used to address the linear buckling of the Nb cavity and conical head.

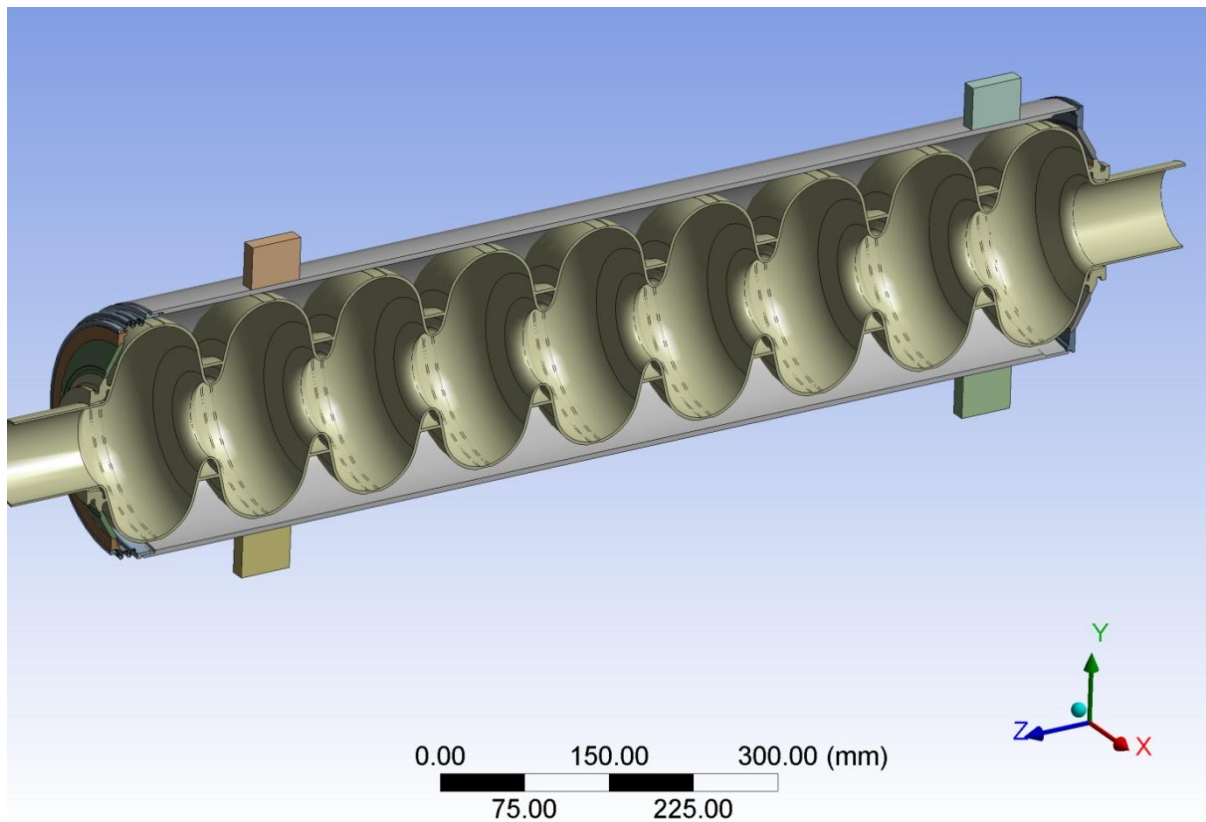


Figure 24. The Finite Element Model



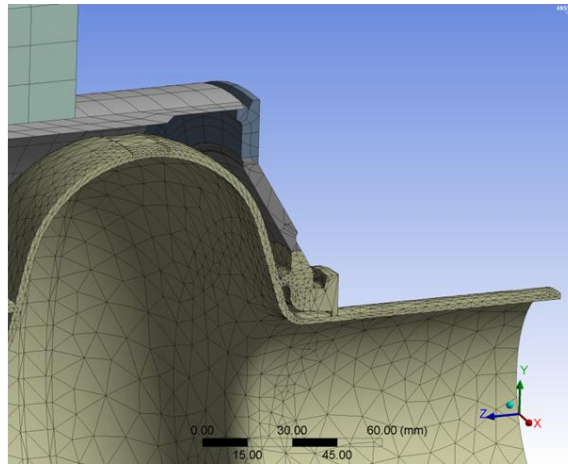
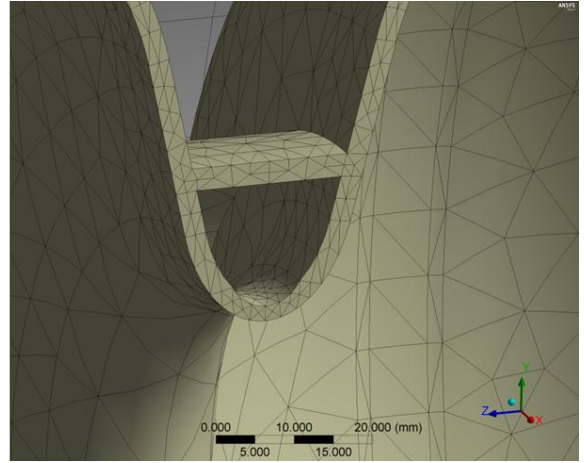
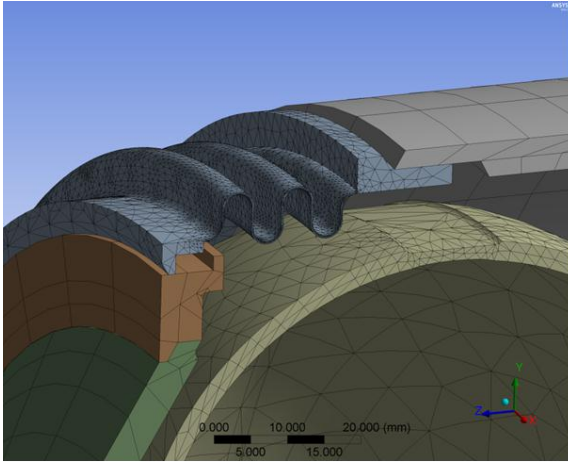


Figure 25. Mesh Details

## *Stress Analysis Results*

### General

The complete finite element model was run for the five load cases. Stress classification lines, shown in Figure 26, were established through the critical sections of the structure. The stresses along these lines were linearized with ANSYS, and separated into membrane and bending components. The linearized stresses (expressed in terms of Von Mises equivalent stress, as required by 5.2.2.1(b)) are categorized according to the Code, Div. 2, Part 5, 5.2.2.2 into primary and secondary stresses.

The primary and secondary stresses along each SCL for each of the five load cases are given from Table 13 to Table 17. Where more than one weld of a given number is present (as indicated in Figure 13 and in Figure 14) the weld with the highest stresses was assessed.

The stresses from Table 13 to Table 17 are used to demonstrate satisfaction of two of the criteria listed in the Stress Analysis Approach of this report: Protection against plastic collapse, and protection against ratcheting. Demonstrating protection against local failure employs the complete model, but requires the extraction of different quantities.

Note: The required minimum thicknesses of the Ti shells for internal and external pressure are calculated by Div. 1 rules in the section Division 1 Calculations by Rule of this report. Therefore, no SCLs addressing the Ti shell thickness far from welds or other discontinuities are established here. See the Appendix B for verification that the FEA produces the correct hoop stress in the Ti shell.

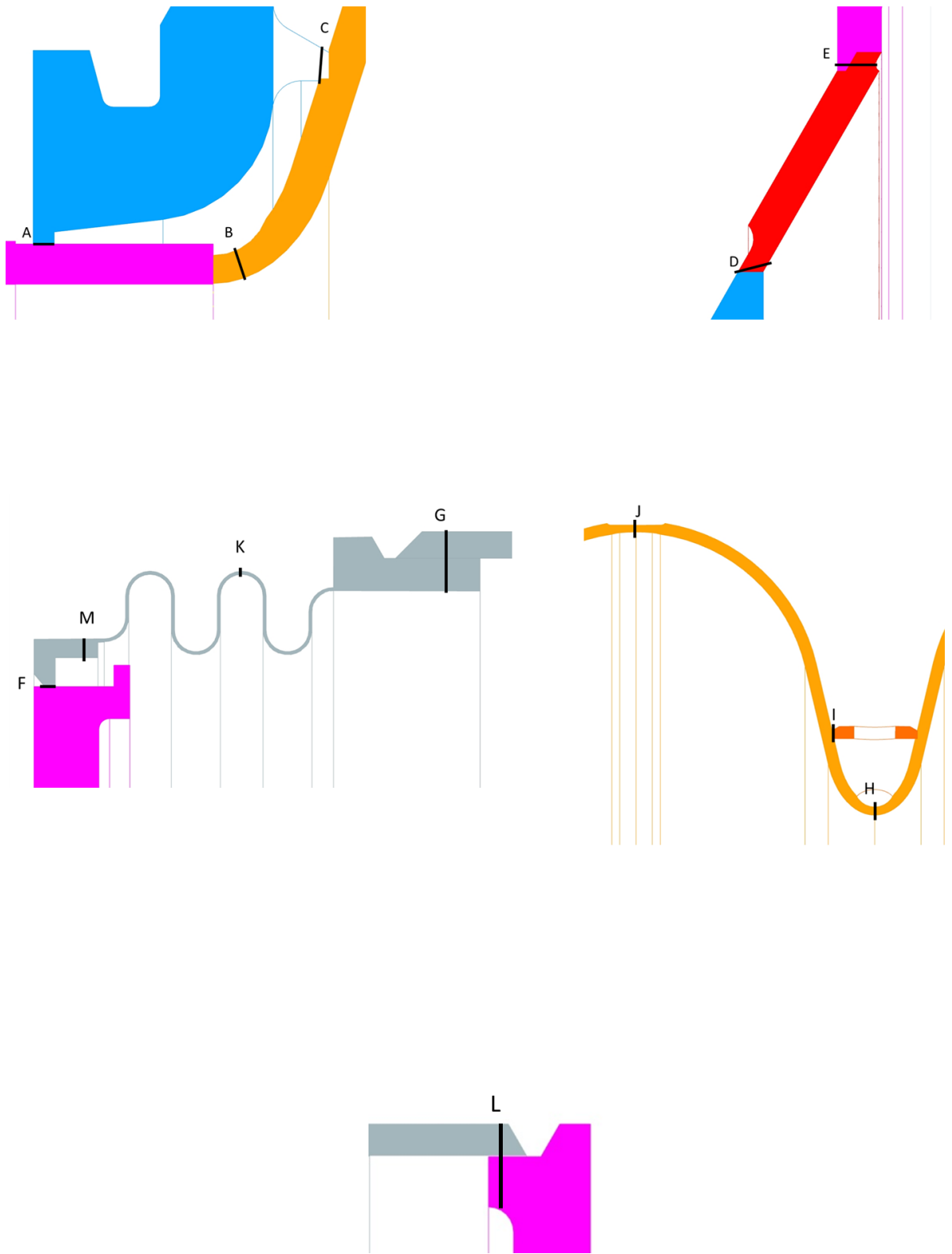


Figure 26. Stress Classification Lines

Table 13. Load Case 1 - Stress Results

Material	SCL	Weld #	Weld Efficiency	Membrane Stress [MPa]	Classification	Allowable Stress [MPa]	Ratio
Nb weld	A	FP1	0.6	1.51	Pm	12	0.12
Nb weld	B	FP2	0.7	1.59	Pl	21	0.07
Nb weld	C	FP3	0.6	2.83	Pm	12	0.23
Nb weld to NbTi	D	MC4	0.6	3.19	Pm	12	0.26
Ti weld to NbTi	E	MC5	0.7	3.5	Pm	55	0.06
Ti weld	F	FP6	0.6	1.62	Pm	47	0.03
Ti weld	G	FP7	0.7	8.22	Pm	55	0.15
Nb weld	H	11	0.6	5.43	Pm	12	0.45
Nb weld	I	9	0.6	3.77	Pm	12	0.31
Nb weld	J	10	0.6	3.41	Pm	12	0.28
Ti	K	--	1	27.14	Pm	79	0.34
Ti weld	L	MC12	0.7	12.37	Pm	55	0.22
Ti weld	M	8	0.6	3.67	Pm	47	0.08
Material	SCL	Weld #	Weld Efficiency	Membrane + Bending [MPa]	Classification	Allowable Stress [MPa]	Ratio
Nb weld	A	FP1	0.6	3.76	Pm+Pb	18	0.21
Nb weld	B	FP2	0.7	2.17	Pl+Q	43	0.05
Nb weld	C	MC3	0.6	17.78	Q	36	0.49
Nb weld to NbTi	D	MC4	0.6	10.08	Pm+Pb	18	0.55
Ti weld to NbTi	E	MC5	0.7	20.18	Pm+Pb	83	0.24
Ti weld	F	FP6	0.6	1.14	Pm+Pb	71	0.02
Ti weld	G	FP7	0.7	10.19	Pm+Pb	83	0.12
Nb weld	H	11	0.6	5.6	Pm+Pb	18	0.31
Nb weld	I	9	0.6	4.5	Q	36	0.12
Nb weld	J	10	0.6	4.72	Pm+Pb	18	0.26
Ti	K	--	1	42.43	Pm+Pb	118	0.36
Ti weld	L	MC12	0.7	12.97	Pm+Pb	83	0.16
Ti weld	M	8	0.6	5.49	Pm+Pb	71	0.08

Table 14. Load Case 2 - Stress Results

Material	SCL	Weld #	Weld Efficiency	Membrane Stress [MPa]	Classification	Allowable Stress [MPa]	Ratio
Nb weld	A	FP1	0.6	3.31	Pm	82	0.04
Nb weld	B	FP2	0.7	3.59	Pl	144	0.02
Nb weld	C	FP3	0.6	5.22	Pm	82	0.06
Nb weld to NbTi	D	MC4	0.6	6.62	Pm	75	0.09
Ti weld to NbTi	E	MC5	0.7	7.39	Pm	87	0.08
Ti weld	F	FP6	0.6	3.17	Pm	153	0.02
Ti weld	G	FP7	0.7	16.43	Pm	179	0.09
Nb weld	H	11	0.6	10.53	Pm	82	0.13
Nb weld	I	9	0.6	7.31	Pm	82	0.09
Nb weld	J	10	0.6	6.8	Pm	82	0.08
Ti	K	--	1	54.07	Pm	255	0.21
Ti weld	L	MC12	0.7	25.67	Pm	179	0.14
Ti weld	M	8	0.6	7.02	Pm	153	0.05
Material	SCL	Weld #	Weld Efficiency	Membrane + Bending [MPa]	Classification	Allowable Stress [MPa]	Ratio
Nb weld	A	FP1	0.6	7.92	Pm+Pb	123	0.06
Nb weld	B	FP2	0.7	4.82	Pl+Q	288	0.02
Nb weld	C	MC3	0.6	33.42	Q	247	0.14
Nb weld to NbTi	D	MC4	0.6	20.37	Pm+Pb	112	0.18
Ti weld to NbTi	E	MC5	0.7	41.47	Pm+Pb	131	0.32
Ti weld	F	FP6	0.6	4.32	Pm+Pb	230	0.02
Ti weld	G	FP7	0.7	21	Pm+Pb	268	0.08
Nb weld	H	11	0.6	10.86	Pm+Pb	123	0.09
Nb weld	I	9	0.6	9.85	Q	247	0.04
Nb weld	J	10	0.6	9.22	Pm+Pb	123	0.07
Ti	K	--	1	83.03	Pm+Pb	383	0.22
Ti weld	L	MC12	0.7	26.91	Pm+Pb	268	0.10
Ti weld	M	8	0.6	10.78	Pm+Pb	230	0.05

Table 15. Load Case 3 - Stress results

Material	SCL	Weld #	Weld Efficiency	Membrane Stress [MPa]	Classification	Allowable Stress [MPa]	Ratio
Nb weld	A	FP1	0.6	11.79	Pm	82	0.14
Nb weld	B	FP2	0.7	3.75	Pl	144	0.03
Nb weld	C	MC3	0.6	29.74	Pm	82	0.36
Nb weld to NbTi	D	MC4	0.6	37.06	Pm	75	0.50
Ti weld to NbTi	E	MC5	0.7	22.74	Pm	87	0.26
Ti weld	F	FP6	0.6	17.71	Pm	153	0.12
Ti weld	G	FP7	0.7	2.38	Pm	179	0.01
Nb weld	H	11	0.6	15.95	Pm	82	0.19
Nb weld	I	9	0.6	29.48	Pm	82	0.36
Nb weld	J	10	0.6	13.31	Pm	82	0.16
Ti	K	--	1	57.81	Pm	255	0.23
Ti weld	L	MC12	0.7	22.83	Pm	179	0.13
Ti weld	M	8	0.6	19.14	Pm	153	0.12
Material	SCL	Weld #	Weld Efficiency	Membrane + Bending [MPa]	Classification	Allowable Stress [MPa]	Ratio
Nb weld	A	FP1	0.6	14.34	Q	247	0.06
Nb weld	B	FP2	0.7	5.3	Q	288	0.02
Nb weld	C	MC3	0.6	51.11	Q	247	0.21
Nb weld to NbTi	D	MC4	0.6	45.91	Q	224	0.20
Ti weld to NbTi	E	MC5	0.7	59.69	Q	262	0.23
Ti weld	F	FP6	0.6	17.85	Q	460	0.04
Ti weld	G	FP7	0.7	23.91	Q	536	0.04
Nb weld	H	11	0.6	20.54	Q	247	0.08
Nb weld	I	9	0.6	42.69	Q	247	0.17
Nb weld	J	10	0.6	16.28	Q	247	0.07
Ti	K	--	1	509.66	Q	766	0.67
Ti weld	L	MC12	0.7	23.73	Q	536	0.04
Ti weld	M	8	0.6	19.87	Q	460	0.04

Table 16. Load Case 4 - Stress Results

Material	SCL	Weld #	Weld Efficiency	Membrane Stress [MPa]	Classification	Allowable Stress [MPa]	Ratio
Nb weld	A	FP1	0.6	11.05	Pm	82	0.13
Nb weld	B	MC2	0.7	1.79	Pl	144	0.01
Nb weld	C	MC3	0.6	28.6	Pm	82	0.35
Nb weld to NbTi	D	FP4	0.6	35.43	Pm	75	0.47
Ti weld to NbTi	E	FP5	0.7	20.99	Pm	87	0.24
Ti weld	F	FP6	0.6	17.61	Pm	153	0.11
Ti weld	G	FP7	0.7	14.35	Pm	179	0.08
Nb weld	H	11	0.6	5.71	Pm	82	0.07
Nb weld	I	9	0.6	30.06	Pm	82	0.37
Nb weld	J	10	0.6	14.76	Pm	82	0.18
Ti	K	--	1	6.65	Pm	255	0.03
Ti weld	L	MC12	0.7	2.89	Pm	179	0.02
Ti weld	M	8	0.6	12.42	Pm	153	0.08

Material	SCL	Weld #	Weld Efficiency	Membrane + Bending [MPa]	Classification	Allowable Stress [MPa]	Ratio
Nb weld	A	FP1	0.6	12.76	Q	247	0.05
Nb weld	B	FP2	0.7	2.64	Q	288	0.01
Nb weld	C	MC3	0.6	72.99	Q	247	0.30
Nb weld to NbTi	D	FP4	0.6	42.59	Q	224	0.19
Ti weld to NbTi	E	MC5	0.7	53.81	Q	262	0.21
Ti weld	F	FP6	0.6	17.91	Q	460	0.04
Ti weld	G	FP7	0.7	31.53	Q	536	0.06
Nb weld	H	11	0.6	13.38	Q	247	0.05
Nb weld	I	9	0.6	48.95	Q	247	0.20
Nb weld	J	10	0.6	14.95	Q	247	0.06
Ti	K	--	1	561.03	Q	766	0.73
Ti weld	L	MC12	0.7	3.17	Q	536	0.01
Ti weld	M	8	0.6	12.93	Q	460	0.03

Table 17. Load Case 5 - Stress Results

Material	SCL	Weld #	Weld Efficiency	Membrane Stress [MPa]	Classification	Allowable Stress [MPa]	Ratio
Nb weld	A	FP1	0.6	1.47	Pm	12	0.12
Nb weld	B	FP2	0.7	1.4	Pl	21	0.07
Nb weld	C	MC3	0.6	2.72	Pm	12	0.22
Nb weld to NbTi	D	MC4	0.6	2.11	Pm	12	0.17
Ti weld to NbTi	E	MC5	0.7	2.23	Pm	55	0.04
Ti weld	F	FP6	0.6	0.82	Pm	47	0.02
Ti weld	G	FP7	0.7	3.11	Pm	55	0.06
Nb weld	H	11	0.6	2.24	Pm	12	0.18
Nb weld	I	9	0.6	2.29	Pm	12	0.19
Nb weld	J	10	0.6	1.74	Pm	12	0.14
Ti	K	--	1	13.3	Pm	79	0.17
Ti weld	L	MC12	0.7	7.28	Pm	55	0.13
Ti weld	M	8	0.6	1.63	Pm	47	0.03
Material	SCL	Weld #	Weld Efficiency	Membrane + Bending [MPa]	Classification	Allowable Stress [MPa]	Ratio
Nb weld	A	FP1	0.6	2.84	Pm+Pb	18	0.16
Nb weld	B	FP2	0.7	1.84	Pl+Q	43	0.04
Nb weld	C	MC3	0.6	6.04	Q	36	0.17
Nb weld to NbTi	D	MC4	0.6	5.24	Pm+Pb	18	0.29
Ti weld to NbTi	E	MC5	0.7	11.44	Pm+Pb	83	0.14
Ti weld	F	FP6	0.6	1.09	Pm+Pb	71	0.02
Ti weld	G	FP7	0.7	4.98	Pm+Pb	83	0.06
Nb weld	H	11	0.6	2.38	Pm+Pb	18	0.13
Nb weld	I	9	0.6	4.15	Q	36	0.11
Nb weld	J	10	0.6	2.09	Pm+Pb	18	0.11
Ti	K	--	1	18.36	Pm+Pb	118	0.16
Ti weld	L	MC12	0.7	7.62	Pm+Pb	83	0.09
Ti weld	M	8	0.6	2.62	Pm+Pb	71	0.04



### Collapse Pressure

The criterion for protection against plastic collapse is given in Div. 2, 5.2.2. The criterion is applied to load cases in which primary (load-controlled) stresses are produced. For this analysis, this is Load Case 1, Load Case 2, and Load Case 5.

The following stress limits must be met (per 5.2.2.4(e)):

1.  $P_m = \text{primary membrane stress} \leq S$
2.  $P_l = \text{primary local membrane stress} \leq 1.5 \cdot S$
3.  $P_l + P_b = \text{primary local membrane} + \text{primary bending} \leq 1.5 \cdot S$

where  $S$  = maximum allowable primary membrane stress.

In this work, the  $P_l$  classification is limited to SCL B (weld 2). All other membrane stresses extracted on the SCLs are classified as the more conservative  $P_m$ , which is then used in place of  $P_l$  in 3 above.

Examining Table 13, Table 14 and Table 17, it is found that the closest approach to the limiting stress for any load case occurs at SCL D (weld #4, the weld between the end disk flange and the transition ring) in Load Case 1, where the primary membrane stress plus the primary bending stress of 10.1 MPa psi compares to an allowable of 18 MPa.

### Ratcheting

Protection against ratcheting, the progressive distortion of a component under repeated loadings, is provided by meeting the requirements of Div. 2, 5.5.6. Specifically, the following limit must be satisfied:

$$\Delta S_{n,k} \leq S_{PS}$$

where:

- $\Delta S_{n,k} = \text{primary plus secondary equivalent stress range}$
- $S_{PS} = \text{allowable limit on primary plus secondary stress range}$

The stress range  $\Delta S_{n,k}$  must take into account stress reversals; however, there are no stress reversals in normal operation of the cavity, so for this analysis  $\Delta S_{n,k}$  is equal to the primary plus secondary stresses given in the tables from Table 13 to Table 17.

Examination of the tables shows that the cavity satisfies the ratcheting criterion; the closest approach to the allowable primary plus secondary stress range limit occurs for Load Case 4 (*gravity + liquid head + 0.4 MPa + blade tuner extension + cool down*) in the Ti bellows. For this load case, the calculated primary plus secondary stress range reaches 73% of the allowable.

Local Failure

The criterion for protection against local failure is given in Div. 2, 5.3.2:

$$\sigma_1 + \sigma_2 + \sigma_3 \leq 4 \cdot S$$

where  $\sigma_1, \sigma_2, \sigma_3$  are the principal stresses at any point in the structure, and  $S$  is the maximum allowable primary membrane stress (see Table 8), multiplied by a joint efficiency factor if applicable.

This criterion is assumed to be satisfied if the sum of the principal stresses calculated at every element centroid in the model meets the stress limit for the material.

Table 18 lists the maximum allowable sum of principal stresses for each material at each load case. These values are four times the full values given for maximum primary membrane stress times a joint efficiency for a Type 3 butt weld of 0.6. For those locations which are not near a joint, or are near one of the Type 2 butt weld joints, this is conservative.

The results for each material and each load case are given in the Tables from Table 19 to Table 21. The closest approach to the allowable limit occurs in the iris support ring welds for Load Case 4 (cold, 0.41 MPa internal pressure, tuner extension), which reaches 0.94 of the allowable. For all other materials/load cases, the principal stress sum lies below the allowable.

Table 18. Maximum Allowable Sum of Principal Stresses

Load Case (Temp)	Maximum Allowable Sum of Principal Stresses [MPa]		
	Nb	TiNb	Ti
1 (293 K)	48	300	190
2 (1.88 K)	329	300	612
3 (1.88 K)	329	300	612
4 (1.88 K)	329	300	612
5 (293 K)	48	300	190

Table 19. Local Failure Criterion - Niobium

Load Case	Maximum Principal Stress Sum (MPa)	Allowable Stress (MPa)	Location	Ratio $S_{fe}/S_a$
1	44	48	Weld #3	0.92
2	115	329	Weld #3	0.35
3	287	329	Weld #3	0.87
4	308	329	Weld #3	0.94

5	11	48	Weld #3	0.23
---	----	----	---------	------

Table 20. Local Failure Criterion - Ti-45Nb

Load Case	Maximum Principal Stress Sum (MPa)	Allowable Stress (MPa)	Location	Ratio S <sub>fe</sub> /S <sub>a</sub>
1	23	300	Weld #5	0.08
2	44	300	Weld #5	0.15
3	53	300	Weld #4	0.18
4	53	300	Weld #4	0.18
5	7	300	Weld #5	0.02

Table 21. Local Failure Criterion - TiGr2

Load Case	Maximum Principal Stress Sum (MPa)	Allowable Stress (MPa)	Location	Ratio S <sub>fe</sub> /S <sub>a</sub>
1	96	190	Bellows – SCL K	0.51
2	197	612	Bellows – SCL K	0.32
3	523	612	Bellows – SCL K	0.86
4	498	612	Bellows – SCL K	0.81
5	43	190	Bellows – SCL K	0.23

## Buckling

### *Ti Shells and Bellows*

The buckling of the Ti shells and bellows is addressed by Div. 1 rules in an earlier section of this report.

### *The Nb Cavity*

The Code, Div. 1, does not contain the necessary geometric and material information to perform a Div. 1 calculation of Nb cavity collapse. Therefore, the procedures of Div. 2, Part 5, 5.4 “Protection Against Collapse from Buckling” are applied.

A linear elastic buckling analysis was performed with ANSYS. A design factor was applied to the predicted collapse pressure to give the maximum allowable external working pressure. This design factor, taken from 5.4.1.3(c) for spherical shells, is 16. Only the cavity was modeled. The ends are constrained in all degrees of freedom to simulate the effect of attachment to the conical heads and Ti shells of the helium vessel.

The predicted buckled shape is shown in Figure 27. The critical pressure is 96.7 MPa. Applying the design factor gives this component a maximum allowable external working pressure of 6 MPa, which is far greater than the required MAWP of 0.1 MPa external.

The ANSYS buckling pressure seems large; as a check, a calculation of the collapse of a sphere of similar dimensions to those of a cell was done using a formula from Ref. 4. This calculation, given in Verification of ANSYS Results at pag.74 of this report, produces a similar result.

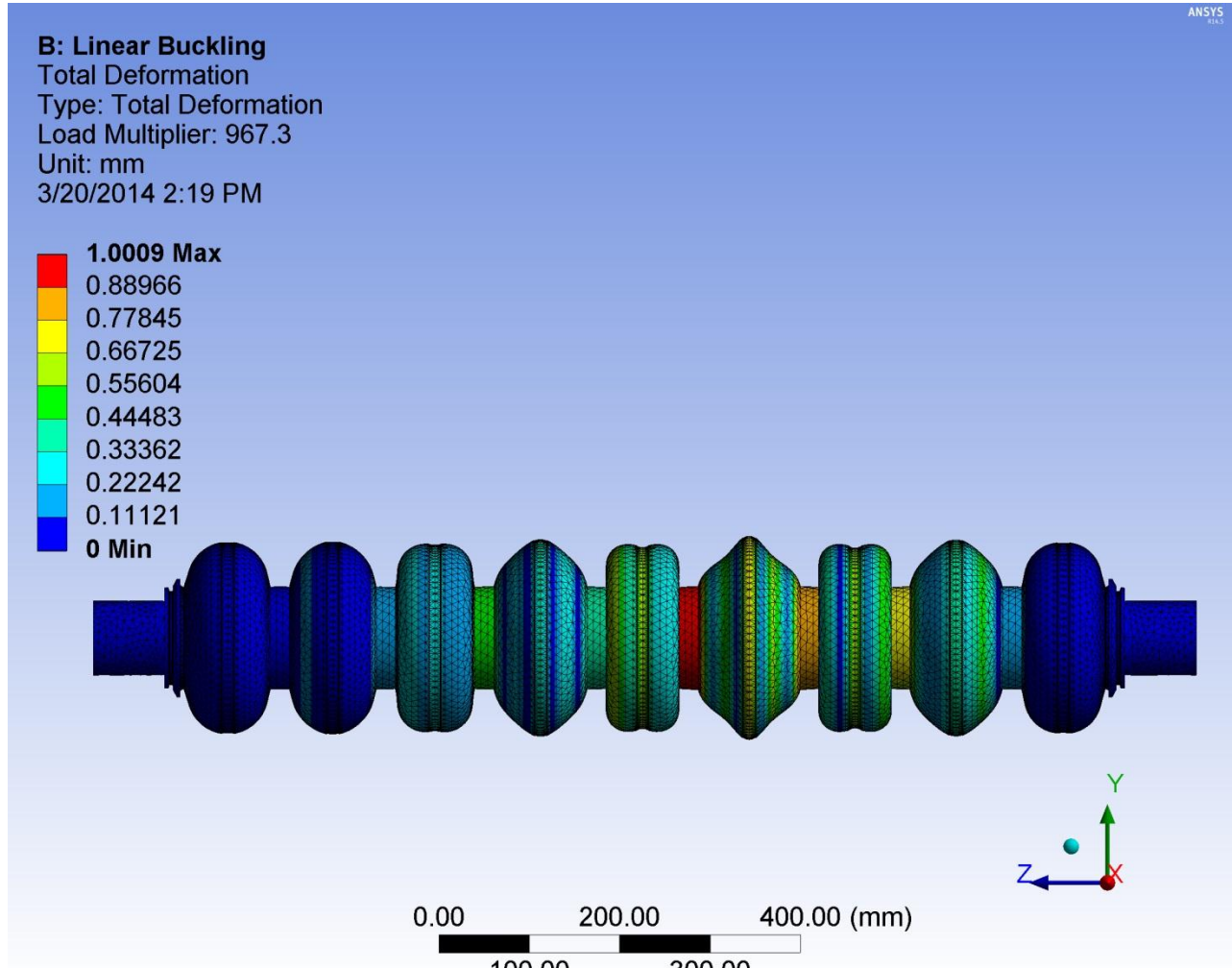


Figure 27. Lowest buckling mode of Nb Cavity ( $P_{cr} = 96.7$  MPa)

*Conical Heads*

The buckling pressure of the conical heads was calculated by the linear buckling approach used for the Nb cavity.

A model of the head only was made. It was constrained against axial motion where it connects to the Ti shell, but allowed to rotate freely, and translate radially.

The predicted buckling shape is shown in Figure 28. The critical buckling pressure is 358 MPa. Applying the design factor of 2.5 (from 5.4.1.3(b) for conical shells under external pressure) gives an MAWP for external pressure of 143 MPa, which is well above the actual maximum pressure of 0.1 MPa.

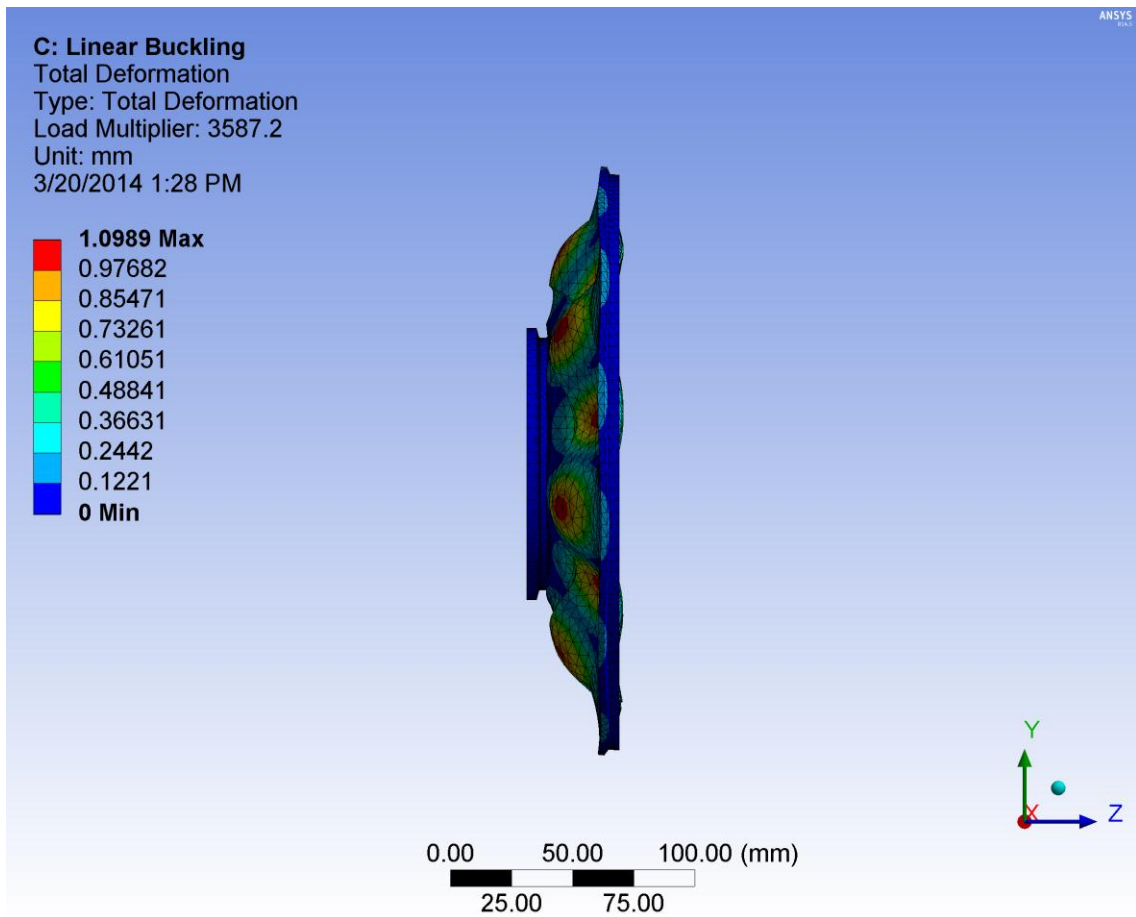


Figure 28. Buckling of the conical heads

Fatigue Assessment

The need for a fatigue analysis can be determined by applying the fatigue assessment procedures of Div. 2, Part 5, 5.5.2.3, "Fatigue Analysis Screening, Method A."

In this procedure, a load history is established which determines the number of cycles of each loading experienced by the Dressed SRF Cavity. These numbers are compared against criteria which determine whether a detailed fatigue analysis is necessary.

The load history consists of multiple cool down, pressurization, and tuning cycles. Estimates for the number of cycles of each load a cavity might experience are given in Table 22.

**Table 22. Estimated Load History of Dressed SRF Cavity**

<b>Loading</b>	<b>Designation</b>	<b>Number of Cycles</b>
<b>Cool down</b>	$N_{\Delta TE}$	<b>100</b>
<b>Pressurization</b>	$N_{\Delta FP}$	<b>200</b>
<b>Tuning</b>	$N_{\Delta tuner}$	<b>200</b>

The information of Table 22 is used with the criterion of Table 23 (a reproduction of Table 5.9 of Part 5 of the Code) to determine whether a fatigue analysis is necessary.

The tuning load has no direct analog to the cycle definitions of Table 23. Therefore, it will be assigned its own definition as a cyclic load ( $N_{\Delta tuner}$ ) and treated additively.

For the Nb cavity, construction is integral, and there are no attachments or nozzles in the knuckle regions of the heads. Therefore, the applicable criterion is

$$N_{\Delta TE} + N_{\Delta FP} + N_{\Delta tuner} \leq 1000$$

$$100 + 200 + 200 = 500 \leq 1000$$

The criterion is satisfied, and no fatigue assessment is necessary for the Nb cavity.

Table 23. Reproduction of Table 5.9 of Part 5, "Fatigue Screening Criteria for Method A"

Description	
<b>Attachments and nozzles in the knuckle region of formed heads</b>	$N_{\Delta FP} + N_{\Delta PO} + N_{\Delta TE} + N_{\Delta T\alpha} \leq 350$
<b>All other components that do not contain a flaw</b>	$N_{\Delta FP} + N_{\Delta PO} + N_{\Delta TE} + N_{\Delta T\alpha} \leq 1000$
<b>Attachments and nozzles in the knuckle region of formed head</b>	$N_{\Delta FP} + N_{\Delta PO} + N_{\Delta TE} + N_{\Delta T\alpha} \leq 60$
<b>All other components that do not contain a flaw</b>	$N_{\Delta FP} + N_{\Delta PO} + N_{\Delta TE} + N_{\Delta T\alpha} \leq 400$
<p><math>N_{\Delta FP}</math> = expected number of full-range pressure cycles, including startup and shutdown</p> <p><math>N_{\Delta PO}</math> = expected number of operating pressure cycles in which the range of pressure variation exceeds 20% of the design pressure for integral construction or 15% of the design pressure for non-integral construction</p> <p><math>N_{\Delta TE}</math> = effective number of changes in metal temperature difference between any two adjacent points</p> <p><math>N_{\Delta T\alpha}</math> = number of temperature cycles for components involving welds between materials having different coefficients of thermal expansion that cause the value of <math>(\alpha_1 - \alpha_2)\Delta T</math> to exceed 0.00034</p>	

*Beam Vacuum MAWP*

The beam vacuum internal MAWP is 3.0-bar (45-psia). Referring to Figure 19 and the Load Case 5 of Table 9, the LHe volume ( $P_1$ ) is set at 0 bar, and the beam vacuum ( $P_3$ ) is set at 1 bar, resulting in a 0.1 MPa differential across the cavity wall. As shown in Figure 26, the stress classification lines (SCL) that show stresses in the cavity are B, C, H, I, and J. As seen in Table 17, the maximum ratio of the calculated stress to the allowable stress occurs in SCL C, which is the weld to the end disk flange. The ratio is 0.22.

At NML, where the string of dressed cavities within the cryomodule is tested, the niobium cavity would operate under vacuum as part of the beam vacuum. The beam pipe venting line has a rupture disk with a set pressure as high as 25-psig (40-psia) (0.27 bar). In the failure mode where liquid helium leaks into the cavity, and then the cavity is warmed up, the helium would expand and pressurize the cavity. For this failure mode of helium expanding inside the cavity, the cavity can be pressurized to 3 bar, while the liquid helium volume ( $P_1$ ) is 0 bar. The ratio of calculated stress to the allowable stress would increase proportionally to the cavity pressure. At 45-psia (3 bar) the ratio increases to 0.66 so the stresses are well within the allowable. The niobium cavity within the helium vessel can safely see an internal pressure of 45 psia (3 bar).



## System Venting Verification

The 1.3-GHz Dressed SRF Cavity will be performance tested in the Horizontal Test Stand (HTS). If the cavity becomes part of a cryomodule, then it will be used at New Muon Lab. The venting system of each location is documented by the AD/Cryo department, which operates the systems. The documents include a description of the venting system, available relief capacities, and pressure drop calculations. This pressure vessel note shows the required relief capacity and compares it to the available relief capacities.

### Summary

The AD/Cryo document titled “Meson Detector Building, Horizontal Test System Main Relief Valve Analysis” (<http://www-cryo.fnal.gov/MDB/SitePages/Calculations.aspx>, under the “HTS” folder) lists the most updated calculations on the relief system for the Horizontal Test System. The system is protected by two safety valves, which are shown on the flow schematic 5520.000-ME-440517. The available relief capacities are listed in Table 1 of the AD/Cryo document.

- SVH2: Set pt. = 15-psig, Leser burst disk, model 4414.7932, nominal size = 1.5” x 2.5”
- SVH1: Set pt. = 12-psig, BS&B burst disk, nominal size 3”

Table 24 shows the available and the required flow capacities for the HTS system.

**Table 24 – Summary of Required and Available Relief Capacities at HTS**

Source of Helium Pressure	Required relief capacity (SCFM air)	Available relief capacity (SCFM Air)
Loss of cavity vacuum	750	1311
Loss of insulating vacuum	683	1202

The AD/Cryo document titled “New Muon Lab Cryomodule, Feed Cap, and End Cap Relief Valve System Analysis” (<http://www-cryo.fnal.gov/NML/SitePages/PipingSystemEngineeringNotes.aspx>, under the folder “Approved”) lists the most updated calculations on the NML relief system. There are two safety relief valves for venting helium from the cryomodule. The valves are shown on drawing 5520.000-ME-458097, the schematic of the cryomodule at NML with the relief valves. Both are rupture disks, as detailed below (see Tables 1, 2, and 3 in the AD/Cryo document):

- SV-803-H: Set pt. = 43 psig (4-bar), Leser Model 4414.4722, nominal size = 6"x8", 8053-SCFM air (16,175-g/sec)
- SV-806-H: Set pt. = 15 psig (2-bar), Leser Model 4414.7942, nominal size = 2"x3", 951-SCFM air (217-g/sec)

Table 25 summarizes the possible sources of helium pressure and the calculated required flow rate for the cryomodule.

Table 25 – Summary of Required Relief Capacities at NML

Source of Helium Pressure	Required relief capacity (SCFM Air)	Available relief capacity (SCFM Air)
Loss of beam vacuum	6061	8053
Loss of insulating vacuum	3737	8053

For the mass flow rates that are listed, the following equation is used for conversion to volumetric flow rate (SCFM-air): <sup>(11)</sup>

$$Q_a = \frac{13.1 \cdot W C_a}{60 \cdot C} \sqrt{\frac{Z T M_a}{M Z T_a}}$$

Where:

- $Q_a$  = volumetric flow rate [SCFM air]
- $W$  = mass flow rate of helium [lbm/hr]
- $C_a$  = air gas constant = 356
- $Z_a$  = compressibility factor of air = 1
- $T_a$  = air temperature at standard conditions [°R]
- $M_a$  = air molecular weight = 4
- $C$  = helium gas constant = 378
- $M$  = helium molecular weight = 28 kg/kmol
- $Z$  = compressibility factor of helium

#### *Detailed Calculations for System Venting*

##### Temperature of relief flow (CGA S-1.3—2008 paragraph 6.1.3)

The CGA specifies a temperature to calculate the flow capacities of pressure relief devices for both critical and supercritical fluids. The temperature to be used is determined by calculating the square root of fluid's specific volume and dividing it by the specific heat input at the flow rating pressure. The sizing temperature would be when this calculation is at a maximum. For the relief pressure of 4.4-bar (110% of the cold MAWP), the temperature is 6.8°K. This results in a compressibility factor of helium equal to 0.58.

##### At HTS: Loss of RF Cavity (Beam) Vacuum and Loss of Insulating Vacuum

Two independent scenarios are considered in calculating the helium boil-off: helium vaporization due to the loss of RF cavity (beam) vacuum and helium vaporization due to the loss of insulating vacuum. For both scenarios, at a helium pressure of 4.4-bar (110% MAWP), the heat absorbed per unit mass of efflux, equivalent to a latent heat but including the effect of significant vapor density is 23-J/g.

For helium boil-off during the loss of RF cavity vacuum due to an air leak, the total surface area of the RF cavity that is used in the calculations is 1302-in<sup>2</sup> (0.84-m<sup>2</sup>). The heat flux of 4.0-

W/cm<sup>2</sup> is used <sup>(12)</sup>.

The helium boil-off during the loss of insulating vacuum is calculated based on the total surface area of the cold mass. At HTS, the cold mass is the total surface area of the helium vessel which is 1550-in<sup>2</sup> (1.0 m<sup>2</sup>) (refer to drawing number 87285). The heat efflux for a superinsulated vacuum vessel with an uninsulated helium vessel is 2.0-W/cm<sup>2</sup> (13).

The total mass flow rate is calculated using the equation:

$$\dot{m} = \frac{A * Q}{\theta}$$

The equivalent volumetric flow rate is calculated based on the total mass flow rate. The detailed list of values for helium vaporization during the loss of cavity vacuum and loss of insulating vacuum at HTS are shown in Table 26:

**Table 26 – Values Used to Calculate the Required Volumetric Flow Rate for Helium Vaporization at HTS**

		Cavity Vacuum Loss	Loss of Insulating Vacuum	
Q	Heat flux	4.0	2.0	W/cm <sup>2</sup>
P <sub>relief</sub>	110% of set pressure of cold MAWP	4.4	4.4	bar
		440	440	kPa
T	temperature when specific heat input is at a minimum for relief pressure	6.8	6.8	K
		12.24	12.24	R
θ	specific heat input for helium at T, P <sub>relief</sub>	23	23	J/g
A	Surface area of helium-to-vacuum boundary	0.84	1.0	m <sup>2</sup>
m <sub>dot</sub>	mass flow rate of helium during vaporization	1461	870	g/sec
W	mass flow rate of helium during vaporization	11570	6887	lbm/hr
C	helium gas constant	378	378	
M	molecular weight of helium	4	4	kg/kmol
ρ	helium density at T, P <sub>relief</sub>	53.39	53.39	kg/m <sup>3</sup>
Z	compressibility factor for helium at flow condition	0.58	0.58	
C <sub>a</sub>	air gas constant	356	356	
Z <sub>a</sub>	air at T <sub>a</sub>	1	1	
T <sub>a</sub>	air at room temperature	520	520	R
M <sub>a</sub>	air molecular weight	28.97	28.97	kg/kmol
Q <sub>a</sub>	volumetric flow rate of helium during vaporization	750	446	SCFM air

At NML: Loss of RF Cavity (Beam) Vacuum and Loss of Insulating Vacuum

At NML, just as at HTS, the required flow rate during the helium vaporization for the loss of beam vacuum and loss of insulating is calculated at 4.4-bar (110% of the cold MAWP of 4-bar). For each scenario, the total surface area of the helium-to-vacuum boundary includes the surface areas of all eight dressed cavities plus the corrector dipole. For the loss of beam vacuum, the total helium-to-vacuum surface area of 6.8-m<sup>2</sup> includes the surface area of eight cavities (0.84-m<sup>2</sup> for each cavity) plus the surface area at the dipole corrector (0.067m<sup>2</sup>). For the loss of insulating vacuum, the total surface area of 8.9-m<sup>2</sup> includes the area of the eight helium vessels (1.0-m<sup>2</sup>), the area of the dipole corrector (0.37-m<sup>2</sup>). Table 27 lists the values that leads to the required volumetric flow rate of helium for the NML relief system.

Table 27 – Values Used to Calculate the Required Volumetric Flow Rate for Helium Vaporization at NML

		Beam Vacuum Loss	Loss of Insulating Vacuum	
Q	Heat flux	4.0	2.0	W/cm <sup>2</sup>
P <sub>relief</sub>	110% of set pressure of cold MAWP	4.4	4.4	bar
		440	440	kPa
T	temperature when specific heat input is at a minimum for relief pressure	6.8	6.8	K
		12.24	12.24	R
θ	specific heat input for helium at T, P <sub>relief</sub>	23	23	J/g
A	Surface area of helium-to-vacuum boundary	6.8	8.9	m <sup>2</sup>
m <sub>dot</sub>	mass flow rate of helium during vaporization	11803.5	7278.2	g/sec
W	mass flow rate of helium during vaporization	93484.6	57643.7	lbm/hr
C	helium gas constant	378	378	
M	molecular weight of helium	4	4	kg/kmol
ρ	helium density at T, P <sub>relief</sub>	53.39	53.39	kg/m <sup>3</sup>
Z	compressibility factor for helium at flow condition	0.58	0.58	
C <sub>a</sub>	air gas constant	356	356	
Z <sub>a</sub>	air at T <sub>a</sub>	1	1	
T <sub>a</sub>	air at room temperature	520	520	R
M <sub>a</sub>	air molecular weight	28.97	28.97	kg/kmol
Q <sub>a</sub>	volumetric flow rate of helium during vaporization	6060.6	3737.1	SCFM air

## Welding Information

The weld characteristics were introduced earlier in this document in the sub-section titled “Welds” in the “Design Verification” section. As stated earlier, welds are produced by either the EBW process or the TIG process. All welds on the Dressed SRF Cavity are designed as full penetration butt welds. All welds are performed from one side, with the exception of the Ti-45Nb to Ti transition welds. Those welds are performed from two sides. No backing strips are used for any welds. Table 28 summarizes the welds, including the drawing, materials joined, weld type, and how the weld was qualified. Figure 25 shows the location of the welds on the vessel.

Table 24. Weld summary for LCLS II cavity

Weld	Weld Descripti	Drawing & Reference	Material s	Weld Type	Weld Qualification
1	End Tube Spool Piece to End Cap Flange	MD-439178	Nb-Nb	EBW	Welded at vessel manufacturer
2	End Tube Spool Piece to RF Half Cell	MD-439178	Nb-Nb	EBW	Welded at vessel manufacturer
3	End Cap Flange to RF Half Cell	MD-439178	Nb-Nb	EBW	Welded at vessel manufacturer
4	End Cap Flange to End Cap Disk	MD-439178	Nb-Ti45Nb	EBW	Welded at vessel manufacturer
5	End Cap Disk to Transition	MD-439180 MD-440003	Ti45Nb-Ti	EBW	Welded at vessel manufacturer
6	1.3GHz 9 Cell RF Cavity (Transition Ring) to Bellow Assembly	F10017493	Ti-Ti	TIG	Welded at FNAL. WPS, PQR, WPQ for Procedure No. TI-1 and TI-6.
7 (FP End)	Bellow Assembly to LCLS II Helium Vessel Assembly	F10017493	Ti-Ti	TIG	Welded at FNAL. WPS, PQR, WPQ for Procedure No. TI-1 and TI-6.
8	Bellows Convolutions to Weld Cuff	F10010529 X-Ray Report	Ti-Ti	TIG	Welded at vessel manufacturer. WPS, PQR, WPQ.
9	Support Ring to Half Cell	MC-439172	Nb-Nb	EBW	Welded at vessel manufacturer
10	Dumbbell to Dumbbell	MD-439173	Nb-Nb	EBW	Welded at vessel manufacturer
11	Half Cell to Half	MC-439172	Nb-Nb	EBW	Welded at vessel manufacturer
12 (MC End)	Transition Ring to LCLS II Helium Vessel Assembly	F10017493	Ti-Ti	TIG	Welded at FNAL. WPS, PQR, WPQ for Procedure No. TI-1 and TI-6.
13	Seam Welds of Helium Tubes	812995, 813005, X-Ray Report	Ti-Ti	TIG	Welded at vessel manufacturer. WPS, PQR, WPQ.
14	2-phase pipe stub to helium vessel	812765, X-Ray Report	Ti-Ti	TIG	Welded at vessel manufacturer. WPS, PQR, WPQ. Final weld was radiographed (weld W1 in x-ray report).

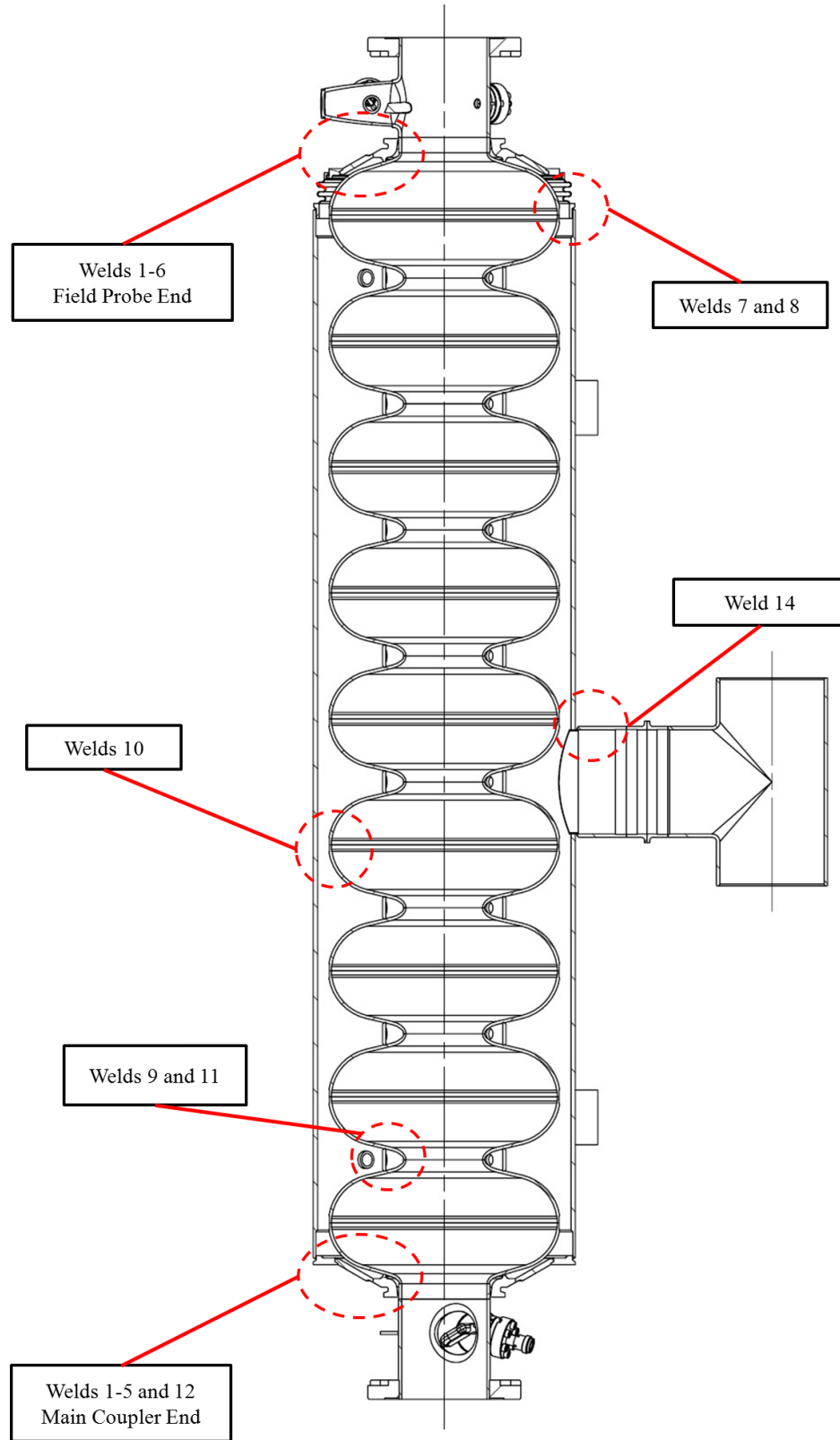


Figure 29. Weld Locations, as numbered in Table 24

According to the Code, the welds must follow certain guidelines. Table 29 summaries the weld guideline, the paragraph in the Code which addresses the weld guideline, and how the weld does not follow the guideline. To accommodate for the exceptions, in the analysis of the design, the joint efficiency is at least 0.6, which is typical for a weld that is not radiographed (see Table 4).

**Table 25. Weld Exceptions to the Code**

Weld Guideline	Code Paragraph	Exception to the Code	Explanation
Electron beam welds in any material must be ultrasonically examined along the entire length.	UW-11(e)	No ultrasonic examination was performed.	In the analysis, the joint efficiency is at least 0.6, as if the weld is not radiographed (see Table 3).
Category B Ti welds must be either Type 1 or Type 2 butt welds.	UNF-19(a)	Some Category B welds are Type 3.	In the analysis, the joint efficiency is at least 0.6, as if the weld is not radiographed (see Table 3).
All Ti welds must be examined by the liquid penetrant method.	UNF-58(b)	No liquid penetrant testing was performed.	In the analysis, the joint efficiency is at least 0.6, as if the weld is not radiographed (see Table 3).
The welds of a bellows expansion joint must be examined by the liquid penetrant method.	26-11	No liquid penetrant testing was performed.	In the analysis of the seam weld, the joint efficiency is at least 0.6, as if the weld is not radiographed.

Three welds are performed at Fermilab (welds 6-7 in Table 28). They are the final closure welds that bring the titanium helium vessel and the niobium RF cavity together to make the complete assembly. According to the Technical Appendix in the FESHM 5031 on Welding Information:

“Welding executed at Fermilab shall be done in a manner equivalent to a generic welding procedure specified and qualified under the rules of the A.S.M.E. Boiler and Pressure Vessel Code Section IX. The system designer of an in-house built vessel shall provide a statement from the welding supervisor or his designee certifying the welding was observed and accomplished in accordance to the specified generic welding procedure by a qualified welder and shall attach a copy of the welder's identification to the statement.”

The Code Section IX requires three documents that specify and qualify a weld procedure and certify a welder. These documents are the Welding Procedure Specification (WPS), the Procedure Qualification Record (PQR), and the Welder/Welding Operator Performance Qualifications (WPQ). For the titanium closure welds that are completed at Fermilab, namely welds 6-7 in Table 28, the relevant documents are titled “TI-1” and “TI-6”. The documents are available online at <http://tdserver1.fnal.gov/tdweb/ms/Policies/Welding/>

All other welds were performed at vendors outside Fermilab. Any available documentation and inspection results are explained in the following paragraphs.



For the niobium cavity electronic beam (EB) welding that took place (welds 1-5, 9-11), no welding documents are available. In most cases the process is proprietary. How the welds and welders are qualified are not known other than what is specified in the engineering drawings. The quality assurance for the niobium cavity is its RF performance. The RF performance is an indirect way of proving full penetration welds because if the weld is not full penetration, the RF performance is not acceptable.

For the bellows assembly, a single weld holds the bellows convolution to the weld cuff at each end (weld 12 in Table 28). The bellows assembly was fabricated at Ameriflex. A WPQ is available.

The titanium helium vessel assembly was manufactured at Incodema, who provided the WPS, PQR, and WPQ weld documents. All of the final welds (including welds 8, 12-14) were radiographed (x-rayed).

A detailed procedure, titled “1.3GHz Cavity Welding to Helium Vessel” lists all of the manufacturing steps that are taken for dressing a bare cavity after vertical testing in preparation for horizontal testing.

The welding documents, x-ray reports, and manufacturing procedure are available online at <http://ilc-dms.fnal.gov/Workgroups/CryomoduleDocumentation/folder.2011-04-14.5879929941/PVnotes/WeldFabrication/Xray/>

## **Fabrication Information**

Fabrication documents for the titanium helium vessel assembly, the bellows assembly are available. These documents are not required by FESHM 5031 but are made available at a centralized location. These documents include material certifications, leak check results, and other quality assurance documents. The documents are available in Fermilab Teamcenter engineering installation.

## Verification of ANSYS Results

### Hoop Stress in Ti Cylinder

The hoop stress in the Ti cylinder, far from the ends or the flanges (which function like stiffening rings) can be calculated from

$$S = \frac{P \cdot r}{t}$$

where:

- $S$  = hoop stress
- $P$  = pressure
- $r$  = mean radius of shell
- $t$  = thickness of shell

Substituting  $P = 0.205$  MPa,  $r = 115$  mm,  $t = 5$  mm gives  $S = 4.7$  MPa.

To check this number against the ANSYS results for 0.205 MPa, a path was created in the ANSYS model, and the hoop stress plotted along the path. Figure 30 shows the path; Figure 31 shows the comparison of the ANSYS results with those calculated from the expression above. Agreement is extremely good over the region away from the ends, averaging less than 1%.

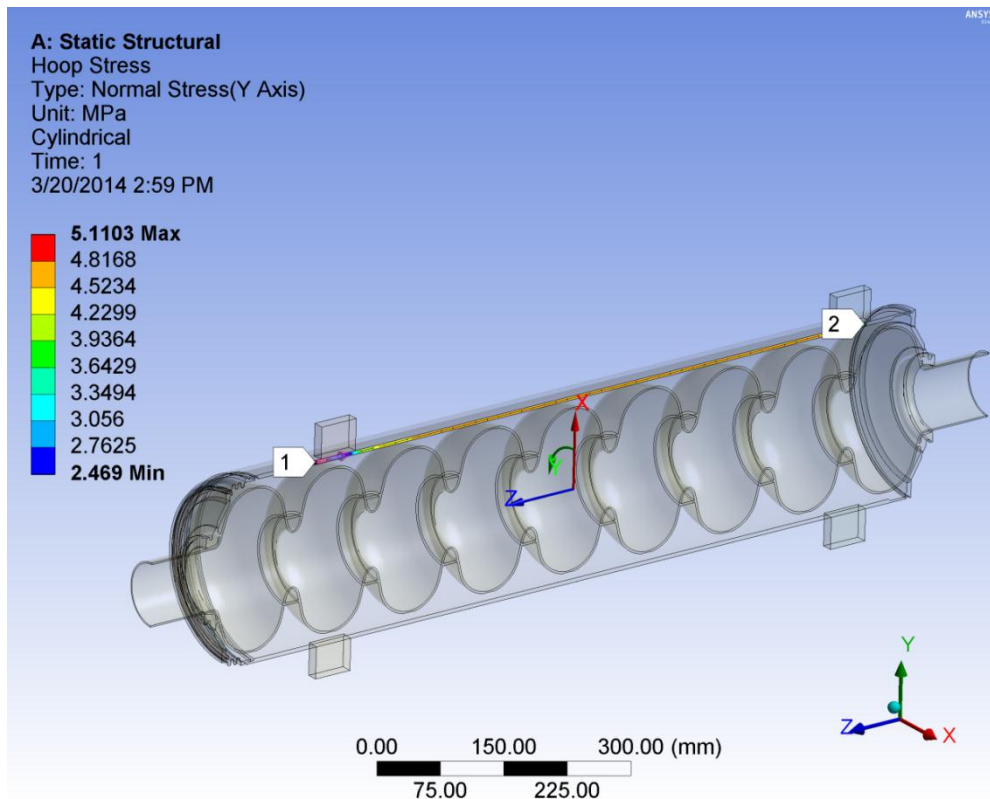


Figure 30. Path for hoop stress plot

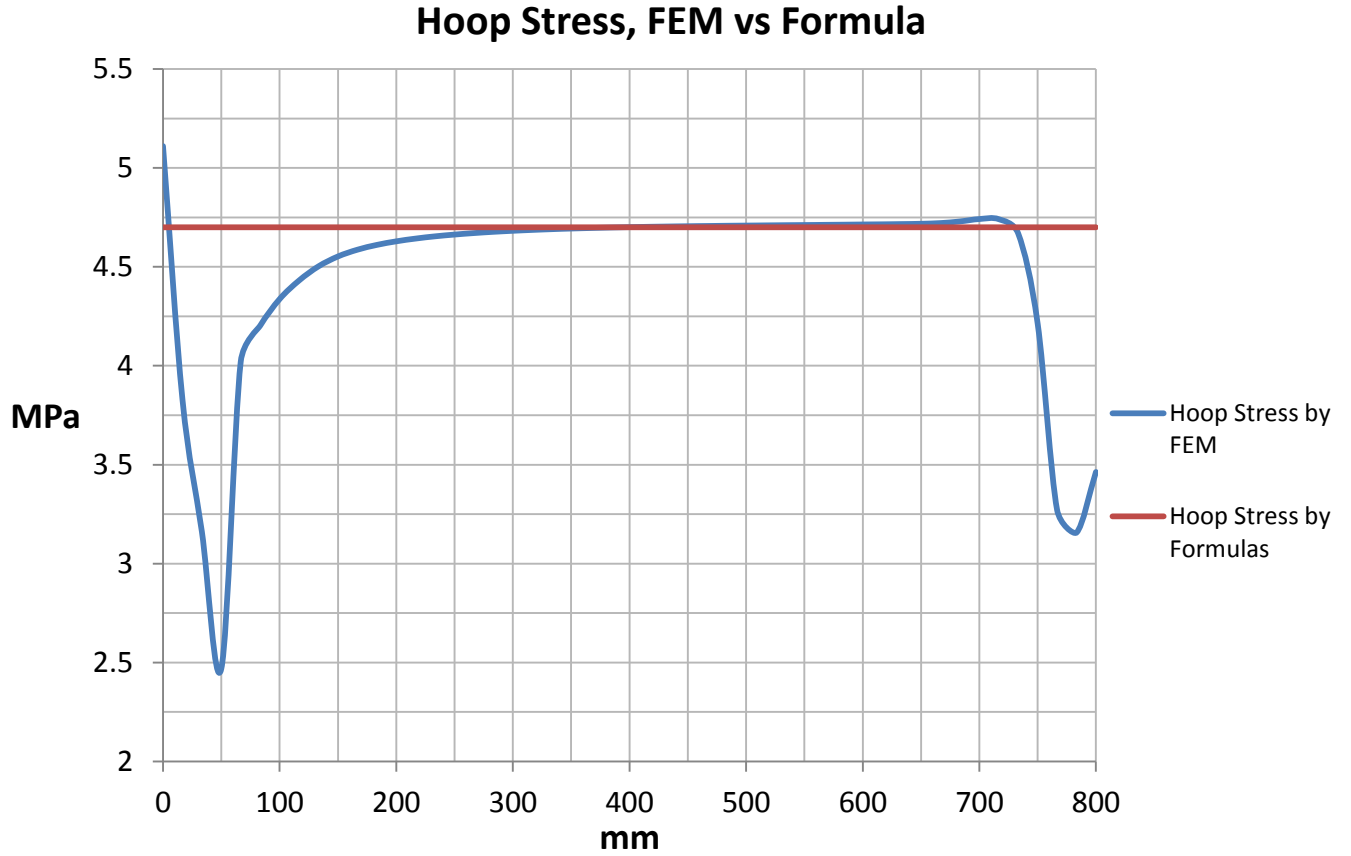


Figure 31. Hoop Stress in Ti Cylinder along line 1-2 for Pressure of 0.205 MPa

*Buckling of Spherical Shell – Approximation to Cell Buckling*

The ANSYS model predicted Nb cavity buckling would occur at a pressure of 358 MPa. This numbers seems very large, so as a check a comparison was performed with the predicted collapse pressure for a thin sphere. <sup>(16)</sup>

From Ref. 16, Table 35, Case 22, the critical buckling pressure of a thin sphere is:

$$q' = \frac{2 \cdot E \cdot t^2}{r^2 \cdot \sqrt{3 \cdot (1 - \nu^2)}}$$

where:

- $q'$  = critical pressure, MPa
- $E$  = Young's modulus = 105000 MPa
- $r$  = radius of sphere = 105 mm
- $\nu$  = 0.38

Substituting gives  $q' = 93$  MPa. This compares well with the ANSYS linear buckling prediction.

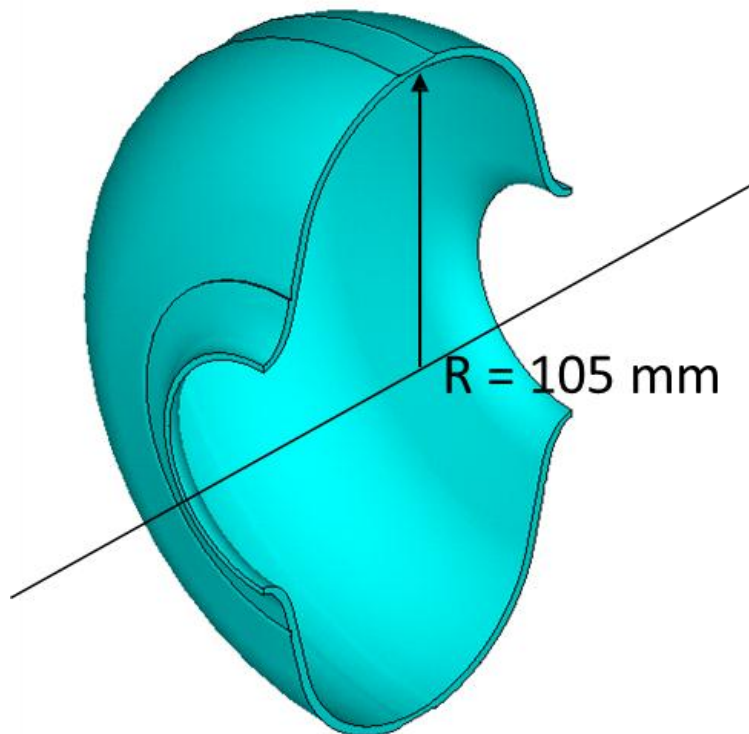


**Figure 32. Single cell - radius for spherical shell buckling calculation**

*Buckling of Ti Cylinder*

The maximum allowable external pressure of the Ti cylinder was determined in section 7.0 of this report using the chart techniques of Div. 1. This calculation can be checked by doing an ANSYS linear buckling calculation on the length of shell used in the Div. 1 calculations, and applying the design factors for linear buckling given in Div. 2, Part 5, 5.4.1. This calculation is also useful for verifying that the buckling pressure of the conical head (calculated as 358 MPa in section 9.0 of this report) is higher than that of the cylinder.

The FE model, which does not include the conical heads, is shown in Figure 33, in its buckled shape. The analysis predicts collapse at 7.3 MPa. The Code calculation of section 7.0 gives an maximum allowable external pressure for this part of 0.2 MPa. These numbers can be compared by noting that the factor  $B = \sigma_{cr}/2$ , where  $\sigma_{cr}$  is the hoop stress at which the cylinder buckles<sup>(17)</sup>. B is a factor dependent on materials and geometrical properties. Given the properties of the case we can infer from Figure NFT-2 (the material chart for Grade 2 TI) in the Code, Section II, Part D, Subpart 3 that the factor B is 10000 (psi) which is about 70 MPa. Substituting  $\sigma_{cr} = P_{cr} r/t$ , where  $P_{cr}$  is the critical buckling pressure, gives a theoretical buckling pressure for the cylinder of 6.1 MPa. This is reasonably close to the ANSYS value of 7.3 MPa.

This alternative calculation of Ti shell buckling pressure also verifies that it lies well below the calculated buckling pressure of the conical head, even when that head is unconstrained by the Nb cavity.

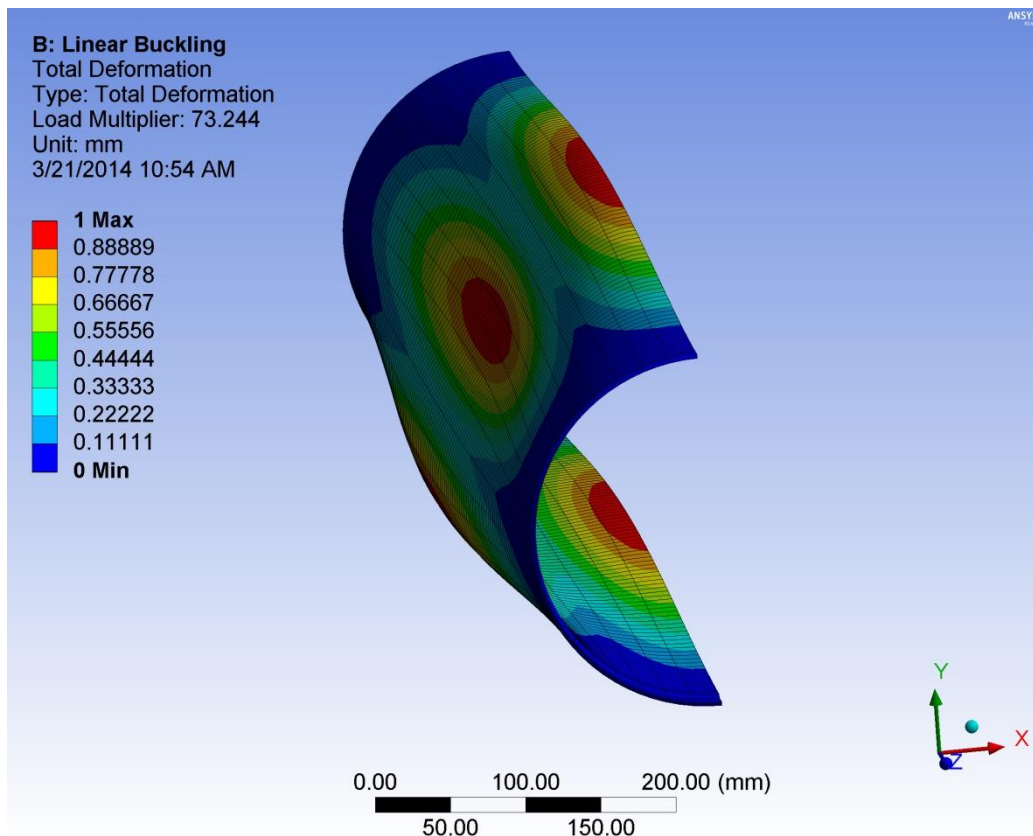
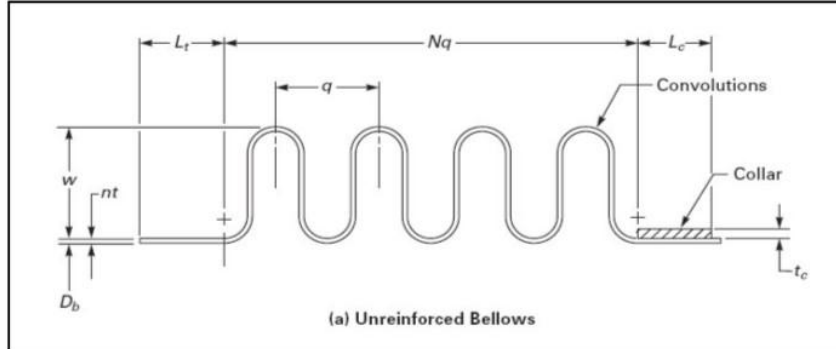


Figure 33. ANSYS linear buckling of the Ti cylindrical shell

## Fatigue Analysis of the Titanium Bellows

Here are the detailed calculations of the titanium bellows following the Code's Div. 1, Appendix 26 guidelines. Mathcad (version 14) was the software that was used.



Detailed calculation of the titanium bellows following the Code's Div.1, Appendix 26 guidelines.

Design pressure (psi)	$P := 30$
Bellows inside diameter (in)	$D_b := 8.64$
Ply thickness (in)	$t := 0.012$
Number of Plies	$n := 1$
Bellows tangent length (in)	$L_t := 0.24$
Bellows Mean Diameter (in)	$D_{mean} := 8.9$
Modulus of Elasticity (psi)	$E_b := 15200000$
Convolution height (in)	$w := 0.25$
Collar length (in)	$L_c := 0.55$
Collar thickness (in)	$t_c := 0.12$
Collar Modulus of Elasticity (psi)	$E_c := 15200000$
Convolution Pitch (in)	$q := 0.341$
Kf coefficient (formed)	$K_f := 3.0$
Allowable stress of bellows (psi)	$S := 11500$
Allowable stress of collar (psi)	$S_c := 11500$
Weld Joint Efficiency	$C_{wc} := 0.6$

Number of convolutions  $N := 2$   
 Bellows Axial Stiffness (N/mm)  $Kb\_SI := 740$   
 (lbf/inch)  $Kb := Kb\_SI \cdot \frac{2.2 \cdot 10^6 \cdot 2.54}{100} = 4.135 \times 10^7$   
 Allowable yield stress (psi)  $Sy := 40000$   
 Poisson's ratio of Ti G2  $\nu_b := 0.37$   
 Bellows live length (in)  $L := 0.87$

Maximum axial extension (mm)  $x\_positive\_SI := 1.8$   
 (in)  $x\_positive := \frac{x\_positive\_SI}{25.4} = 0.071$

Maximum axial compression (mm)  $x\_negative\_SI := 0.33$   
 (in)  $x\_negative := \frac{x\_negative\_SI}{25.4} = 0.013$

$$Dm := Db + w + n \cdot t = 8.902$$

$$k := \min \left[ \left( \frac{Lt}{1.5 \cdot \sqrt{Db \cdot t}} \right), 1.0 \right] = 0.497$$

$$tp := \left( t \cdot \sqrt{\frac{Db}{Dm}} \right) = 0.012$$

$$A := \left[ \left( \frac{\pi - 2}{2} \right) \cdot q + 2 \cdot w \right] \cdot n \cdot tp = 8.212 \times 10^{-3}$$

$$Dc := Db + 2 \cdot n \cdot t + tc = 8.784$$

$$c1 := \frac{q}{2 \cdot w} = 0.682$$

$$c2 := \frac{q}{2.2 \cdot \sqrt{Dm \cdot tp}} = 0.478$$

$$cp := 0.59$$

$$I_{xx} := n \cdot t_p \cdot \left[ \frac{(2 \cdot w - q)^3}{48} + 0.4 \cdot q \cdot (w - 0.2 \cdot q)^2 \right] = 5.429 \times 10^{-5} \quad \text{moment of inertia}$$

$$e_{eq} := \sqrt[3]{12 \cdot (1 - \nu_b^2) \cdot \frac{I_{xx}}{q}} = 0.118 \quad \text{equivalent thickness}$$

$$D_{eq} := D_b + w + 2 \cdot e_{eq} = 9.126 \quad \text{equivalent outside diameter for instability due to external pressure}$$

$$\text{Total axial movement per convolution (mm)} \quad \Delta q := \frac{(x_{\text{positive}} + x_{\text{negative}})}{N} = 0.042$$

$$S1 := \frac{(D_b + n \cdot t)^2 \cdot L_t \cdot E_b \cdot k \cdot P}{2[n \cdot t \cdot (D_b + n \cdot t) \cdot L_t \cdot E_b + t_c \cdot D_c \cdot L_c \cdot E_c \cdot k]} = 427.83$$

$$S11 := \frac{D_c^2 \cdot L_t \cdot E_c \cdot k \cdot P}{2[n \cdot t \cdot (D_b + n \cdot t) \cdot L_t \cdot E_b + t_c \cdot D_c \cdot L_c \cdot E_c \cdot k]} = 440.984$$

$$S2e := \frac{P \cdot [q \cdot D_m + L_t \cdot (D_b + n \cdot t)]}{2 \cdot (A + n \cdot t_p \cdot L_t + t_c \cdot L_c)} = 995.218$$

$$S2i := \frac{P \cdot q \cdot D_m}{2 \cdot A} = 5.545 \times 10^3$$

$$S3 := \frac{P \cdot w}{2 \cdot n \cdot t_p} = 317.203$$

$$S4 := \left( \frac{w}{t_p} \right)^2 \cdot \frac{P \cdot c_p}{2 \cdot n} = 3.958 \times 10^3$$

$$P_{sc} := 0.34 \cdot \frac{\pi \cdot K_b}{N \cdot q} = 6.476 \times 10^7$$

$$\delta_{\text{w}} := \frac{S4}{3 \cdot S2i} = 0.238$$



$$\alpha := 1 + 2 \cdot \delta^2 + \sqrt{1 - 2 \cdot \delta^2 + 4 \cdot \delta^4} = 2.062$$

$$S_{y\_eff} := 2.3 \cdot S_y = 9.2 \times 10^4$$

$$P_{psi} := (\pi - 2) \cdot \frac{A \cdot S_{y\_eff}}{Dm \cdot q \cdot \sqrt{\alpha}} = 197.879$$

$$C_f := 1.85$$

$$C_d := 1.95$$

$$S_5 := \frac{1}{2} \cdot \frac{E_b \cdot t_p^2}{w^3 \cdot C_f} \cdot \Delta q = 1.541 \times 10^3$$

$$S_6 := \frac{5}{3} \cdot \frac{E_b \cdot t_p}{w^2 \cdot C_d} \cdot \Delta q = 1.03 \times 10^5$$

$$S_t := 0.7 \cdot (S_3 + S_4) + (S_5 + S_6) = 1.076 \times 10^5$$

Calculating the buckling pressure for the bellows as an equivalent cylinder

$$\frac{D_{eq}}{e_{eq}} = 77.25$$

$$\frac{L}{D_{eq}} = 0.095$$

$$A_{factor} := 0.039$$

$$P_a := \frac{2}{3} \cdot A \cdot E_b \cdot \frac{e_{eq}}{D_{eq}} = 1.077 \times 10^3$$

Circumferential membrane stress in bellows tangent (MPa)	S1 = 427.83
Circumferential membrane stress in collar (MPa)	S11 = 440.984
Circumferential membrane stress in bellows (MPa)(for end convolution)	S2e = 995.218
Meridional membrane stress in bellows (MPa)	S2i = 5.545 × 10 <sup>3</sup>
Meridional bending stress in bellows (MPa)	S3 = 317.203
Allowable internal pressure to avoid column instability (MPa)	S4 = 3.958 × 10 <sup>3</sup>
Allowable internal pressure based on in-plane instability (MPa)	Psc = 6.476 × 10 <sup>7</sup>
Allowable external pressure based on instability (MPa)	Psi = 197.879
Meridional membrane stress (MPa)	S5 = 1.541 × 10 <sup>3</sup>
Meridional bending stress (MPa)	S6 = 1.03 × 10 <sup>5</sup>
Total stress range due to cyclic displacement (MPa)	St = 1.076 × 10 <sup>5</sup>

## ACCEPTANCE CRITERIA

$$S1 = 427.83$$

$$S2e = 995.218$$

$$S2i = 5.545 \times 10^3$$

$$S = 1.15 \times 10^4$$

$$S11 = 440.984$$

$$Cwc \cdot S = 6.9 \times 10^3$$

$$S3 + S4 = 4.275 \times 10^3$$

$$Kf \cdot S = 3.45 \times 10^4$$

$$P = 30$$

$$Psc = 6.476 \times 10^7$$

$$Psi = 197.879$$

$$Pa = 1.077 \times 10^3$$

$$a := 3.4$$

$$b := 54000$$

$$Stpsi := 122465$$

$$c := 1.86 \cdot 10^6$$

$$Nc := \frac{1}{2} \cdot \left( \frac{c}{Stpsi - b} \right)^a = 3.756 \times 10^4$$

## RF Analysis

The cavity is immersed in a saturated Helium liquid bath which is pumped in order to control the bath temperature. The bath is kept at a certain pressure and the cavity resonant frequency depends on this pressure. The pressure fluctuation in the Helium bath inevitably due to the compressibility of the fluid cause cavity detuning by elastic deformations and micro-oscillations of the cavity walls. This detuning implies that the resonant frequency of the cavity changes because of the deformation of the Niobium core of the cavity. Any small shift from the resonant frequency of the cavity requires significant increase in power to maintain the electromagnetic field constant. For a cavity on resonance, the electric and magnetic stored energies are equal. If a small perturbation is made on the cavity wall. This will generally produce an unbalance of the electric and magnetic energies, and the resonant frequency will shift to restore the balance. The Slater perturbation theorem describes the shift of the resonant frequency, when a small volume  $V$  is removed from a cavity of volume  $V$ . For these reasons, the cavity sensitivity to Helium pressure is an important parameter which must be taken in consideration during the design of a dressed cavity system. The evaluation of  $df / dp$  involves a series of electromagnetic and structural analyses that can be performed with multiphysics software such as COMSOL Multiphysics. The pressure sensitivity characterization is named Coupled Evaluation and these are the several steps to follow in order to calculate the pressure sensitivity:

- **Electro Magnetic analysis** Eigen frequency simulation to find the resonant frequency ( $f_0$ )
- **Static Structural analysis** Find the deformation under given pressure load ( $p$ )
- **Moving Mesh analysis** Update the mesh after deformation induced by the applied pressure
- **Electro Magnetic analysis** Eigen frequency simulation to find the resonant frequency after deformation ( $f_1$ )
- **Evaluation** At this point the pressure sensitivity can be found as

$$\frac{df}{dp} = \frac{f_1 - f_0}{p}$$

All the analyses were done using the software COMSOL Multiphysics version 4.4.

The first step of the approach is to calculate the Eigen frequency simulation to find the resonant frequency. The 1.3GHz 9 cell cavity is designed to resonate at a frequency near to 1.3GHz as the name itself suggests. So the radiofrequency analysis is made near this resonant frequency and between all the resonant frequencies we find out we have to choose the one that amplifies the Electric field in all the cells which is the right one because the particles are in this way accelerated or decelerated in each cell. The part of the model that matters in this step is the RF Volume which simulates the vacuum properties and is thus involved in the research of the resonant frequency.

The results of the analysis are shown in Figure 34 and the resonant frequency we are interested in is  $f_0 = 1.300706 \text{ GHz}$ .

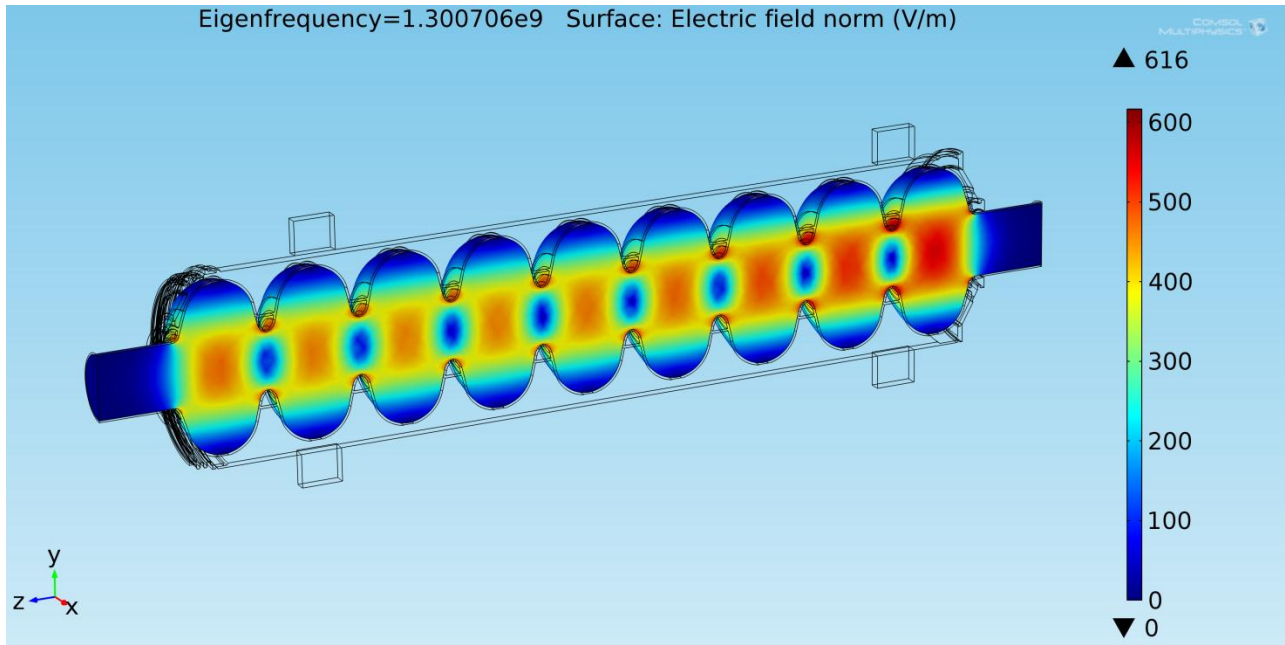


Figure 34. Result of the Electro Magnetic analysis to find the resonant frequency  $f_0$

Now that we have found  $f_0$  it is time to switch to the second step and apply the pressure on the model. The pressure used for the evaluation is  $p = 1 \text{ bar}$  and it is where the Helium bath is located, so it is applied on the external surfaces of the cavity and on the internal surfaces of the Helium vessel. The pressure applied is important because it deforms the shape of the cavity and thus the RF volume contained inside. In the end flange near the bellow is applied the Tuner constraint. For this analysis the tuner is considered to be of infinite stiffness so it has been replaced by a Fixed Constraint. Later we will show the influence of the Tuner Stiffness in the  $df/dp$  analysis. The displacement that really matters in this analysis is the axial displacement which is greater than the other ones because the pressure applied on the End plates acts as a normal force on the cavity which is then stretched. This is shown in XXX where the Z component of the displacement field is plotted.

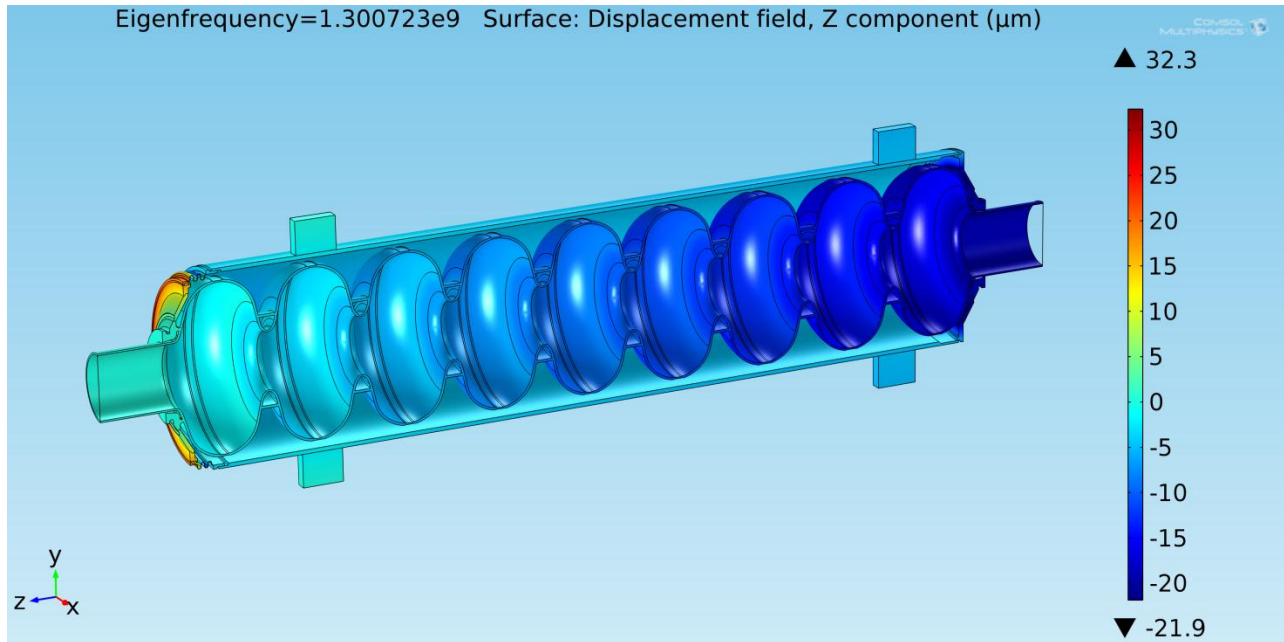


Figure 35. Axial displacement of the dressed cavity assembly when a pressure of 1 bar is applied in the zones where is located the Helium bath

Now that the displacement under the pressure is found it is time to move on the third step of the Coupled Evaluation. The third step is the mesh update. To do so the displacement field just found need to be applied to the external surfaces of the RF volume thus its shape will be deformed and different from the starting one. COMSOL Multiphysics allows us to do that in a command named Moving Mesh which requires a displacement field as an input. Hence we put the displacement field just found from the Static structural analysis as input and we update the solution.

After that passage we should now do the last step: another Electro Magnetic analysis to find the new resonant frequency after the application of the deformation at the mesh of the RF volume. The analysis is the same done in the first step of the evaluation thus the Electric Field found in the vacuum volume should be the same. The only thing that should change is the Eigen frequency ( $f_0$ ) at which that particular Electric field is situated. The results can be seen in Figure 36 where the resonant frequency is found to be  $f_1 = 1.300723\text{GHz}$ . We can observe that like explained in advance the Figure 34 and Figure 36 are equal in terms of Electric field and the only thing changed is indeed the resonant frequency of the cavity.

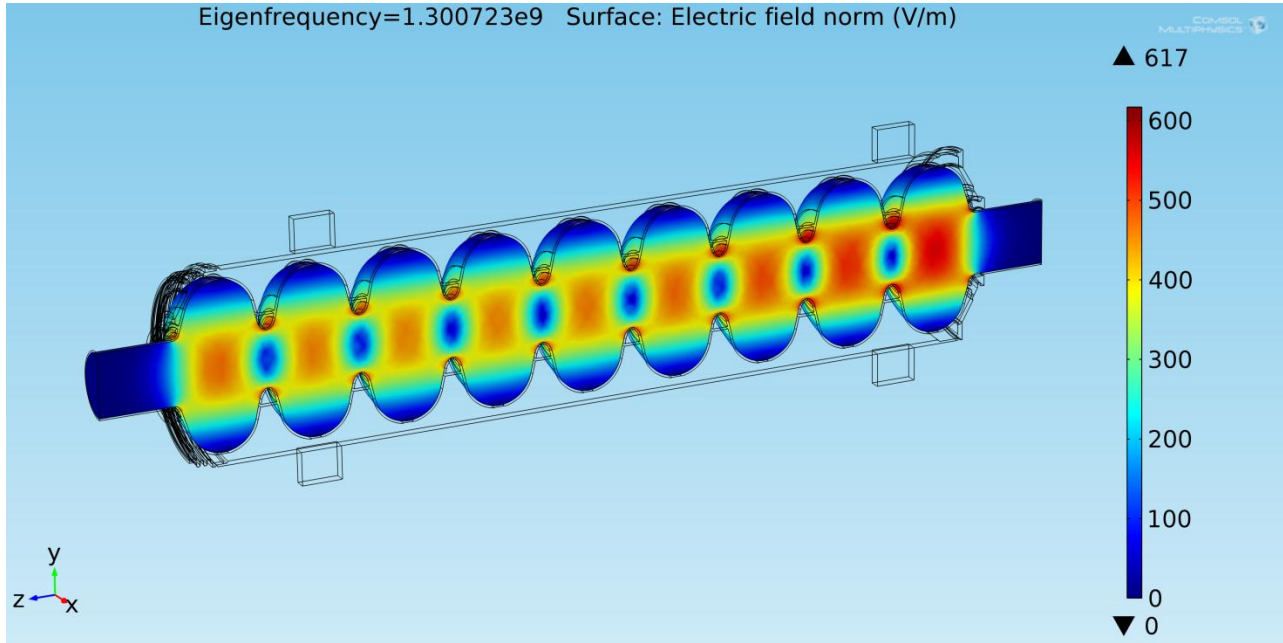


Figure 36. Result of the Electro Magnetic analysis to find the resonant frequency  $f_1$

Now we have all the necessary data to calculate the  $df/dp$ . The pressure sensitivity is thus given by:

$$\frac{df}{dp} = \frac{f_1 - f_0}{p} = \frac{1.300723 \cdot 10^9 \text{ Hz} - 1.300706 \cdot 10^9 \text{ Hz}}{10^3 \text{ mbar}} = 17 \text{ Hz/mbar}$$

In addition to this result we can note from Figure 35 (and of course by more accurate measurement of the solution) that the displacement between the two ends of the Helium vessel in this case is  $17 \mu\text{m}$ .

#### *Influence of the Tuner Stiffness*

Now that we have calculated the pressure sensitivity in the case of an infinite stiffness of the Tuner is time to investigate how the Tuner Stiffness will affect that measurement. The Tuner for the new design has not been created yet so this analysis is very important because it give a benchmark to follow in the Tuner design and it also allow to skip another Pressure Sensitivity Evaluation when the Tuner stiffness will be determined.

To investigate this influence we simply have to do several coupled evaluation with the fixed constraint simulating the Tuner stiffness replaced by a spring constraint which value will be updated every analysis with the stiffness we want to simulate. We decided to have smaller stiffness steps when the tuner stiffness is low because the  $df/dp$  was seen to have a rise in this range and we want an accurate representation of the curve. Before proceeding with the analysis we can say that we expect a rise of the pressure sensitivity with decreasing stiffness, because such dressed cavity is more flexible and its shape will be more deformed.

The analyses are coupled evaluations which have been well explained above. The outcomes are shown in the Table 26 and in the Figure 37. The reference resonant frequency is the one of the undeformed cavity so it is the same of the previous analysis that is  $f_0 = 1.300706 \text{ GHz}$ .

Table 26. Results of the influence of the tuner stiffness over the pressure sensitivity of the dressed cavity

<i>Stiffness [kN/mm]</i>	<i>f<sub>1</sub> [GHz]</i>	<i>df/dp [Hz/mbar]</i>
0	1.300868	162
1	1.300831	125
2.5	1.300800	94
5	1.300776	70
10	1.300755	49
20	1.300741	35
40	1.300732	26
80	1.300728	22

These results are in accordance with what we expected before the analysis was made and explains us that it is important to go towards a more stiffness tuner and in general we should maximize the tuner stiffness for this cavity because doing so the assembly is more rigid and it will deform less when a pressure fluctuation is applied. In results the resonant frequency will be closer to the undeformed one. Thus the power required to tune the cavity, the process that modify the length of the cavity applying a displacement on the tuner, is less and this bring us to an energy saving and, in consequence, a money saving.

From Figure 37 we notice that the pressure sensitivity has a trend tending to the value we calculated before (*17 Hz/mbar*) when the tuner stiffness tend to infinite, which confirms the validity of the coupled analysis made. We also notice that the *df /dp* has a rapid increase when the tuner stiffness drops below *10 kN/mm*. Thus it will be very important in the design of the tuner to tray to maintain a stiffness higher than this value otherwise the pressure sensitivity will rise and the power to maintain the resonant frequency of the cavity the same of the undeformed cavity will be too high.



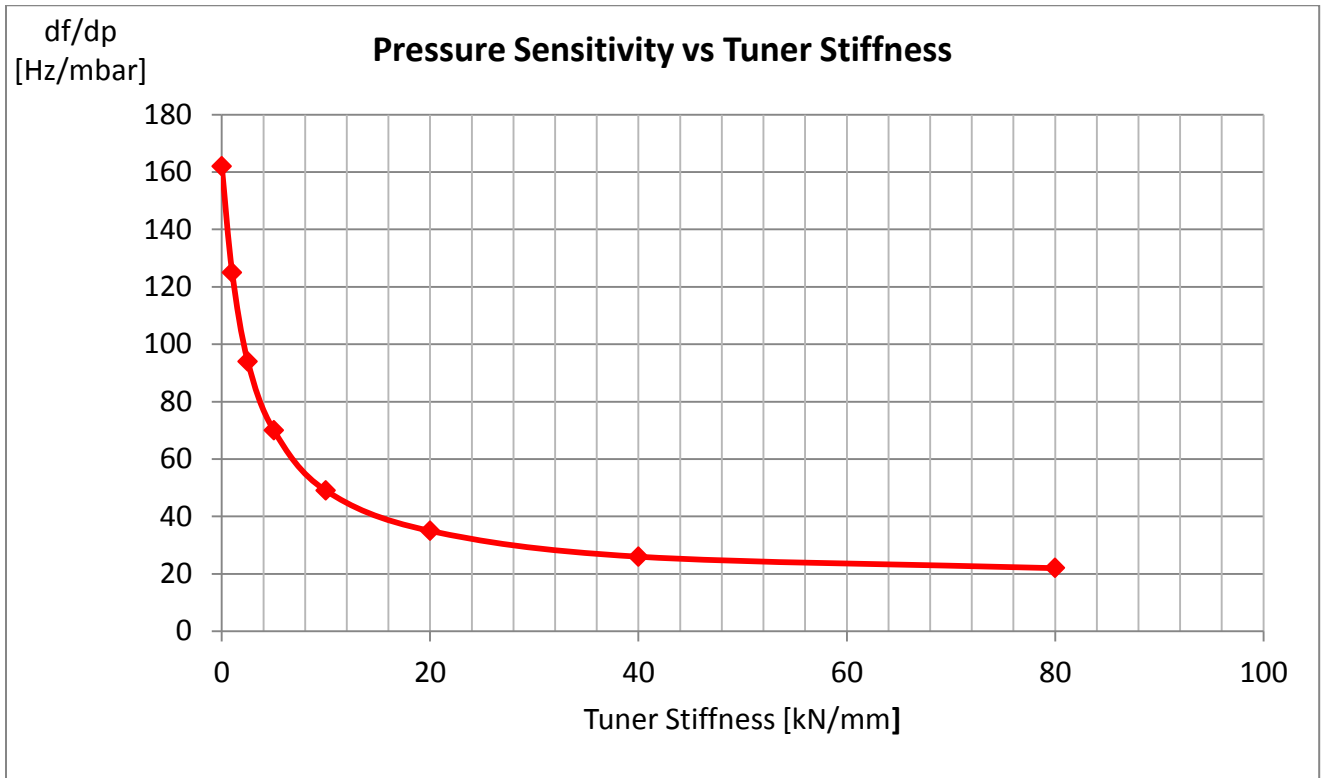


Figure 37. Graph putting in evidence the influence of the tuner stiffness in the analysis of the pressure sensitivity

## Magnetic Shielding

Fermilab has developed a double-layer magnetic shield design for the 1.3GHz LCLS-II Prototype Cryomodule. The first layer is assembled close around the helium vessel with approx. 3mm radial clearance, and the second layer is spaced 20mm out radially from the first layer using spacers. Both layers will be physically connected from cavity-to-cavity using interconnect shields, these will be screwed on around the tuner end of one cavity and designed with a floating joint at the coupler end of the opposite cavity. This will allow for movement in the interconnect region due to thermal contraction/expansion during cavity cool down/warm up (~1.8K/300K). The cavity string will consist of eight, 9-cell superconducting, Radio Frequency (RF) cavities.

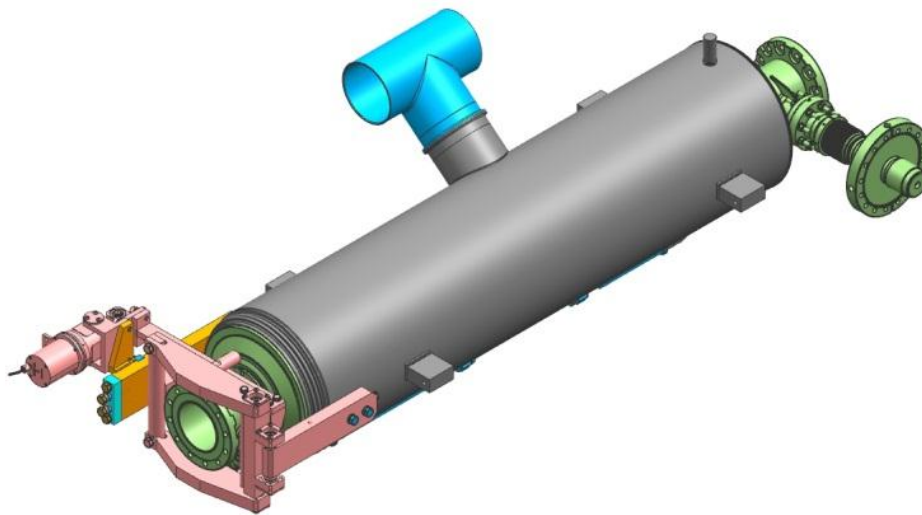


Figure 38. Cavity prior to Magnetic Shield Installation

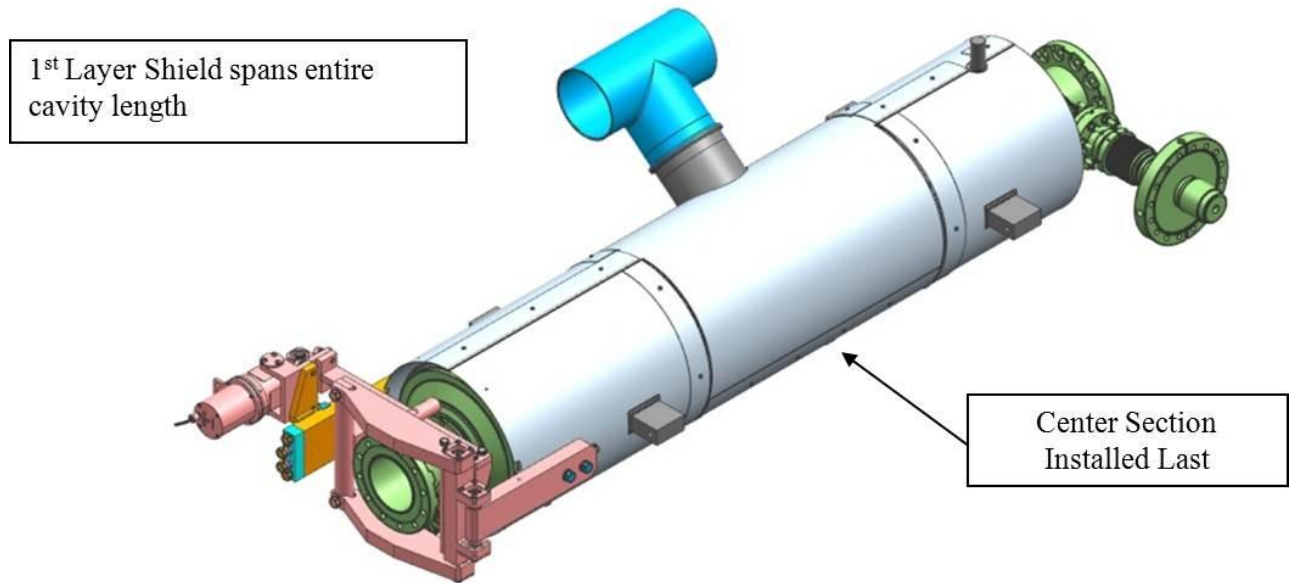


Figure 39. Cavity Complete with 1<sup>st</sup> layer Magnetic Shielding

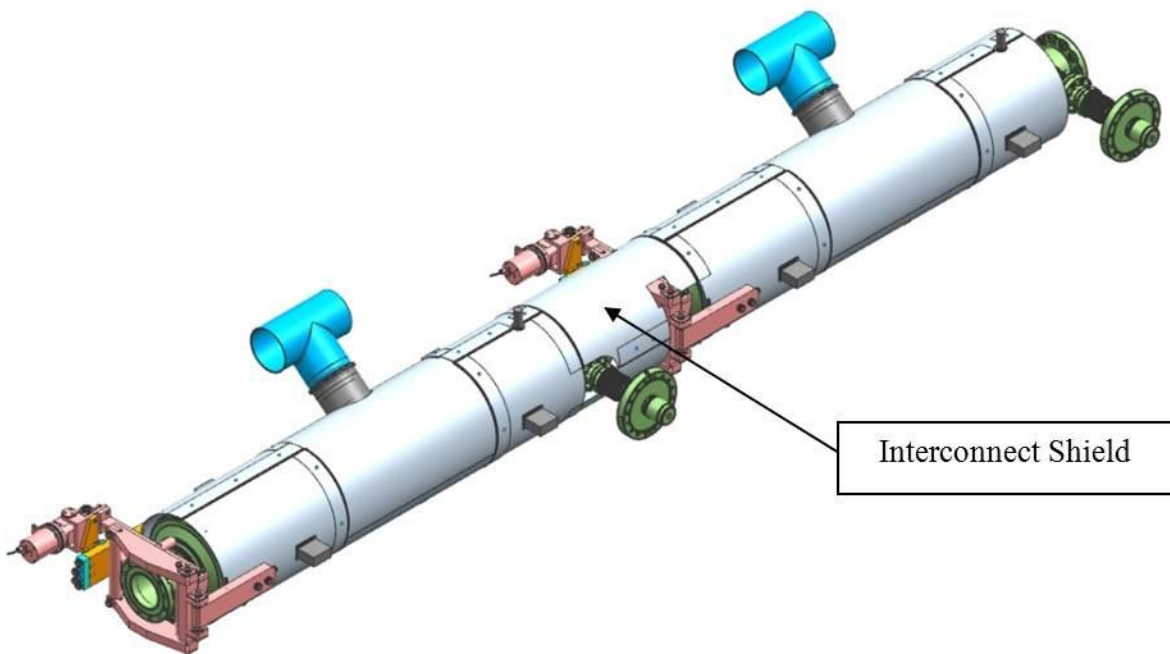


Figure 40. 2-Cavity string with complete 1<sup>st</sup> layer shielding

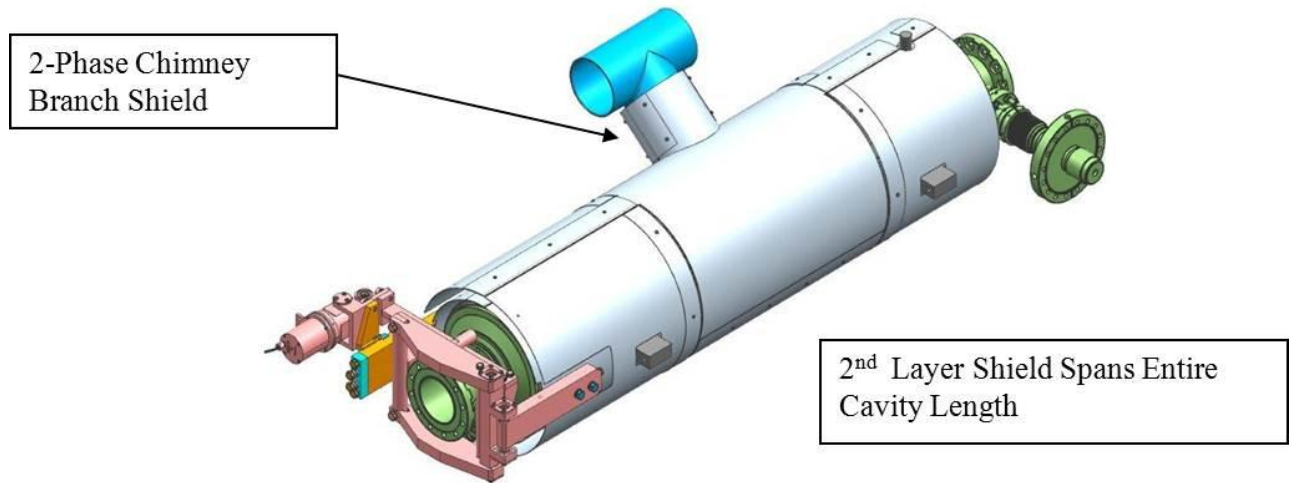


Figure 41. Cavity complete with 2<sup>nd</sup> layer Magnetic Shielding

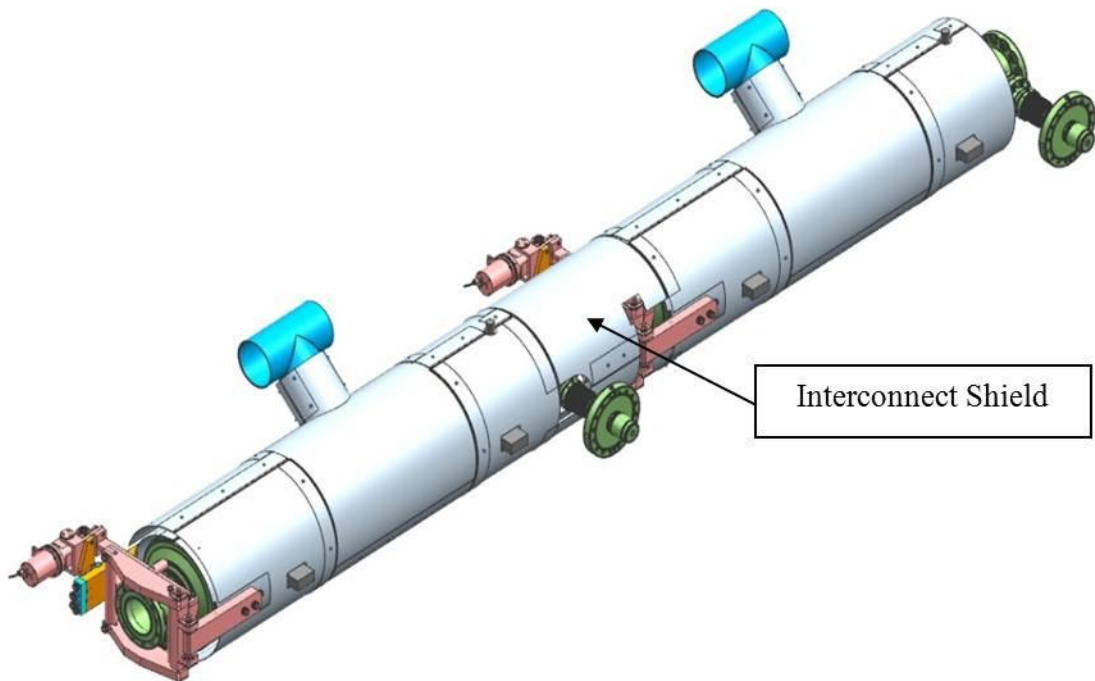


Figure 42. 2-Cavity string with complete 2 layers of Shielding

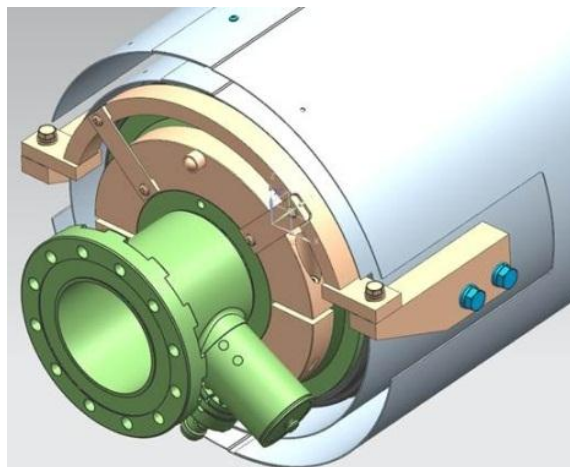


Figure 43. Close-up of Shields with bellows restraint

The cavity and shielding is at the core of the cryomodule. This shell acts as the primary layers of magnetic shielding for the internal cavities.

#### *Shield Fasteners*

Fermilab requires that the shield components be fastened together using PEM fasteners but does not specify the style or required torque. The installation details of the fasteners, such as torque, are to be specified by the vendor and must be accepted in writing by Fermilab before the fabrication begins. Fermilab will specify the location of the fasteners per the manufacturing drawings.

#### *Shield Spacers (2nd Layer)*

Fermilab requires that the shield components be spaced radially 20mm between the first layer and second layer shields. The spacers will fastened together using PEM fasteners but does not specify the style or required torque. The location and details of the spacers and fasteners, are to be specified by the vendor and must be accepted in writing by Fermilab before the fabrication begins. Vendor will specify the location of the spacers and fasteners as to avoid vessel penetrations and shield overlaps.

#### *Shield Material*

Magnetic shields must be fabricated from Cryoperm10, Amumetal 4K, or an equivalent material that is specially prepared to have high permeability over a wide range of temperature; materials must be approved by FNAL. Suitable performance is illustrated in Figure 1. The relative magnetic permeability of the completed shields, after installation in the cryomodule, must exceed 10,000 over the temperature range  $1.6\text{K} < T < 300\text{K}$ . Note that this value for relative permeability is the minimum requirement after all mechanical and handling procedures have been completed and is based on the assumption that the permeability will be degraded significantly by mechanical stress and shock.



Results on initial permeability vs measurement temperature

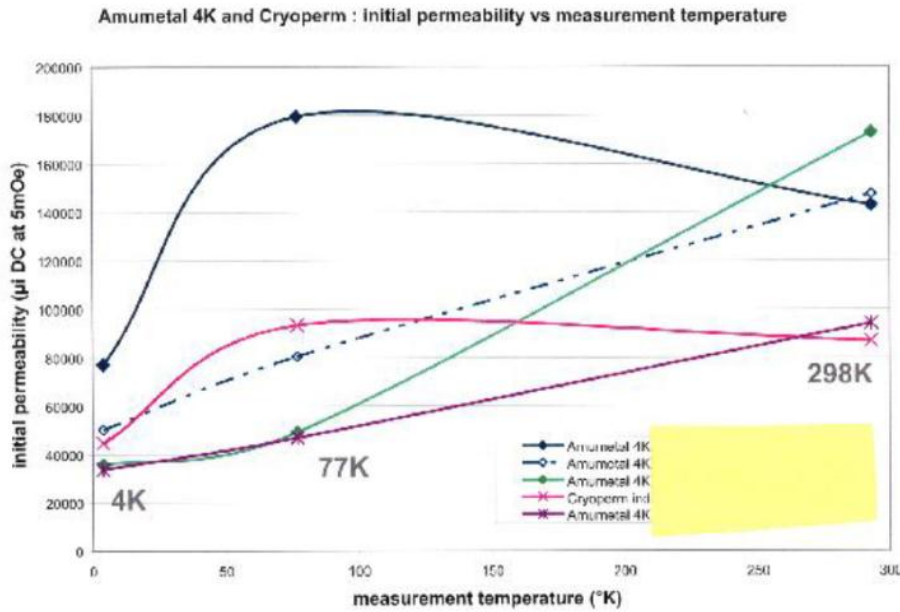


Figure 44. Permeability vs. Temperature curves for Cryoperm10 and for Amumetal 4K

*Magnetic Fields*

The magnetic field inside the magnetic shield under normal operating conditions as well as during cryomodule cooldown must not exceed 5 milliGauss (0.5 microTesla). The shields will consist of two concentric layers of 1mm thick high magnetic permeability material separated by a radial gap of approximately 20 millimeters. Any spacers used between the shielding layers must be made from material with relative magnetic permeability less than 1.05. It must be ensured that there are no magnetic “shorts” present that would allow flux to pass easily from the outer shield layer to the inner layer. It is anticipated that the ambient flux outside the magnetic shield will be less than 500 milliGauss (50 microTesla).

*Labeling*

Each piece of shielding will be properly identified with minimal 1/8 inch high lettering, embossed or engraved onto each shield in a location that is viewable after the shield is assembled. Each shield will be bagged in plastic and labeled with a tag identifying the part number and revision level.

*Fastener Material*

The fasteners to join the shield components together must be made from 316L stainless steel or similar low magnetic permeability steel.

### *Forming*

The material will be formed via normal sheet metal operations. Laser cutting of the flat stock and rolling to final size is permitted. The fabrication techniques, from design to the final configuration, are identical to that of Amumetal®, the 80% Nickel alloy used for room temperature applications. The only difference between these two metals is the special annealing cycle used for Cryoperm®.

### *Heat Treatment (Annealing)*

After forming, the shields must be annealed and processed accordingly to optimize the magnetic field properties at 4.2K. This process cannot be specified by Fermilab since, in most cases, this is a proprietary process.

### *Grinding & Snipping*

Before annealing, grinding and snipping are permissible to create a better fit with mating parts. No metal work is permitted once the annealing process has been completed.

### *Handling*

Before and after annealing, white cotton gloves must be worn to prevent cosmetic defects from dirty hands and skin oils. After processing of the shields, care must be taken in handling and shipping to not damage the developed magnetic characteristics of this material. Therefore, the shields are to be cautiously handled, packaged in bubble wrap and Styrofoam, and shipped in crates that will prevent impact to the shields and also minimize vibrations. Prior to awarding the contract, the vendor must explain their process and describe the method and container used for shipping.

**Appendix A – Pressure Test Results**



**Pressure Testing Permit\***

Type of Test:  Hydrostatic  Pneumatic  
 Test Pressure 34.5 psig Maximum Allowable Working Pressure 29.7 psid

**Items to be Tested**

TB9RI026 Cavity Helium Vessel

Note1: Cavity beam-line is backfilled to atmospheric pressure with boiled off argon gas, outside of the helium vessel is at atmospheric pressure in air

Note 2: The mini Conflat flange at the bottom of the helium vessel will be used to backfill the helium vessel with boiled off nitrogen gas during the test. The Conflat flange on the 2-phase pipe of the helium vessel will be blanked off during the test.

Note 3: The blade tuner is installed to the cavity. It is imperative that the safety rods are engaged between the tuner and the cavity tuner support rings on the helium vessel before the pressure test. This will ensure that the load on the piezo stack will not exceed the allowable limit. The tuner assembly also ensures that the titanium bellows in the middle of the helium vessel is supported during the pressure test.

Note 4: The pressure test will also include an RF frequency measurement before, during, and after pressurization

Location of Test CAF-MP9 Date and Time 10/22/13

**Hazards Involved**

Contact with high velocity jet of test gas.

**Safety Precautions Taken**

System designed, fabricated, and inspected per ASME Boiler & Pressure Vessels code. Test will be conducted by trained personnel as described in ASME code. Access to test area will be limited only to those involved in the test during pressurization.

**Special Conditions or Requirements**

Operating pressure = 29.7 PSID, test pressure = 1.16\*OP = 34.5 PSIG, pneumatic per ASME code.

1. First pressurize to 9-PSI and check for leaks.
2. Repeat at pressure levels listed in Table D-1.
3. Increase pressure gradually to the test pressure for 5minutes.
4. Reduce pressure to design pressure.
5. Close valve on regulator.
6. Maintain test for at least 10min. without loss of pressure.

Qualified Person and Test Coordinator Ken Pu 10/22/2013  
 Dept/Date TD/SRF Department

Division/Section Safety Officer Richard Ruthe 10/22/13  
 Dept/Date TD/ESH

**Results**

Pressure remained at 30 psig for 10 minutes without dropping.

Witness Richard Ruthe Dept/Date 10/22/13  
 Rich Ruthe or designee



## Details for the pressure test steps.

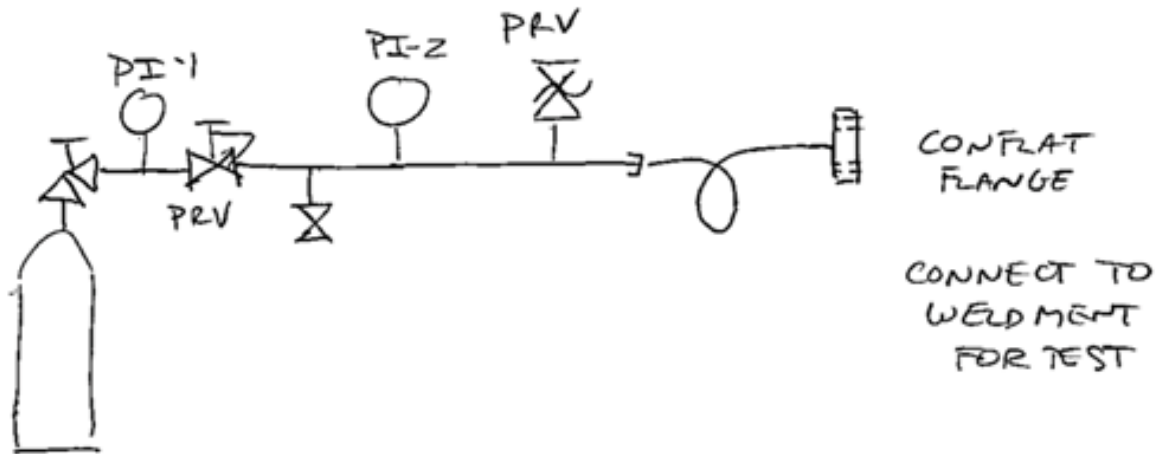
The table below shows the pressure levels for each pause and what should be done at that pressure. Total time for the test, not including setup and tear-down time, will be about 20 minutes.

**Table 27. Pressure Test Steps**

Pressure (psig) (psig equals differential pressure for this test)	Dwell time (minutes)	Activity at pressure
0	--	Baseline RF test
9.0	As needed	Snoop line fitting, RF check
17.0	As needed	Snoop line fitting, RF check
20.5	~1	
24.0	As needed	RF check
27.0	~1	
31.0	As needed	RF check
34.5	5	Peak test pressure of 1.15 x MAWP
30.0	10*	Test pressure hold point*, RF check
25.0	As needed	RF check
17.0	As needed	Visual inspection, RF check
0	--	RF check

\*The pressure hold point of 30 psig is approximately the MAWP. Dwell time is set long enough to assure us that pressure is not dropping.

### Test Setup



Test Pressure  
19 psig

PI-2  
0-100 psig

PRV  
35.4 psig relief



Figure 45. Typical Set-Up of Dressed SRF Cavity for Pressure Test.

**Appendix B - FESHM 5031.6 DRESSED SRF CAVITY ENGINEERING NOTE FORM**Prepared by: \_\_\_\_\_ Preparation Date: 2014SRF Cavity Title: Pressure Vessel Engineering Note For the 1.3-GHz Helium Vessel, Dressed Cavity RI-026 (Cavity TB9RI026, Vessel INC-XXX)

Lab Location / Cryomodule ID:

- As single dressed cavity: tested at Meson Detector Building (FIMS #408)
- Installed in cryomodule: tested at New Muon Lab (FIMS #700)

Purpose of system / System description: Liquid helium containment for nine-cell 1.3-GHz Superconducting Radio Frequency (SRF) cavityPressure Vessel ID Number: IND-202

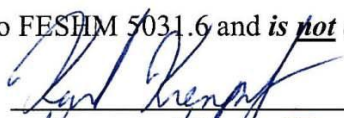
Design Pressure 1: 2.0 bar                      Design Temperature 1: 80 – 300 K  
 Design Pressure 2: 4.0 bar                      Design Temperature 2: 1.8 – 80 K  
 Beam Vacuum: 3.0-bar (45-psia)

Materials: Niobium, titanium, niobium-titaniumDrawing Numbers (PID's, weldments, etc.):  
\_\_\_\_\_Designer/Manufacturer: FNAL / Incodema / RI / Sciaky

Test Pressure: \_\_\_\_\_ Test Date: \_\_\_\_\_

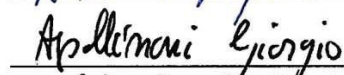
## Statements of Compliance

SRF Cavity conforms to FESHM 5031.6 and is not exceptional: Yes  No

Reviewer's Signature: 

Date: 10/23/13

Print name: KURT KREMETSZ

D/S Head's Signature: 

Date: 11/26/13

Print name: Giorgio APOLLINARI

---

### Additional approvals if vessel is exceptional

ES&H Director's Signature: 

Date: 12-3-13

Print name: Martha Michels #8971

Director's Signature: 

Date: 12/3/13

Print name: Stewart D. Housner

---

## References

1. Fermilab's ES&H Manual, Chapter 5031.6, "Dressed Niobium SRF Cavity Pressure Safety," Aug 2010.
2. ASME, Boiler and Pressure Vessel Code, 2007.
3. "Vacuum Vessel Engineering Note for SMTA Horizontal Test Cryostat," ATA-010, February 2007
4. Y. Pischalnikov, et al, "Resonance Control in SCRF Cavities," September, 2008.
5. "Pressure Vessel Engineering Note for the 3.9-GHz Helium Vessel, Cavity #5," IND- 102, July 2008.
6. Peterson, T., "3.9-GHz Helium Vessel, Low Temperature Maximum Allowable working Pressure," March, 2009
7. Standards of the Expansion Joint Manufacturers Association, Inc., 7<sup>th</sup> Edition.
8. American Institute of Steel Construction, Manual of Steel Construction, 8<sup>th</sup> Edition, 1980.
9. Compressed Gas Association, Inc., "Pressure Relief Device Standards, Part 3 – Stationary Storage Containers for Compressed Gases," CGA S-1.3-2008, 8<sup>th</sup> Edition.
10. Soyar, B., private email, December 2007.
11. Kropschot, R.H., et al, "Technology of Liquid Helium," National Bureau of Standards, Monograph 111, October 1968.
12. G. Cavallari, et al, "Pressure Protection Against Vacuum Failures on the Cryostats for LEP SC Cavities", European Organization for Nuclear Research, 27 Sep, 1989. CERN internal note AT-CR/90-09 presented at 4th Workshop on RF Superconductivity, Tsukuba, Japan (1998).
13. W. Lehmann, et al, "Safety Aspects for LHe Cryostats and LHe Transport Containers," Proceedings of the 7th International Cryogenic Engineering Conference, London, 1978.
14. TTF Design Report, Section 5.5.1.
15. Crane, Flow of Fluids, Technical Paper 410, 1988.
16. Roark, R.J. and Young, W.C., Formulas for Stress and Strain, 5<sup>th</sup> Edition, McGraw-Hill, 1975.
17. Rao, K.R., et al, Companion Guide to the ASME Boiler and Pressure Vessel Code, Vol. 1.